SULFUR DIOXIDE AND PARTICLE EMISSIONS FROM MOUNT ETNA, ITALY

by

Robert J. Andres

Submitted in Partial fulfillment
of the Requirements for the Degree of
Master of Science in Geochemistry

New Mexico Institute of Mining and Technology
Socorro, New Mexico

June, 1988

ACKNOWLEDGEMENTS

This project was aided by my advisor and friend, Philip Kyle. He initiated the project and later guided and supported it. In addition to Phil, the following are also acknowledged:

R. Cristofolini, V. Scribano and the Istituto di Scienze della Terra, Universita di Catania, Catania, Italy provided crucial support and local knowledge during my stay in Sicily;

J. Lowenstern for acting as liaison and interpreter during the first half of my stay in Catania;

SITAS for use of the Torre del Filosofo and occasional transportation up and down Mount Etna;

Vittoria and Giovanni Cuccimotto for making my time in Italy more enjoyable;

R. Chuan for use of the QCM, help in identifying particles with the SEM, and lodging during my visit to California;

J. Mabon for operating the SEM at New Mexico Institute of Mining and Technology;

K. Meeker and Los Alamos National Laboratory for analyzing the aerosol filter packs;

J. Ruff and Dr. A. Guthjar for aid in the Fourier transform evaluations of the data;

J. Murray for his latest summit map and levelling results;

C. Behr, N. Dunbar, P. Kyle, K. Meeker, P. Sylvester, C. Popp and A. Campbell for helpful reviews of the text;

S. Krukowski, D. Johnson, A. Campbell and the New Mexico Bureau of Mines and Mineral Resources for aid in preparing slides for my thesis defense; and

Research and Development Division, New Mexico Institute of Mining and Technology; Geological Society of America; and Sigma Xi (two grants) for financial support.

Thanks also goes to Tina Behr, without whose support this project would never have been completed.

Finally, I must acknowledge Him who created it all.

ABSTRACT

The sulfur dioxide and particle emissions of Mount Etna were sampled from June to August 1987. Only two of the four summit craters were active at that time. SO_2 fluxes for the entire system averaged 1056.17 $\pm$ 1842.74 tonnes per day. Variations in system SO_2 fluxes may be due to subsurface magma movement and highlight the futility of SO_2 monitoring for prediction of volcanic eruptions. The two degassing craters emitted from 165 to 5229 tonnes per day with wide, short-term variations measured in both craters. Particles identified include silicates, chlorides, chlorates, sulfites, and sulfides. Chlorine was only a constituent of one crater's particles. Similar elemental enrichment factors were calculated for most elements from each crater with chlorine, bromine and sulfur the most enriched elements in the sampled fume. Differences observed in particle compositions and size distributions for each crater are likely due to the differing eruption style of each crater. Atmospheric implications of Etnean emissions were negligible compared to the region's anthropogenic sources.

Table of Contents

List of Tables

List of Figures

INTRODUCTION

Volcanic emission products include solid, liquid, and gaseous phases. Many studies address the lavas erupted from volcanoes, but few studies examine the gases and aerosol particles. The major gaseous phases emitted from volcanoes are water, carbon dioxide, and sulfur dioxide. Micron-sized aerosols consist mainly of silicates, metals, sulfates, chlorides, and oxides.

One of the first sites where volcanic gases were studied was Kilauea Volcano, Hawaii. In 1912, Day and Shepherd (1913) collected gas samples from Halemaumau lava lake. Later, Jaggar (1940) completed a study of magmatic gases from Halemaumau which served as the best available compilation of magmatic gas compositions for decades (Gerlach, 1980).

Modern studies at Kilauea have progressed beyond the characterization of volatiles to those which examine the mechanisms controlling volatile release from the magma. This has allowed calculation of pre-eruptive magma volatile contents and volatile mass balances from mantle magma generation to surficial vent emission, such as those of Gerlach and Graeber (1985) and Greenland et al. (1985). Despite different approaches, their calculations showed similar results. In addition, Gerlach (1986) determined the shallow saturation of Hawaiian magmas with respect to sulfur. His results indicated that significant sulfur

exsolution occurs only at depths less than 125 meters below the surface. Hence, regular monitoring of sulfur emissions can provide information on magmatic processes occurring in the near-surface environment.

Sulfur dioxide gas (SO_2) is a major gaseous sulfur species emitted by volcanoes and can be monitored with the Barringer correlation spectrometer (COSPEC). The COSPEC was first applied to volcanic SO_2 emissions in 1971. Early studies grossly characterized SO_2 fluxes for several volcanoes (Stoiber et al., 1983). Today, detailed COSPEC investigations reveal systematic variations in SO_2 emissions from individual volcanoes over short time periods (Chartier, 1986; Kyle, personal communication). Interpretations of fluxes has led to models for magma movement (Casadevall et al., 1981; Malinconico, 1979), models for predicting eruptions (Malinconico, 1987), and calculations of volcanic gas emissions to the atmosphere (Lambert et al., 1988; Stoiber et al., 1987; Berresheim and Jaeschke, 1983; Cadle, 1980).

Volcanic gas and particle research provides a better understanding of atmospheric processes. Studies of the conversion of SO_2 to H_2SO_4 and its subsequent precipitation as acid rain have been aided by volcanic gas research (Finlayson-Pitts and Pitts, 1986). Likewise, studies of volcanic particles have provided theories for the causes of short term climatic changes (Devine et al., 1984; Rampino and Self, 1984).

An assessment of the effects of volcanic emissions on the atmosphere is aided by compiling characterization studies of emissions from active volcanoes. Mount Etna, Italy is one of the most active volcanoes in Europe; it is constantly degassing and frequently erupts. The magma composition and volcanic activity of Mount Etna differ from other, more thoroughly studied volcanoes. Because the composition of the gaseous species emitted by volcanoes is in part a function of its lava composition, Mount Etna is an ideal location for a volcanic emissions study.

The main objective of this study is to assess the SO_2 and particulate input to the atmosphere from Mount Etna. This will be accomplished by

1) determining the emission rates of SO_2 and other trace gases and aerosols,
2) correlating the variations in SO_2 emissions to magmatic processes,
3) characterizing the size distributions and compositions of particulate material, and
4) evaluating the impact of these emissions on the atmosphere.

Observations for this study were made at Mount Etna between 22 June and 10 August 1987.

GEOLOGY OF MOUNT ETNA

Volcanic History

Modern Mount Etna (Figure 1) is the result of a long history of volcanic activity. Built upon sialic, continental crust near the boundary of the African and European plates (Lentini, 1982; Barberi et al., 1974), Mount Etna has evolved from subaquatic tholeiitic pillow lavas, to subaerial alkali basalts, and then to hawaiite-tephrite lava flows and cinder cones (following classification of de la Roche et al., 1980) (Cristofolini et al., 1987; Cristofolini et al., 1984; Romano, 1982; Rittmann, 1973). Mount Etna's volcanic history includes four main phases.

The first phase of activity was dominated by tholeiitic volcanism from approximately 700,000 to 200,000 years before present (B.P.) (Romano, 1982). Pillow basalts, hyaloclastic breccias, and intrusions were typical products of this early phase. Extensive, subaerial, plateau basalts erupted after regional uplift occurred.

The second phase of activity erupted hawaiites and phonotephrites from approximately 200,000 to 80,000 years B.P. (based on Th/U dates, Condomines et al., 1982). Numerous eruptive centers emitted flows and local pyroclastics to form domes and stratovolcanoes during this time (Romano, 1982; Rittmann, 1973).

Figure 1. Mount Etna Location Map. Figure 1a shows the relationship of Sicily to mainland Italy. Figure 1b contains the areal extent of Etnean volcanics and other regional features. The area portrayed in Figure 1c is located within the 3000 meter contour of Figure 1b and shows the positions of the four summit craters. Figure 1 compiled from Murray, 1987; Chester et al., 1985; Murray et al., 1981; and Romano et al., 1979.

FIGURE 1A.

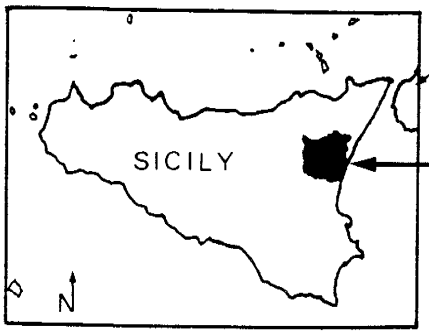

FIGURE 1B.

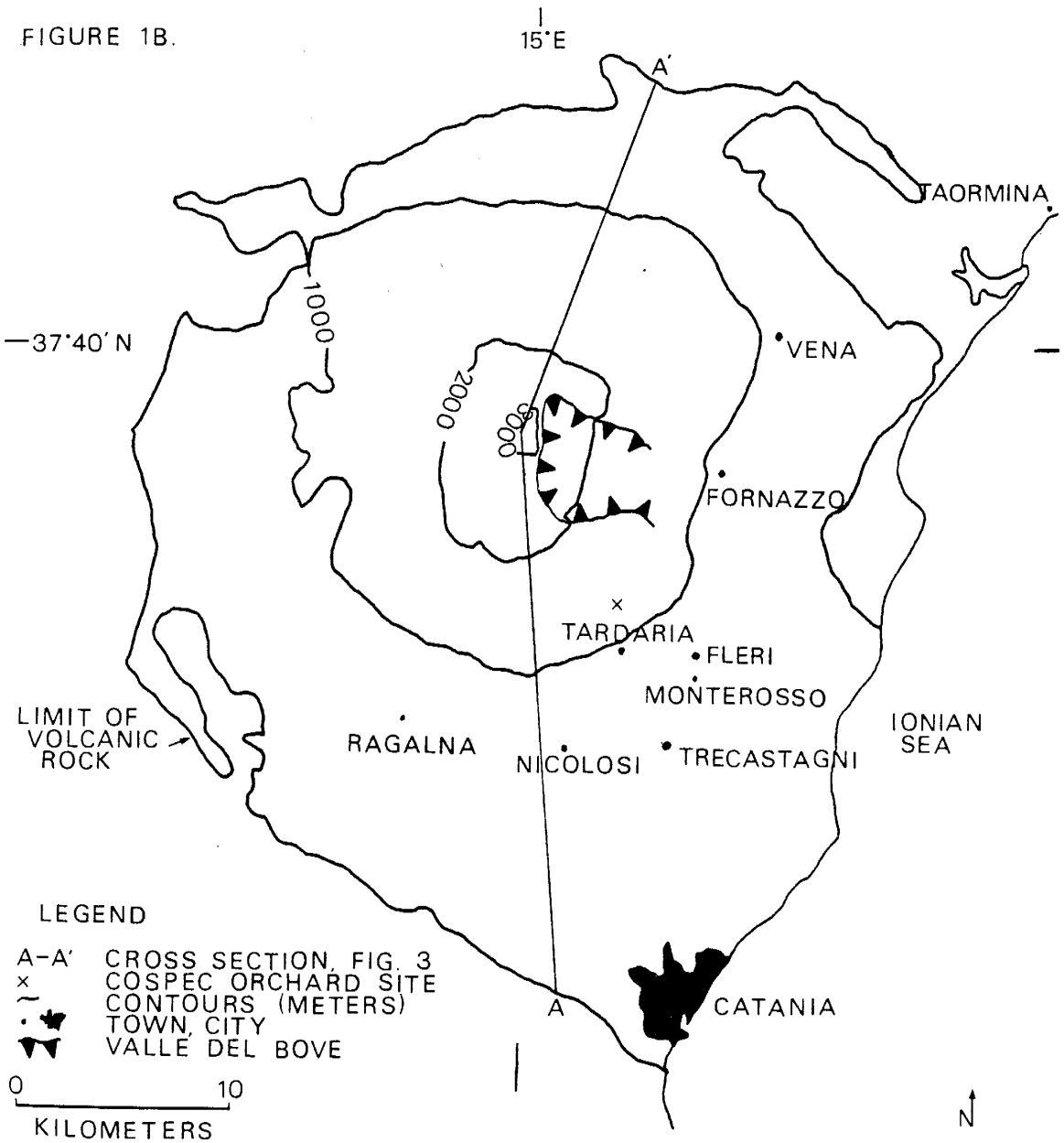

FIGURE 1C.

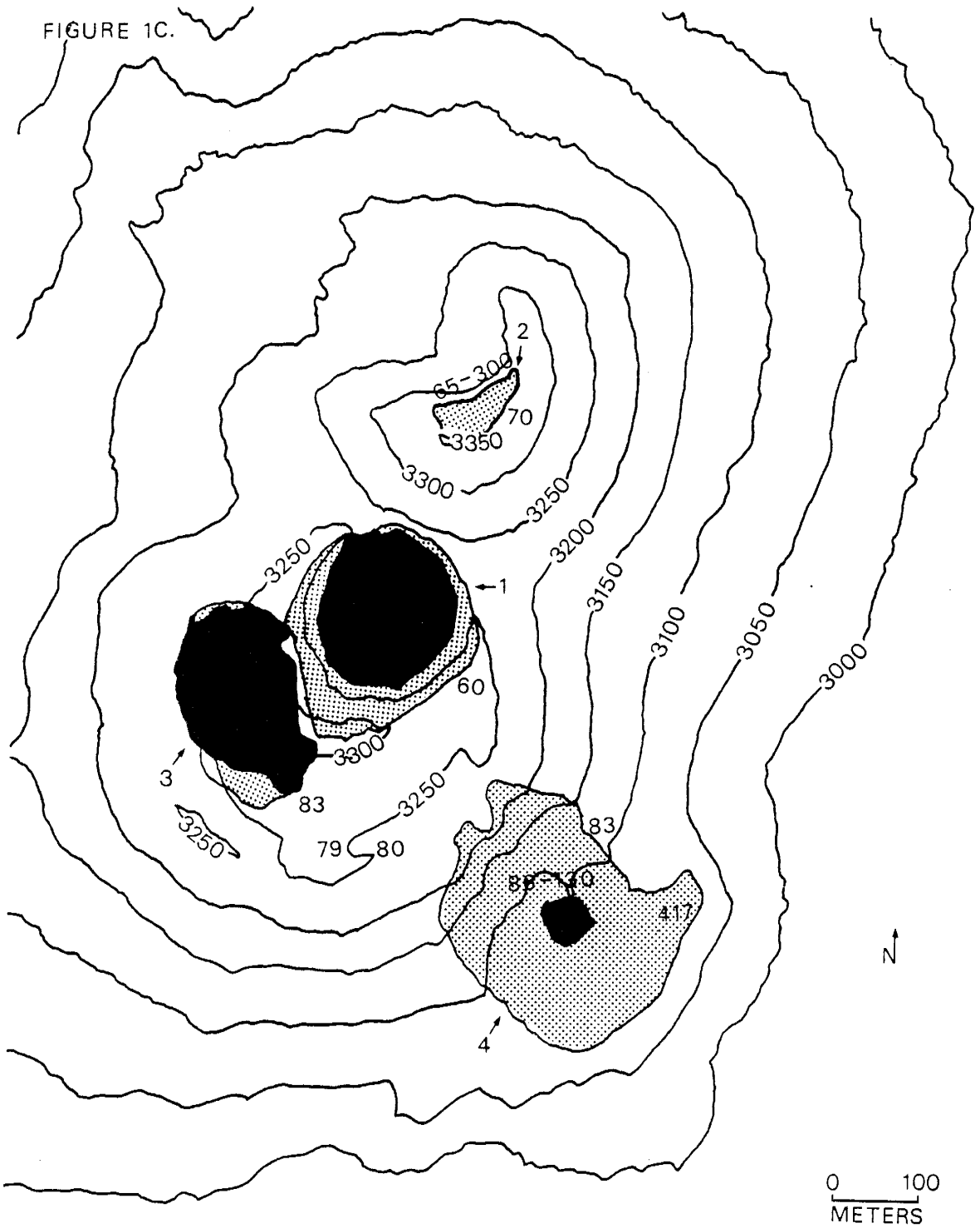

LEGEND

~ CONTOURS (METERS)

AREAL EXTENT OF CRATER

AREA WITHIN VERTICAL CRATER WALL

FUMAROLE AND FLOW TEMPERATURES

1 THE CHASM
2 NORTHEAST CRATER
3 BOCCA NUOVA
4 SOUTHEAST CRATER

The third phase of activity is characterized by mugearites, hawaiites, tephrites, and latite andesites. These were erupted as flows and pyroclastics from a 3000 meter high stratovolcano and many, smaller, eruptive centers. This activity lasted from 80,000 to 30,000 years B.P. (Romano, 1982; Rittmann, 1973). Later, the stratovolcano was largely eroded during the formation of the Valle del Bove, a large valley now present on the east-southeast side of modern Mount Etna (Figure 1b).

The fourth and present phase began 30,000 years B.P. and is characterized by the eruptions of hawaiites and alkali basalts. Numerous widespread eruptive centers have built flows, cones, and localized pyroclastics to form a volcanic pile which ranges from 33 to 45 kilometers in basal diameter and over 3500 meters in height (Romano, 1982; Romano et al., 1979; Rittmann, 1973). The modern summit of Mount Etna rises sharply from the underlying volcanic pile, and it consists of four craters, several parasitic cones, and lava flows (Figure 1c).

Modern Volcanic Activity

Modern volcanic activity on Mount Etna can be classified as summit and flank eruptions. Both eruption types are dominated by aa flows, but pahoehoe flows with extensive tube systems also occur (Guest, 1982; Wadge, 1977).

Summit activity usually originates from the craters. The craters show various types of activity including lava filling and draining the craters, crater collapse, strombolian eruptions, and non-explosive lava effusion. Although the summit craters are spatially close, their activities are independent (V. Scribano, personal communication; Guest, 1982).

Flank activity is less common than summit activity, and usually occurs as fissure-fed flows. The flows typically have higher effusion rates than summit-fed flows. Guest (1982) has found a positive correlation between flank flow volumes and the duration of repose periods between flank eruptions. This suggests that magma storage occurs within the Etnean complex. Strombolian flank eruptions are less common and build isolated cinder cones, or cones associated with fissure-fed flows (Guest, 1982; Wadge, 1977).

The eruptive history of Mount Etna has been used to calculate the rate of magma influx into the Etnean system. Wadge (1977) reports a magma influx rate of 0.34 cubic meters per second (cms) and an eruption rate of 0.26 cms for a period from 1759 to 1975. The difference between these rates represents internally stored magma, i.e. in dikes. The 1759 to 1975 magma influx rate was revised to 0.27 cms (Wadge, 1979) in a reply to criticism of the original estimate by Tanguy (1979). Wadge and Guest (1981) calculate a 0.7 cms magma influx rate for 1971 to 1981. Subsequent estimates of magma influx rates have yet to be published.

However, the latest, reported magma influx is double the rate of the previous 250 years and signifies some unknown change in the Etnean plumbing system.

The Etnean Subsurface

Mount Etna is the largest and one of the most active European volcanoes. It lies at the intersection of four, fault zone alignments (Figure 2. Lo Giudice et al., 1982; Rittmann, 1973). These faults facilitate magma rise and differentiation and align eruption locations.

A comprehensive physicochemical subsurface model has been assembled from the petrographic, isotopic, geochemical, and seismological data of Mount Etna. Analyses of Etnean lavas reveal their mantle sources have within plate geochemical characteristics which have later been modified by a subduction zone component (Cristofolini et al., 1987; Cristofolini et al., 1984). Partial melts of this source collect in dikes and sills 20 kilometers below the surface in Mount Etna's deep magma reservoir (Figure 3, Lombardo and Patanè, 1982). These partial melts can differentiate and mix in this deep reservoir. Seismic evidence indicates that this reservoir is approximately 22 by 31 kilometers in areal extent and 4 kilometers thick (Sharp, 1982). Initial ^{230}Th-^{232}Th ratios suggest this reservoir has existed for 200,000 years (Condomines et al., 1982).

Reservoir magmas eventually rise through the Etnean plumbing system in a plexus of dikes and sills which result

Figure 2. Relationship of Mount Etna and Regional Fault Zones. Figure 2 is modified from Grindley, 1973.

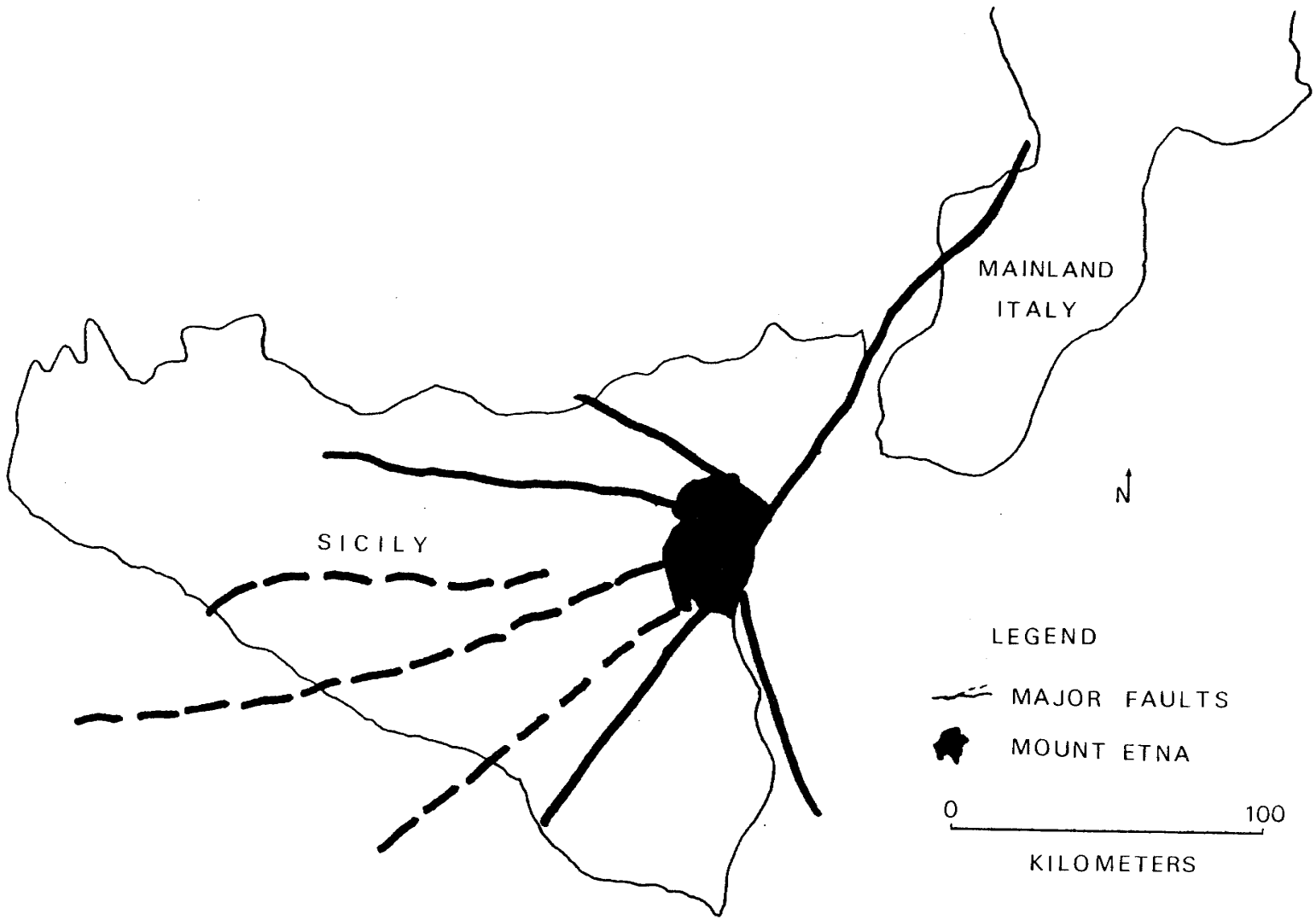
MAINLAND
ITALY
N
SICILY
LEGEND
MAJOR FAULTS
MOUNT ETNA
0
100
KILOMETERS

Figure 3. Cross-section of Mount Etna. Location of deep magma reservoir determined by seismic studies. Areal trace of cross-section depicted in Figure 1b. Figure 3 is modified from Lombardo and Patanè, 1982.

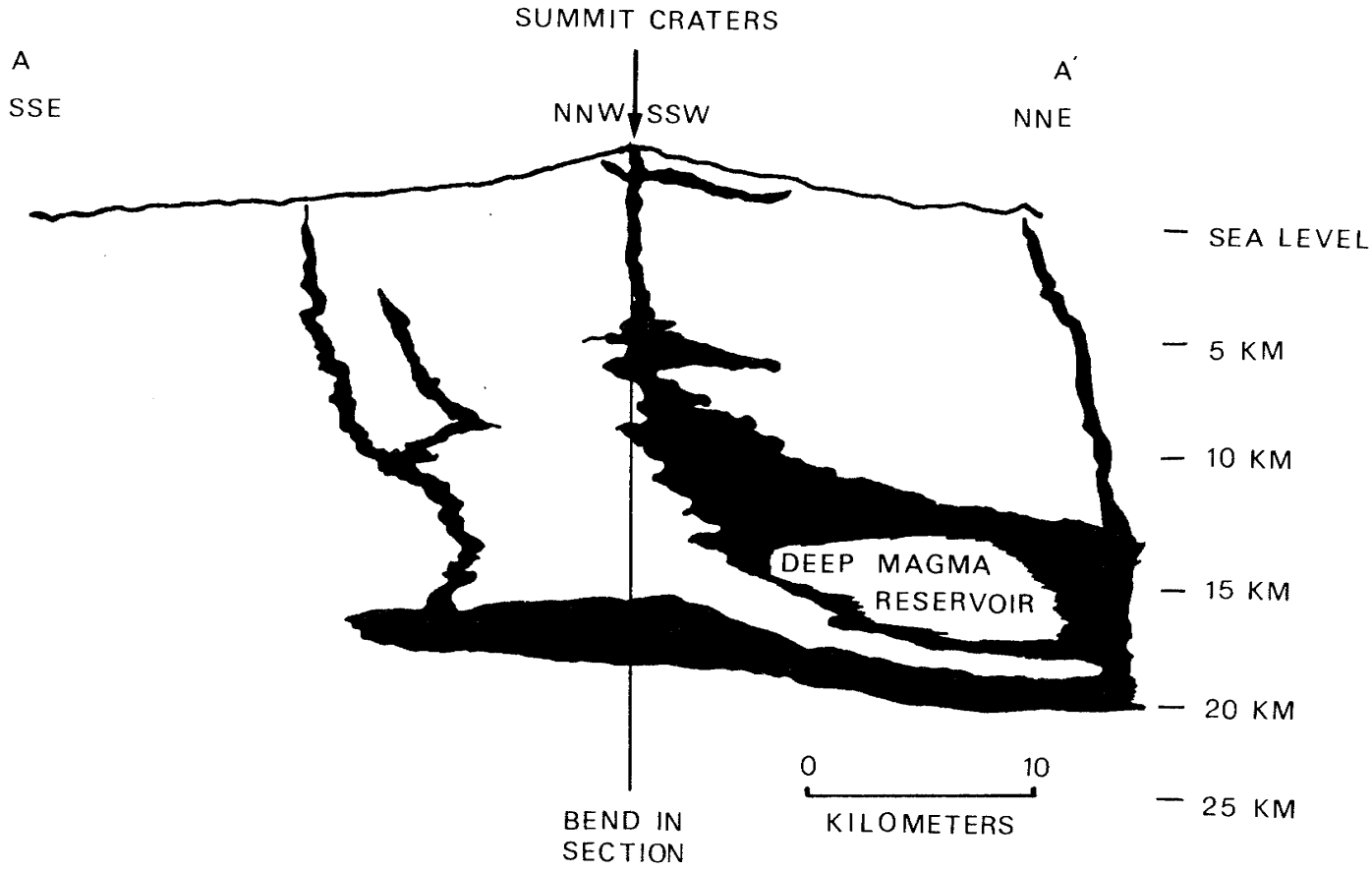
SUMMIT CRATERS
A
SSE
NNW
SSW
A'
NNE
SEA LEVEL
5 KM
10 KM
DEEP MAGMA
RESERVOIR
15 KM
20 KM
0
10
KILOMETERS
25 KM
BEND IN
SECTION

from the tensional stress regime of the region (Cristofolini et al., 1985; Cristofolini et al., 1984; Wadge, 1977). Olivine, titanomagnetite, and clinopyroxene crystallize during the magma's ascent; the last phase to crystallize is plagioclase which forms at 2 to 3 kilometers depth in shallow magma reservoirs (Cristofolini et al., 1987; Cristofolini and Tranchina, 1980). Little evidence exists for crustal contamination of the ascending magmas; however, isotopic and geochemical evidence strongly suggest magma mixing is common prior to magma eruption (Cristofolini et al., 1987; Cristofolini et al., 1984; Cristofolini and Romano, 1982; Carter and Civetta, 1977).

Seismic resonance data indicate there are discrete, individual conduits for each summit crater at shallow levels (Figure 4, Schick et al., 1982); however, these conduits do not contain homogeneous magmas. Individual lava flows can show variations in composition upon eruption, reflecting the various processes which affect the magmas at depth (Cristofolini et al., 1984). It should be noted that most magmas erupted over the last few centuries have been from a homogeneous deep reservoir source; subsequent crystallization and mixing processes have not changed their bulk chemistry significantly prior to eruption (Cristofolini et al., 1984).

Figure 4. Subsurface Relationship of Mount Etna's Craters. Subsurface structure modelled from seismic resonance data. Bends in cross-sectional view are not noted. Figure 4 is modified from Schick et al., 1982.

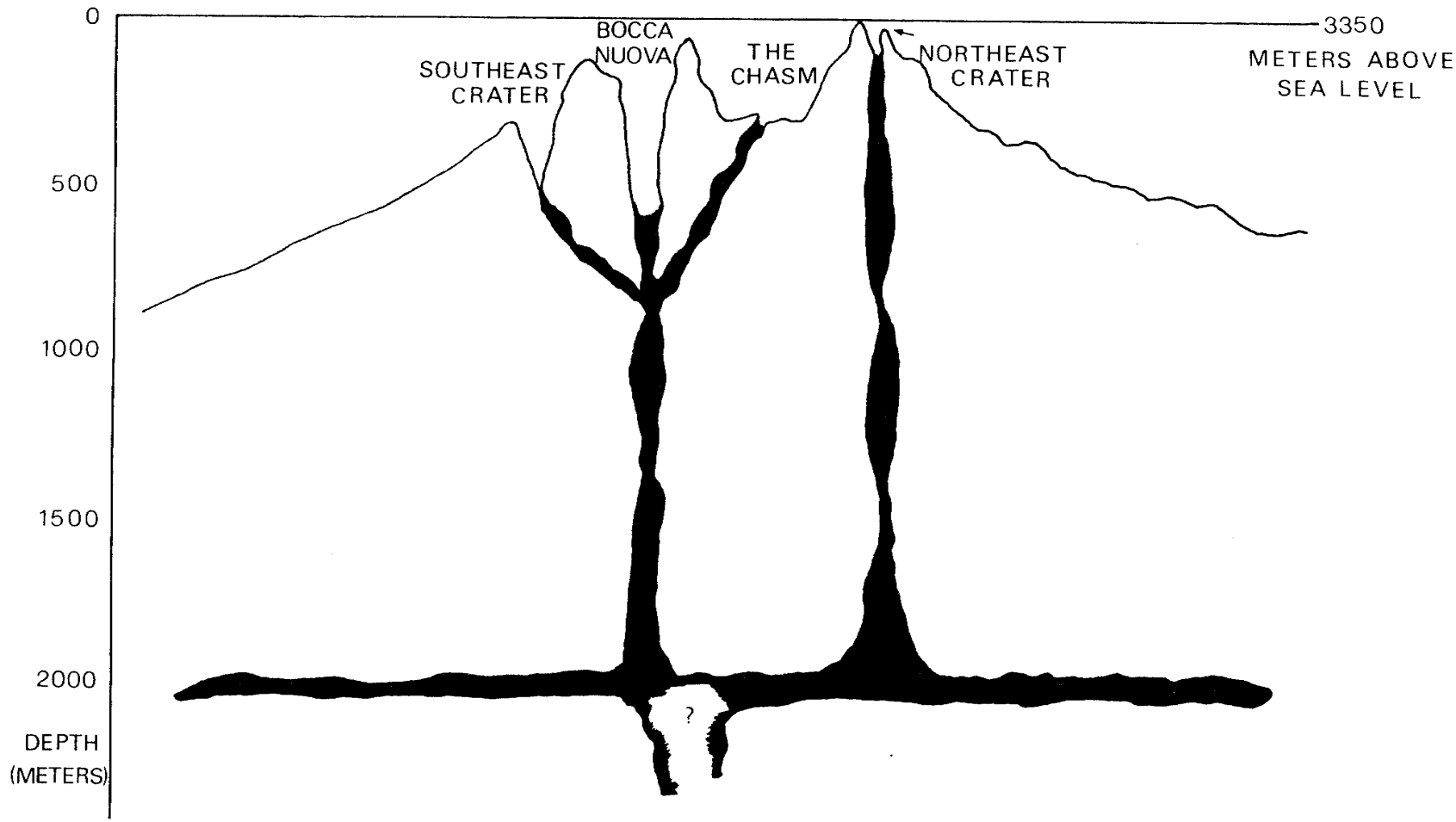
0
500
1000
1500
2000
DEPTH
(METERS)
SOUTHEAST
CRATER
BOCCA
NUOVA
THE
CHASM
NORTHEAST
CRATER
3350
METERS ABOVE
SEA LEVEL
?

Previous Studies of Mount Etna SO_2 and Particle Emissions

A comprehensive study of gas and particle emissions of Mount Etna has yet to be undertaken. Previous studies have been limited in scope and variable in quality. The results of these studies are usually not directly comparable because of differing objectives, different sampling methods, and the dynamic state of Mount Etna's volcanic activity.

Tazieff (1971) sampled the plume of one of Mount Etna's summit craters in September 1968 and June 1969. He measured on site SO_2 concentrations of 330 $\pm$ 33 to 4 $\pm$ 0.4 parts per million.

Le Guern (1973) sampled gases emitted from an active hornito and a recently opened vent on 11 July 1970 and 27 August 1971, respectively. Gas chromatography analyses showed varying proportions of SO_2, CO_2, and H_2 in the atmospheric-contaminated gas samples.

Huntingdon (1973) sampled hornito-emitted gases with an evacuated sampling bottle technique. Sample contamination was induced by his sampling apparatus and resulted in the loss of oxygen and sulfur from the samples. The resulting analyses showed the gases were unusually reduced and of non-equilibrium compositions.

Gerlach (1979) restored Huntingdon's data to thermodynamic equilibrium compositions. The average of 9 analyses show SO_2 is second to water in abundance (Table 1); water, SO_2, and carbon dioxide compose greater than 98

Table 1. Comparison of average volcanic gas compositions from Mount Etna, Italy; Kilauea, Hawaii; and Erta'Ale, Ethiopia. All data are reported in mole percentages and corrected to thermodynamic equilibrated compositions (Gerlach, 1979, 1980, 1981).

	H_2O	H_2	CO_2	CO	SO_2	S_2	H_2S	HCl
Etna, 1075°C								
1970	49.14	0.53	23.41	0.49	25.94	0.25	0.21	n.d.
Kilauea, 1140°C								
1918	52.30	0.79	30.87	1.00	14.59	0.12	0.16	0.14
Erta'Ale								
1971, 1075°C	69.56	1.57	17.80	0.78	8.79	0.51	0.95	n.d.
1974, 1130°C	77.13	1.59	11.70	0.52	7.39	0.29	0.92	0.42

n.d. = not determined

percent of the average analysis. Reduced species such as H_2, CO, H_2S, and S_2 are insignificant, highlighting the oxidized nature of emitted volcanic gases. Similar oxidized emissions have been found at other volcanoes (Table 1). These other analyses show carbon dioxide replacing SO_2 as the second most abundant gas species. This is likely due to sampling of more pristine, or less degassed, magma. A more pristine magma would have degassed less carbon dioxide relative to SO_2 because of the different solubilities of the respective gases (Allard, 1983).

Since the early 1970's, no accessible, high-temperature fumaroles have been available for gas bottle sampling on Mount Etna. So, instead of determining compositions of emitted gases, workers began to measure fluxes of various species, or the mass of a particular species emitted over time. SO_2 flux studies have been carried out periodically at Mount Etna. Most of these studies have used a COSPEC to remotely determine the SO_2 flux. Zettwoog and Haulet (1978) employed a COSPEC II to measure SO_2 emitted from Mount Etna during various types of activity from 1975 to 1977 (Table 2). Their results show increasing SO_2 fluxes associated with increasing volcanic activity.

Malinconico (1979) employed a similar technique to that of Zettwoog and Haulet (1978) during July through August 1977 (Figure 5). His results give a baseline SO_2 flux of approximately 1000 tonnes per day during periods of non-

Table 2. Published SO_2 fluxes obtained at Mount Etna. Results from Malinconico (1979) given in Figure 5. SO_2 fluxes are given in tonnes per day.

Date	SO_2 flux	Remarks
Zettwoog and Haulet, 1978		
14 June 1975	4800 3800 3200 2700 3900 3600 4200 3700	During a period of quiet, summit effusion.
15 June 1975	3300 4200 3800 4000	Same as above.
18 June 1975	4100 3700 3600 3600 3400	Same as above.
31 Jan. 1976	5400 12400 7400	Weak flank eruption.
14 June 1976	1600 1300 2300 2200	Prior to opening of 17 June summit vent.
15 June 1976	2900 3700	Same as above.
16 June 1976	6100 6500	Same as above.
22 May 1977	1200 1100	Post-eruptive phase.
23 May 1977	1100	Same as above.
Jaeschke et. al., 1982		
September 1978	142	Post-eruptive phase.
June 1979	955 1600	Pre-eruptive phase.
Martin et al., 1986		
22 Sept. 1983	2680	Post-eruptive phase.
23 Sept. 1983	2250	Same as above.
25 Sept. 1983	3370 5010	Same as above.

Figure 5. Results Obtained by Malinconico (1979) During Summer of 1977. Measured SO_2 fluxes are located above activity bars which depict the volcanic activity associated with the SO_2 fluxes. Figure 5 is modified from Malinconico, 1979.

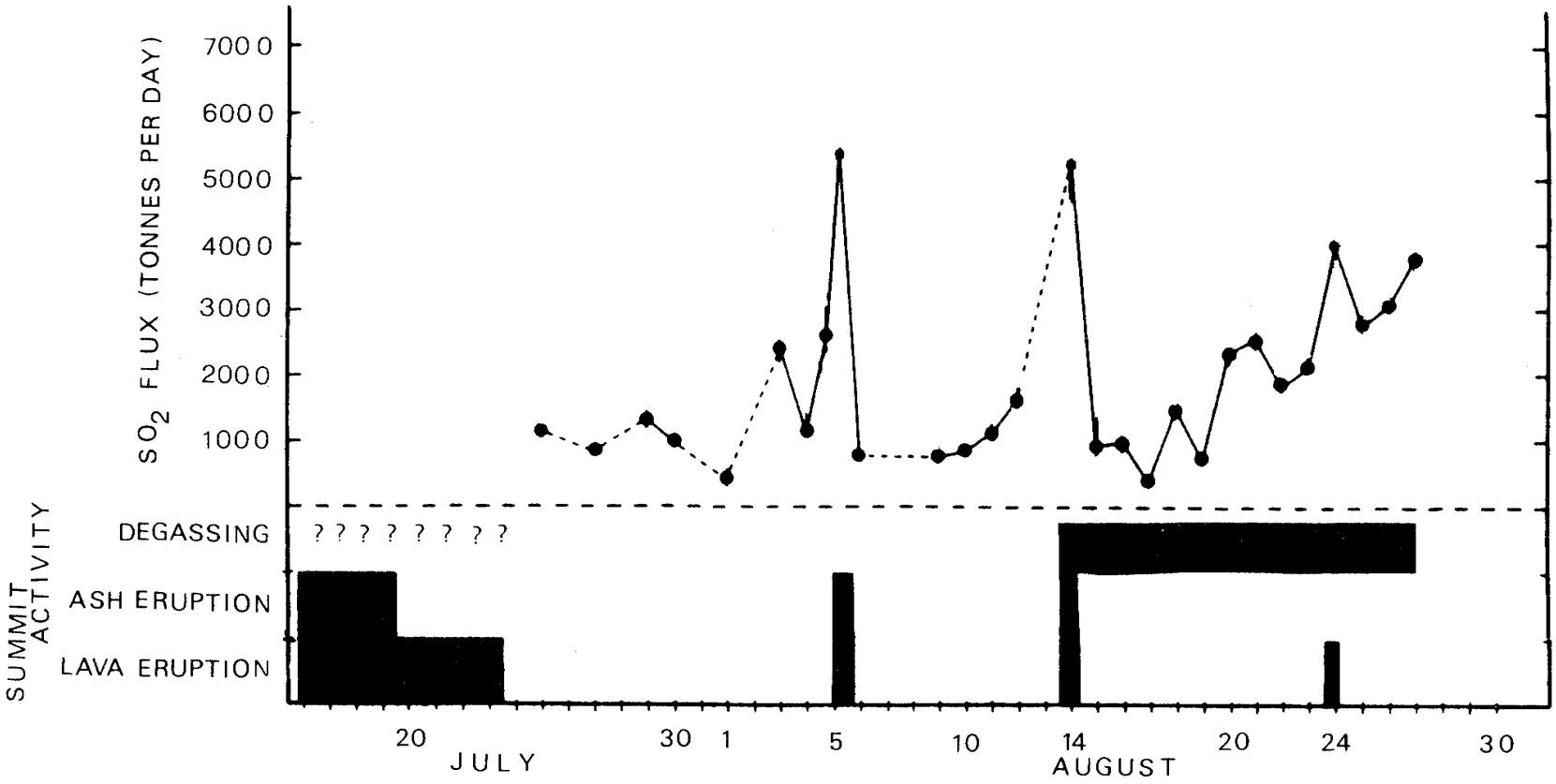
SO_2 FLUX (TONNES PER DAY)
7000
6000
5000
4000
3000
2000
1000
SUMMIT ACTIVITY
DEGASSING
? ? ? ? ? ? ? ?
ASH ERUPTION
LAVA ERUPTION
20
JULY
30
1
5
10
14
20
24
30
AUGUST

explosive summit degassing. Prior to eruptions on 5 and 14 August, SO_2 fluxes increased and peaked at greater than 5,000 tonnes per day during the summit eruptions. Measured SO_2 fluxes again increased from baseline after the 14 August eruption, but no summit eruption ensued. However, a small lava flow was observed on 24 August in one of the summit craters.

Both Zettwoog and Haulet (1978) and Malinconico (1979) made SO_2 flux measurements with an automobile-mounted COSPEC. This technique is discussed later, but it should be noted that this technique can give rise to large errors in flux determinations. It is not presently possible to determine the accuracy of these SO_2 measurements, but the correlation of increasing SO_2 fluxes with increasing volcanic activity is noted and will be discussed later.

Jaeschke et al. (1982) employed a flame-photometric detector-equipped instrument to measure SO_2 fluxes. Their airborne plume measurements during a post-eruptive phase in September 1978 and a pre-eruption phase in June 1979 gave a 142 to 1600 tonnes per day SO_2 flux (Table 2). The higher flux readings were recorded during the pre-eruptive phase sampling.

Martin et al. (1986) used an airborne COSPEC IV during September 1983 to monitor the plume during a post-eruption phase. Their SO_2 flux measurements were taken 9 to 164 kilometers downwind of the summit and recorded 2250 to 5010

tonnes per day (Table 2). Their sampling was done at large distances from the summit in order to study the loss of SO_2 from the plume as a function of distance. Their results of SO_2 plume decay rates are an order of magnitude lower than Jaeschke et al. (1982); this may be due to a greater sampling distance from the summit or different sampling techniques.

In the past, particle research on Mount Etna has not been emphasized. Buat-Ménard and Arnold (1978) examined particles collected on filters from the Etnean plume in June 1976. Their scanning electron microscope studies show volcanic ash dominates 1 to 10 micron-sized particles. Copper and zinc halides were found, as well as sulfur-rich particles. Varekamp et al. (1986) found the small, sulfur-rich particles to be sulfuric acid droplets which are likely formed from the conversion of SO_2 to sulfate. Aluminum, iron, calcium, copper, zinc, and ammonium sulfates, as well as iron and iron-titanium oxides were also detected. Burtscher et al. (1987) measured particles in the 0.01 to 1 micron size range with an aerosol photoemission technique. Their measurements show that the Etnean craters were emitting particles in the 0.02 to 1 micron size range during June 1986.

Elemental fluxes can be determined from analyses of filter-collected particles by energy spectral techniques (e.g. X-ray fluorescence, instrumental neutron activation analysis). Buat-Ménard and Arnold (1978) calculated fluxes

from a summit vent for 25 elements (Table 3). Similar calculations were done on samples collected 9 kilometers from the summit by Martin et al. (1986); 7 elements, sulfate, and ^{210}Po were identified (Table 3). For the 4 elements common to both studies, the samples collected at greater distances from the summit record a lower flux than those samples taken at the summit vent. This is likely a function of particle deposition and the variable fluxes emitted from the summit vents.

Table 3. Elemental fluxes as measured by other workers. All fluxes are reported in tonnes per day, except Po^{210} which is in curies per day. First column of fluxes is from Buat-Ménard and Arnold (1978) and second column is from Martin et al. (1986). The fluxes reported are for particles only and thus are not directly comparable to data obtained in this study which includes acidic gases also (Table 12).

Species	Flux	Flux
S	420	
Cl	300	
K	28	10.8
Na	26	
Ca	20	0.99
Br	6.3	
Al	6.0	1.1
Fe	3.0	0.97
Zn	3.0	
Cu	1.0	
Se	0.63	
Pb	0.36	
As	0.11	
Hg	$7.5E^{-2}$	
Cd	$2.8E^{-2}$	
Cr	$2.0E^{-2}$	
Sb	$1.0E^{-2}$	
Co	$8.0E^{-3}$	
Cs	$4.0E^{-3}$	
Au	$2.4E^{-3}$	
Sc	$5.4E^{-4}$	
SO_4^{2-}		29
Si		5.9
P		0.2
Ti		0.1
Po^{210}		0.26

METHODS

Crater Descriptions and Temperature Measurements

Descriptions of the four summit craters were taken during the field study period; crater morphology, sulfur deposition sites, and activity were noted. Fumarole and lava flow temperatures were measured with an Omega 450 AKT Thermocouple Thermometer with a Type K thermocouple. Temperatures were recorded when the 1 meter long thermocouple was inserted into the fumarole or lava flow and the temperature had stabilized.

SO_2 Flux Measurements

Sulfur dioxide emission rates were measured with a Barringer correlation spectrometer (model COSPEC V). The COSPEC's output signal was recorded on a Hewlett-Packard 7155B strip chart. Both instruments were powered by a 12 volt car battery.

The principles of correlation spectrometry are well documented (Millan and Hoff, 1978; Millan et al., 1976; Moffat and Millan, 1971; Newcomb and Millan, 1970) and its application to volcanic SO_2 emission studies is well established (Malinconico, 1987; Stoiber et al., 1983). Therefore only a brief review of COSPEC theory and operation is necessary.

The major components of a COSPEC are the telescope, grating and correlator, and circuitry (Figure 6).

Figure 6. Internal Configuration of the COSPEC. Figure 6 is not drawn to scale and is modified from Stoiber et al., 1983.

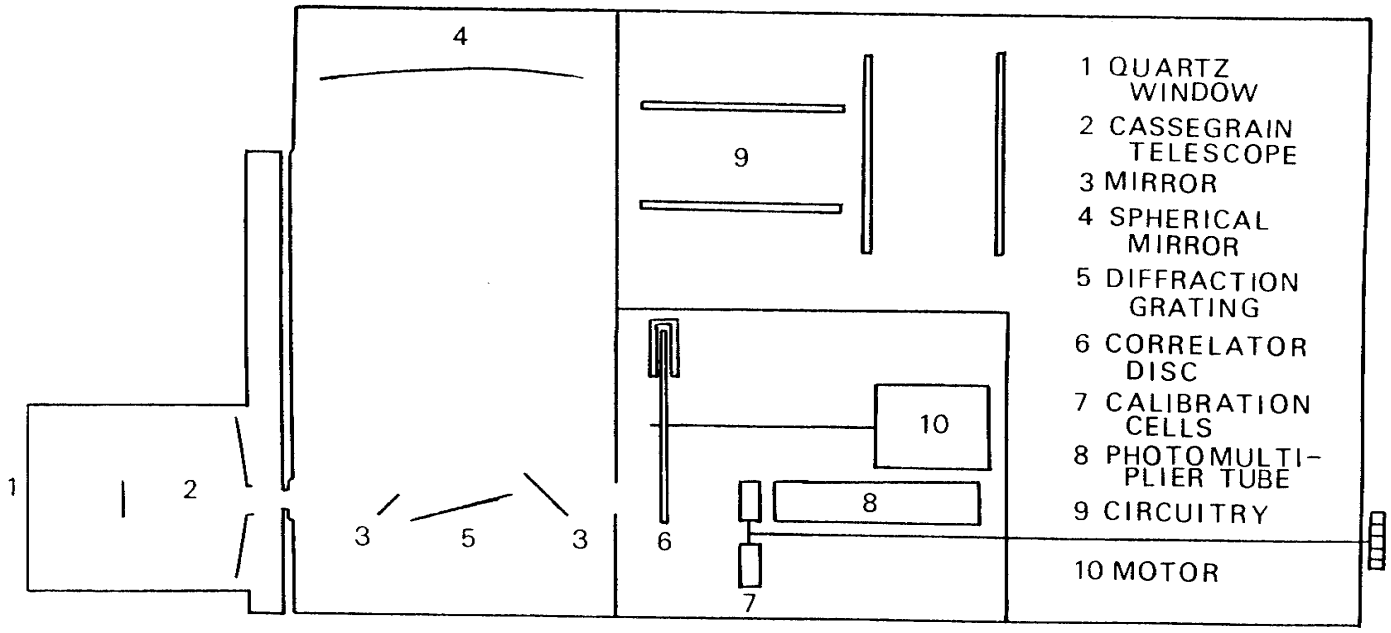
4
9
1
2
3
5
3
6
10
8
7
1 QUARTZ WINDOW
2 CASSEGRAIN TELESCOPE
3 MIRROR
4 SPHERICAL MIRROR
5 DIFFRACTION GRATING
6 CORRELATOR DISC
7 CALIBRATION CELLS
8 PHOTOMULTI-PLIER TUBE
9 CIRCUITRY
10 MOTOR

The Cassegrain telescope has a field of view of 10 by 30 milliradians which collects and focuses incoming light. The diffraction grating separates ultraviolet wavelengths which are sensitive to absorption only by SO_2. The correlator disc creates a high resolution reference spectrum which is electronically converted to determine the amount of SO_2 present in the light path. The circuitry consists of a photomultiplier tube and other electronics. The photomultiplier tube senses the amount of incoming light and converts it to an electronic signal proportional to the SO_2 concentration multiplied by the distance to the SO_2 source. The electronics amplifies the signal and sends it to the strip chart. Internal signal calibration is achieved by inserting cells of known SO_2 concentration and pathlength into the incoming light path. Short term variations in the solar radiation source are minimized by signal calibrations performed before and after each measurement. Long term variations in the solar radiation source are corrected by an internal automatic gain control.

Both stationary and automobile-mounted techniques were employed with the COSPEC for SO_2 monitoring (Stoiber et al., 1983; Millan et al., 1976). The stationary technique involved tripod mounting of the COSPEC and rotating it to scan the volcanic plume at a constant rate. The rotation through the plume was horizontal when measuring a vertically rising plume and vertical when measuring a horizontally

moving plume (Figure 7). The automobile-mounted technique involved mounting a mirror at 45^0 to the telescope so that the COSPEC's field of view was vertical. The vehicle was then driven beneath the horizontally moving plume on roads as near to the summit as possible. With this technique, data corrections were made for varying vehicle speeds and for road segments which were not perpendicular to the wind-driven plume trace.

The stationary technique was preferred over the automobile-mounted technique because it allowed SO_2 monitoring on the Etnean summit. Summit monitoring (1 kilometer from vent) allowed for measurements of a plume which had yet to dissipate. During summit SO_2 monitoring, wind speeds did not exceed 3.5 meters per second and blew constantly from northwest to southeast. Additionally, summit monitoring allowed for visual observation of the plume as it was measured. Suitable roads were unavailable on the summit for automobile techniques. Also, automobile techniques do not allow for simultaneous plume observation during measurements and are subject to more errors as discussed below. However, automobile techniques were necessary when summit monitoring was impossible due to high wind velocities which caused the plume to move along the ground. These high winds were not detrimental to automobile-mounted measurements.

SO_2 fluxes were calculated from the strip chart data, wind speed, and plume width (Chartier, 1986; Stoiber et al.,

Figure 7. Relative Position of COSPEC and Plume During Stationary SO_2 Monitoring. Figure 7 is not drawn to scale.

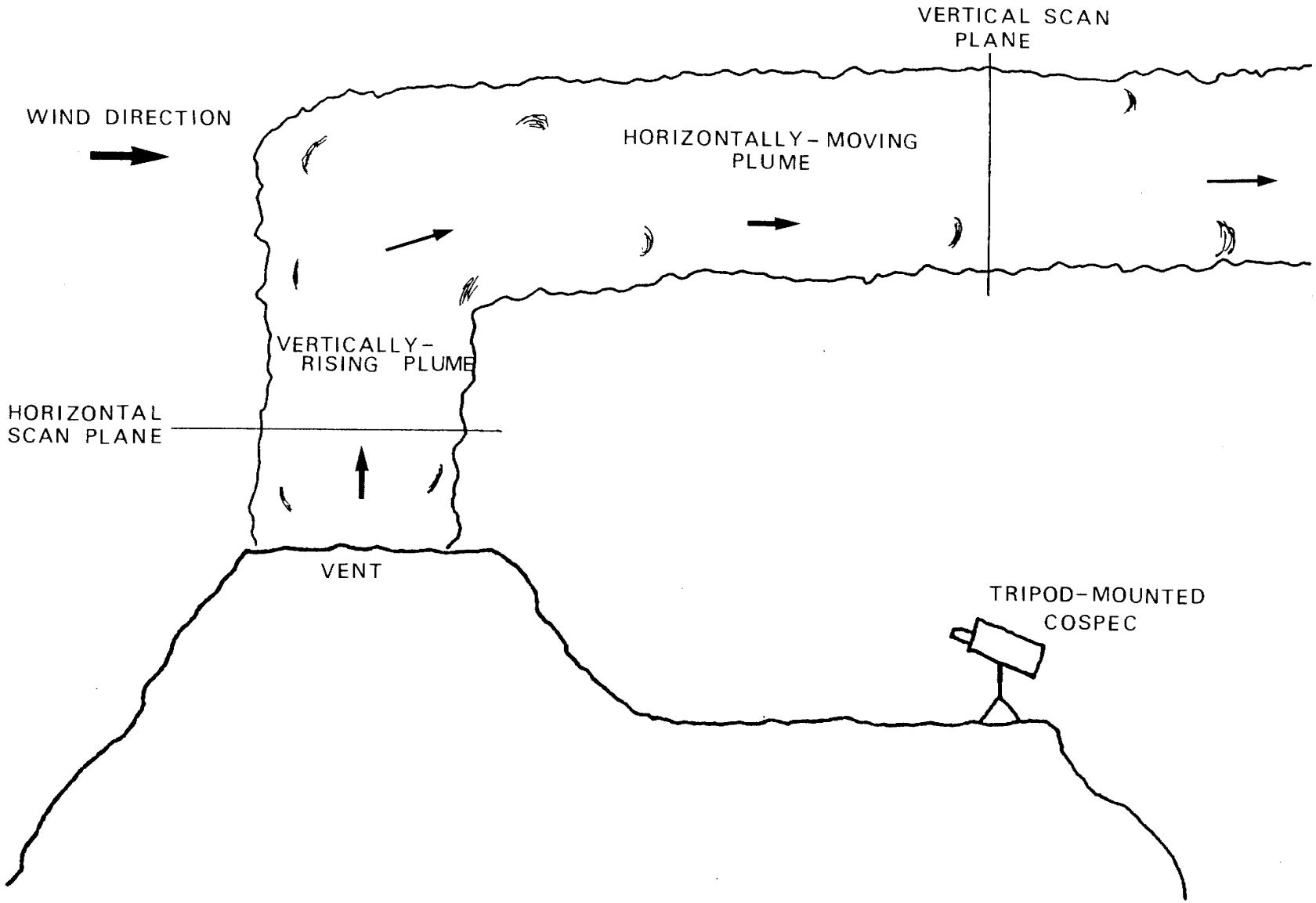
VERTICAL SCAN PLANE
WIND DIRECTION
HORIZONTALLY-MOVING PLUME
VERTICALLY-RISING PLUME
HORIZONTAL SCAN PLANE
VENT
TRIPOD-MOUNTED COSPEC

1983; Millan et al., 1976). The area beneath the recorded curve on strip chart data was determined by hand. Wind speeds were measured with a hand-held anemometer (Davis Instruments Turbometer Wind Speed Indicator) or calculated on a visually-tracked plume. Wind speed was replaced by plume rise rate when no wind was present and the plume rose vertically. Plume width was calculated from the recorded data, scan rate, and the distance to the plume.

Errors associated with stationary COSPEC measurements stem from inaccurate measurement of wind speed or plume rise rate, estimation of the distance to the plume from the monitoring site, scan rate, and data reduction procedures. Agreement between the anemometer and trigonometrically-determined wind speeds on horizontal plumes was excellent. Wind speed error associated with horizontal or vertical plumes is estimated to be 10 percent. Errors associated with scan rates and distances to the plume are believed to be less than 5 percent each. Data reduction errors are estimated to be less than 1 percent. Total error associated with SO_2 measurements is $\pm$ 12 percent (Table 4).

Errors associated with automobile-mounted COSPEC measurements are similar to errors associated with stationary COSPEC measurements. An additional source of error possible with the automobile technique is the loss of portions of the plume due to gravitational settling. This mechanism of plume loss will be discussed in more detail

Table 4. Estimated error percentages associated with COSPEC data collection and results.

Source of Error	Estimated Error (%)
Wind speed	10
Scan rate	5
Distance to plume	5
Data Reduction	1
TOTAL ERROR*	12

* Calculated from the square root of the sum of the squares of the individual sources of error.

==========

later. The occurrence of plume loss is undetectable at the distances used during automobile-mounted COSPEC measurements. Loss of portions of the plume can result in decreased flux measurements when the separated plume is not traversed, or can result in increased flux measurements when the traverse crosses ponded SO_2. Another error associated with plume separation and the automobile technique is the differing velocities of the SO_2 in the visible and separated plumes. Separated plume velocity is a function of the ground slope. However this velocity was not determined and visible plume velocities were used to calculate SO_2 fluxes. If the separated SO_2 plume moves at 1 to 2 meters per second, than a maximum of an additional 50 percent error exists in the 15 July 1987 SO_2 fluxes (the other automobile-collected fluxes used wind speeds of 1 to 2 meters per second).

Typically, measurements of volcanic SO_2 fluxes vary greatly. This variation is not a result of experimental

error, but represents the natural fluctuations of SO_2 emissions over time (Malinconico, 1987; Stoiber et al., 1983).

COSPEC measurements are known to underestimate SO_2 emissions due to the nature of the experimental conditions. Measured SO_2 fluxes are reduced by increasing plume opacity caused by entrained volcanic ash and water vapor; loss of portions of the plume due to wind currents; increasing distance of the COSPEC from the plume; and loss of SO_2 from the plume through oxidation and deposition processes (Malinconico, 1987; Rose et al., 1985; Williams et al., 1981; Malinconico, 1979; Moffat and Millán, 1971). However, reductions due to plume opacity are considered negligible during this study because ash-rich plumes were not observed, and very opaque plumes resulting from co-escaping water were not measured. Likewise, no measurements were made on plumes noticeably divided by wind currents. SO_2 flux reductions due to the distance between the COSPEC and the plume are believed negligible since distance limits discussed by Rose et al. (1985) were not approached. Oxidation and deposition processes were not quantitatively determined but are assumed to be negligible over the short distances involved in the SO_2 measurements.

Particle Measurements

A four stage, quartz crystal microbalance cascade impactor (QCM) was used to obtain particle information from

the plumes of the active Etnean craters. The QCM has been previously used for aerosol sampling at other volcanoes (Casadevall et al., 1984; Chuan et al., 1981; Rose et al., 1980; Cadle et al., 1979).

The QCM (Figure 8) pumps air through a series of stages (Marple and Willeke, 1976). Each stage contains electronic circuitry, and two vibrating quartz plates; one plate collects particles while the other provides a reference frequency for the electronic circuitry. The plates are coated with successive layers of chromium, silver, and nickel. Particles are separated by size due to their relative inertia and are retained on the quartz plates by the particles' inherent adhesiveness to the nickel plating. The electronic circuitry detects changes in the resonant frequency of each collecting plate. Frequency changes of a plate are a function of the mass accumulation. Each stage collects a specific size range of particles. From the top to the bottom of the QCM, the four stages collect particles in size ranges of greater than or equal to 2 microns, 2 to 0.9 microns, 0.9 to 0.3 microns, and 0.3 to 0.07 microns. Particles less 0.07 micron in diameter are not collected and pass through the QCM.

Field particle collections were taken by placing the QCM in the wind-driven plume travelling on the ground surface 15 to 20 meters from the vent. Power was provided by a portable, rechargeable, 12 volt battery. Sampling times varied from 2 to 5.5 minutes.

Figure 8. QCM Components and Stage Interior. Only major components are depicted and figure is not drawn to scale.

STAGE INTERIOR

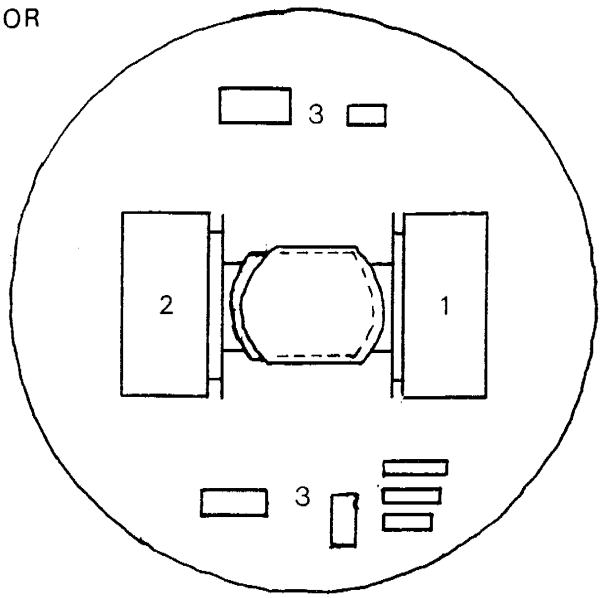

1 COLLECTING PLATE ASSEMBLY

2 REFERENCE PLATE ASSEMBLY

3 OTHER ELECTRONICS

QCM

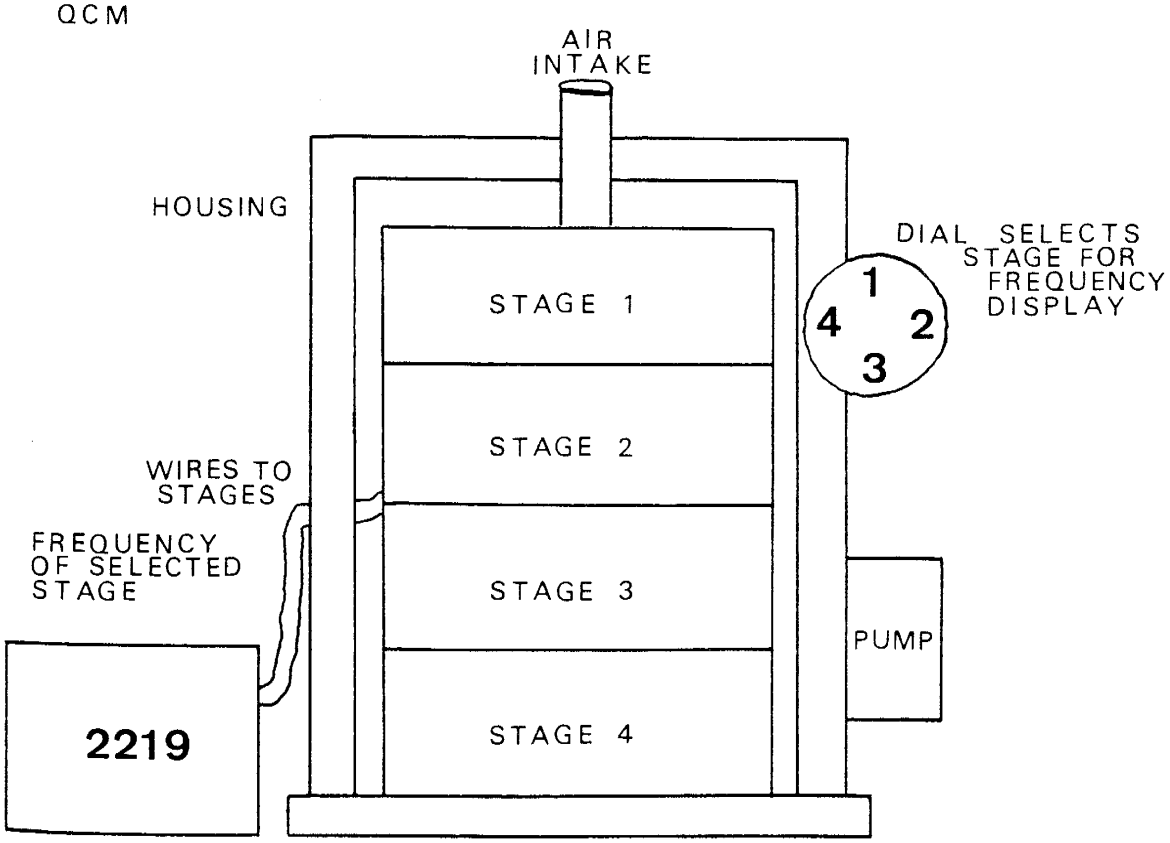

Scanning electron microscope (SEM) analyses of the quartz plates were later performed to constrain particle identities on each stage. Thin silver coatings were applied to the plates making them conductive, this was necessary for SEM imaging. Half of the samples were analyzed on a Kevex ISI-SR-50 SEM with a Kevex Analyst 800 Microanalyzer (Photometrics, Huntingdon Beach, California), the remaining samples were completed on a Hitachi HHS-2R SEM with a Tracor Northern 5400 Analyzer (New Mexico Institute of Mining and Technology, Socorro, New Mexico). Morphological characteristics, mineralogic associations, and semiquantitative chemical analyses provided by energy dispersive x-rays (EDX) were used to help constrain particle compositions.

Errors associated with normal operation of the QCM are negligible. The accuracy of mass distributions calculated is dependent upon the quality of the electronic circuitry. These calculations are assumed to be accurate because of the circuitry's high quality. However, vapors sometimes collected and condensed on the stages during field operation of the QCM. This caused the liquid-soaked stages to electronically malfunction; thus complete mass distributions were not obtained for these samples.

Errors associated with identifying particles are possible, but cannot be assessed. The particle morphologies and compositions suggested by the SEM and EDX data do not

usually give unique solutions to particle identities.

Aerosol Filter Measurements

Particle and gas samples were collected with aerosol filter packs described by Finnegan et al. (1988). Each 47 millimeter diameter pack consisted of one 0.4 micron Nuclepore aerosol filter followed by four ^{7}LiOH-treated Whatman 41 filters. The treated filters retain acidic gases. Volcanic fume was pumped through the filters by a vacuum pump with flow rates monitored by a steel-ball flow-meter attached to the pump's exhaust pipe. Power was provided by a 12 volt car battery.

Three plume samples were collected with separate filter packs which were elevated on a pole 1.5 meters above the ground to be better situated in the volcanic fume. Sampling times ranged from 20 to 38 minutes. Average flow rates during the sampling period varied from 46 to 13.5 liters per minute.

The individual filters were analyzed by instrumental neutron activation analyses (INAA) as described by Finnegan et al. (1988). Details of the INAA sample preparation and analytical procedure were described by Meeker (1988).

Errors in these procedures result from both field and laboratory techniques. Field errors include the varying nature of the plume, filter saturation, and contamination. The volcanic plume was wind-driven and thus the fume admitted to the filters was variable over time with respect

to elemental concentration. Filter saturation can greatly reduce quantitative accuracy. Contamination by non-volcanic, atmospheric, particulate matter during filter replacement was difficult to identify. Contamination from salts and oils on the hands was kept to a minimum by wearing surgical gloves during filter replacement.

Laboratory derived errors include inaccuracy of standards, variable neutron fluxes, and high detector-dead-times for chlorine-rich samples. Errors can also result from improper sample preparation techniques. Analytical errors for various elements range from 1 to 29 percent as estimated by Meeker (personal communication) (Appendix IV).

RESULTS

Volcanic Activity from June to August 1987

Field work on Mount Etna was conducted from June to August 1987. During this time, all visible activity was centered on two of the summit craters, Bocca Nuova and Southeast Crater (Figure 1c). No flank activity was observed.

The Chasm, or La Voragine, is the oldest of the four summit craters. It was approximately 300 meters wide and about 300 meters deep. The walls were nearly vertical and actively caving. The floor was capped with the crust of a lava lake, and a small cinder cone projected through this carapace (V. Scribano, personal communication). Few fumaroles were active along the lightly sulfur-covered walls. A faint odor of SO_2 was present in the low temperature fumaroles (Figure 1c). During this study, no plumes were seen originating from the Chasm.

Northeast Crater opened in 1911 and has had the most explosive history of the summit craters (V. Scribano, personal communication). It was 130 meters in diameter and approximately 100 meters in depth. Its inter-crater slopes were moderate. The floor of the crater was full of volcanic rubble which surrounded three eruptive vents. Fumarole activity was weak, yet a faint smell of SO_2 was present. Fumarole temperatures were generally comparable to the Chasm's fumarole temperatures except for one fissure which

contained 140^{0}C and 300^{0}C vents (Figure 1c). Extremely warm ground was also present on the northern side of the crater. The crater interior was lightly covered with sulfur-rich sublimates, except for the southern wall and immediate vent areas which were heavily blanketed. Only rarely during the course of the fieldwork was a plume seen originating from the Northeast Crater.

Bocca Nuova crater opened in 1968 as a 1 meter diameter pit crater. It was about 260 meters in diameter during the 1987 summer. Its walls were near vertical and caving, including the wall separating Bocca Nuova from the Chasm. The floor was estimated to be 400 meters below the rim (V. Scribano, personal communication). Many fumaroles existed in the crater and in fumarole fields to the south; no temperatures greater than 90^{0}C were measured (Figure 1c). The walls of Bocca Nuova had traces of sulfur deposition. Strombolian eruptions occurred on the floor of the crater, but ash or bombs from these eruptions were not observed. The eruptions were of varying audible intensity and duration. Repose times between eruptions ranged from 9 to 339 seconds with no apparent periodicity (Appendix I, Figure 9). Bocca Nuova emitted a constant plume.

Southeast Crater first formed in 1978 and in 1987 its active vent was about 35 meters in diameter and located on the northern edge of the crater. Since formation, the active vent has continually eroded its northwestern wall. Due to periodic ponding of lava in the crater during flow

Figure 9. Repose Times Between Eruptions of Bocca Nuova.

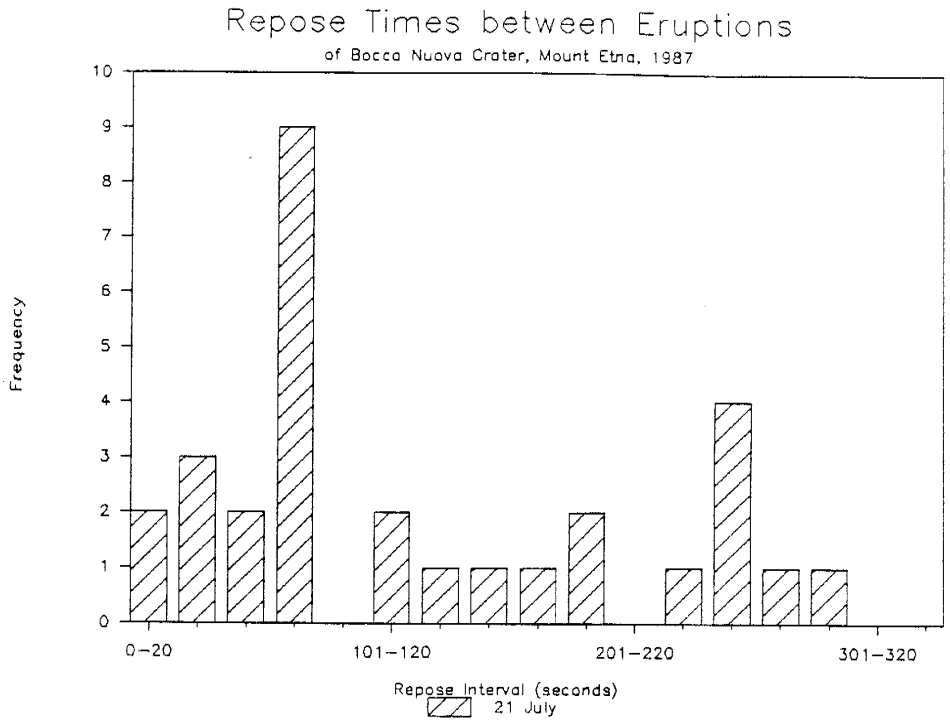
Repose Times between Eruptions
of Bocca Nuova Crater, Mount Etna, 1987
Frequency
10
9
8
7
6
5
4
3
2
1
0
0–20
101–120
201–220
301–320
Repose Interval (seconds)
21 July

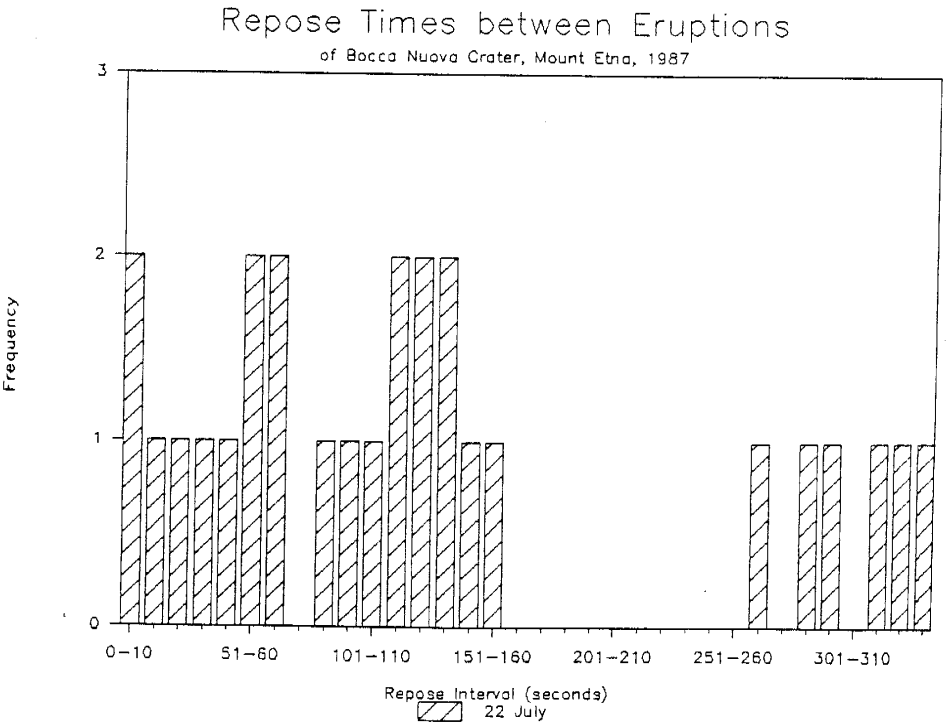
Repose Times between Eruptions
of Bocca Nuova Crater, Mount Etna, 1987
Frequency
3
2
1
0
0–10
51–60
101–110
151–160
201–210
251–260
301–310
Repose Interval (seconds)
22 July

events, the southwestern wall has solidified keeping the vent size relatively constant as the crater enlarged northwestward (Figure 10, V. Scribano, personal communication). Vent walls were near vertical, while crater walls had a more gentle slope due to the solidified ponded lava (Figure 10). The crater floor was strewn with cracked, lava lake crust and push ups, while the vent floor could not be observed. Several large fissures were located north of the vent. Two new collapse pits, each 5 meters deep, formed northeast of the vent during fieldwork activities. Very few, permanent fumaroles existed in the crater; a few fumaroles existed atop the 31 October 1986 flow (V. Scribano, personal communication, Figure 10). Temperatures measured in permanent fumaroles ranged from 85^{0}C to 131^{0}C. A dry vent atop the October 1986 flow measured 417^{0}C (Figure 1c). Sulfur deposition was minor in the crater, but thickened in the immediate vent area. The vent constantly emitted gas, as well as stronger, periodic discrete gas bursts. Individual gas bursts were of varying intensity and duration (0 to 2 seconds). Repose periods between bursts were from 1 to 101 seconds with no apparent periodicity (Appendix I) (Figure 11). Ash and incandescent particles were rarely seen to erupt from the vent. The vent showed no incandescence during the day, but each night the vent glowed red with differing intensities. Southeast Crater emitted a pulsating plume.

Figure 10. Views of Southeast Crater. The periodic ponding of lava in the crater has maintained a constant vent diameter despite the vent's erosion of the northern crater wall. The ponded lava also produces less steep walls than the eroded northern wall. Figure 10 is not drawn to scale.

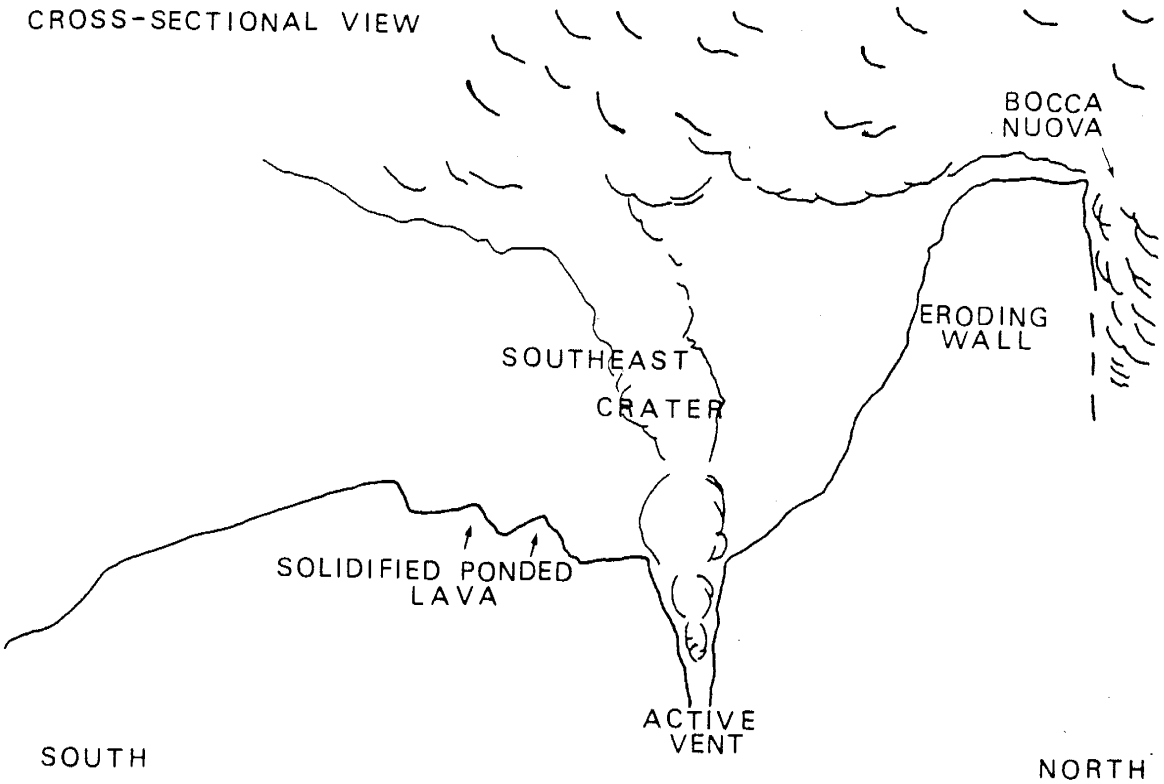
CROSS-SECTIONAL VIEW
BOCCA NUOVA
ERODING WALL
SOUTHEAST CRATER
SOLIDIFIED PONDED LAVA
ACTIVE VENT
SOUTH
NORTH

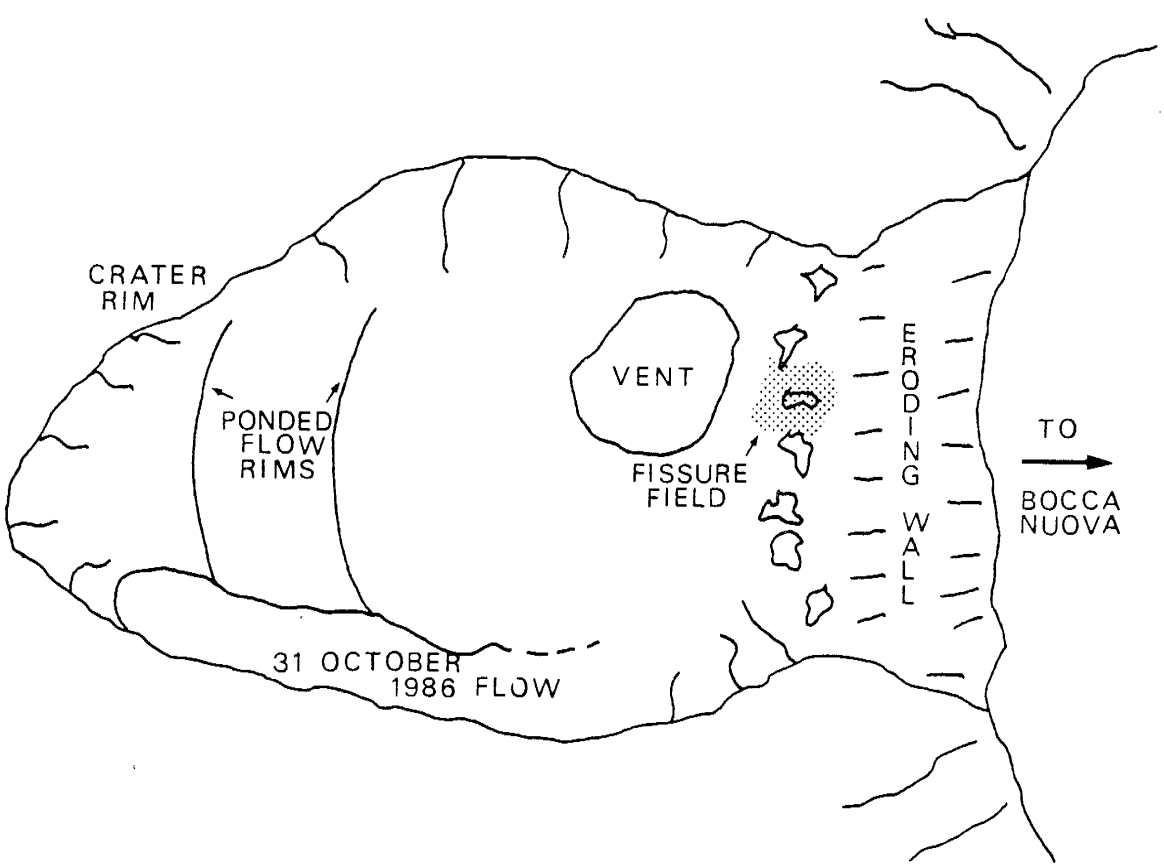
PLAN VIEW
CRATER RIM
PONDED FLOW RIMS
VENT
FISSURE FIELD
ERODING WALL
TO
BOCCA NUOVA
31 OCTOBER 1986 FLOW

Figure 11. Repose Times Between Degassing Bursts of Southeast Crater.

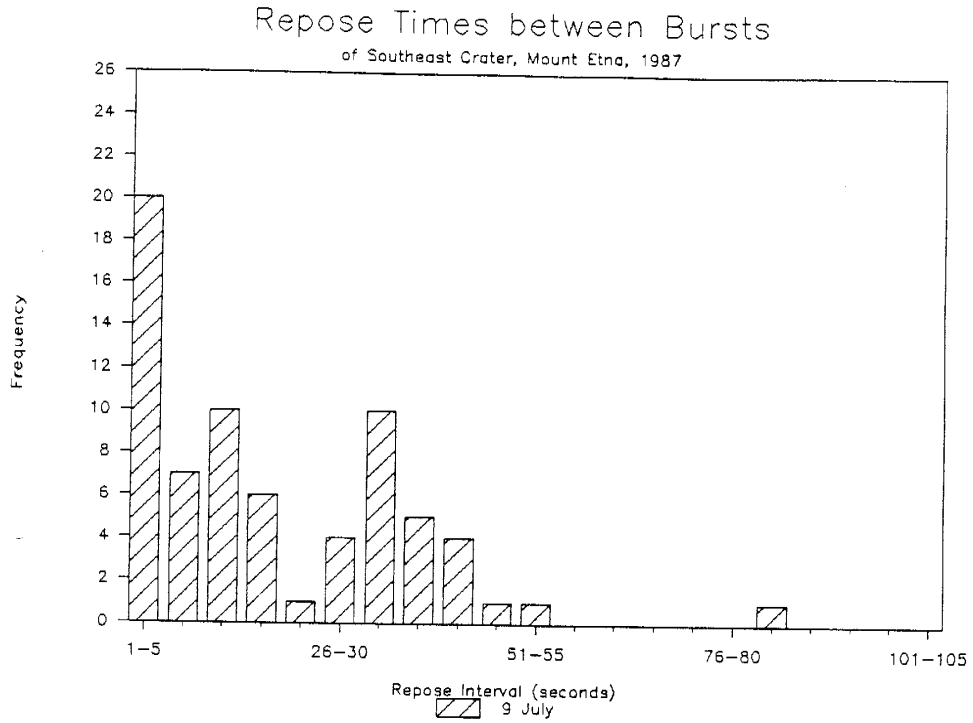
Repose Times between Bursts
of Southeast Crater, Mount Etna, 1987
Frequency
26
24
22
20
18
16
14
12
10
8
6
4
2
0
1–5
26–30
51–55
76–80
101–105
Repose Interval (seconds)
9 July

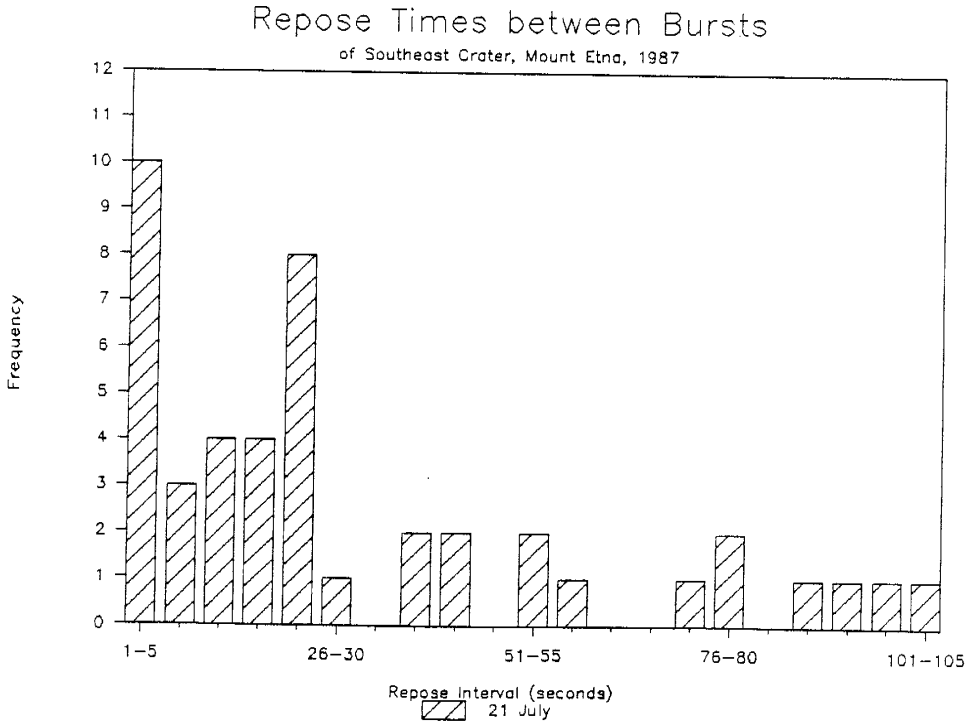
Repose Times between Bursts
of Southeast Crater, Mount Etna, 1987
Frequency
12
11
10
9
8
7
6
5
4
3
2
1
0
1–5
26–30
51–55
76–80
101–105
Repose Interval (seconds)
21 July

SO_2 Fluxes

SO_2 fluxes were measured with tripod-mounted and automobile-mounted techniques on 12 days throughout the study period. The number of determinations per day varied from 2 to 48 and reveal SO_2 fluxes from 117 to 6534 tonnes per day.

The individual contributions of the SO_2 plumes from Bocca Nuova and Southeast Crater to the total SO_2 flux were measured on 19, 20, and 22 July 1987 (Table 5) (Appendix II). On these days, the individual emissions of the two craters could be determined because of the close proximity of the tripod-mounted COSPEC to the craters and the existence of low-velocity winds. The low-velocity winds allowed for each crater's plume to rise individually and be measured separately before the plumes coalesced. Bocca Nuova emitted SO_2 fluxes ranging from 277 to 3898 (average equaled 1166) tonnes per day; Southeast Crater emitted 165 to 5229 (average equaled 625) tonnes per day. While Bocca Nuova emitted the greater average flux, Southeast Crater SO_2 emissions showed greater range.

SO_2 flux data for the entire Mount Etna system, and the collection technique used daily are summarized in Table 6. These fluxes were measured on coalesced crater plumes or individual crater plumes which were later summed. The average SO_2 flux is 1056.17 ± 1842.74 tonnes per day with a range of 117 to 6534 tonnes per day (Figure 12) (Appendix

Table 5. SO_2 flux data for Bocca Nuova and Southeast Craters. All fluxes are reported in tonnes per day; standard deviation is computed at 95% confidence interval (2σ). Table 5 is compiled from data in Appendix II.

Date	Number of Runs	Minimum Flux	Maximum Flux	Average Flux	$\pm 2\sigma$
Bocca Nuova					
19 July 87	19	392.65	3898.33	1590.06	2188.45
20 July 87	44	277.60	1751.03	999.81	725.78
22 July 87	1	433.99	433.99	433.99	0.00
TOTAL	64	277.60	3898.33	1166.20	2903.08
Southeast Crater					
19 July 87	9	427.47	5229.31	1528.25	2727.00
20 July 87	39	165.33	771.49	427.56	336.41
22 July 87	1	217.02	217.02	217.02	0.00
TOTAL	49	165.33	5229.31	625.43	2961.80

Table 6. Summary of Mount Etna sulfur dioxide flux data. All fluxes are reported in tonnes/day; standard deviation computed to 95% confidence interval (2σ); scan types abbreviated A for automobile-mounted COSPEC, H for tripod-mounted COSPEC with horizontal scans, and V for tripod-mounted COSPEC with vertical scans. Two sets of data are reported for 27 June (see Appendix III). Table 6 is compiled from data in Appendix III.

Date	Scan Type	Number of runs	Minimum Flux	Maximum Flux	Average Flux	$\pm 2\sigma$
27 June 87	A	2	176.09	273.98	225.04	97.89
27 June 87	A	5	531.21	917.06	731.37	311.42
3 July 87	H	8	177.90	621.84	371.49	264.65
4 July 87	H	15	250.10	494.51	346.52	136.77
12 July 87	A	2	1015.09	1362.63	1188.86	347.54
13 July 87	H	7	117.93	343.34	186.53	152.29
14 July 87	A	3	556.16	751.47	681.62	177.81
15 July 87	A	3	859.26	1247.25	1010.53	339.06
16 July 87	A	5	391.53	684.66	516.89	208.46
19 July 87	H	9	1490.60	6534.77	3195.56	3460.06
20 July 87	H	48	598.72	2387.29	1411.47	852.33
22 July 87	H	5	651.01	1026.95	772.70	264.68
29 July 87	V	14	384.49	859.46	648.74	250.13
TOTAL		126	117.93	6534.77	1056.17	1842.74

Figure 12. Average SO_2 Fluxes Obtained Throughout This Study. The range of fluxes for each day is shown by the shaded area.

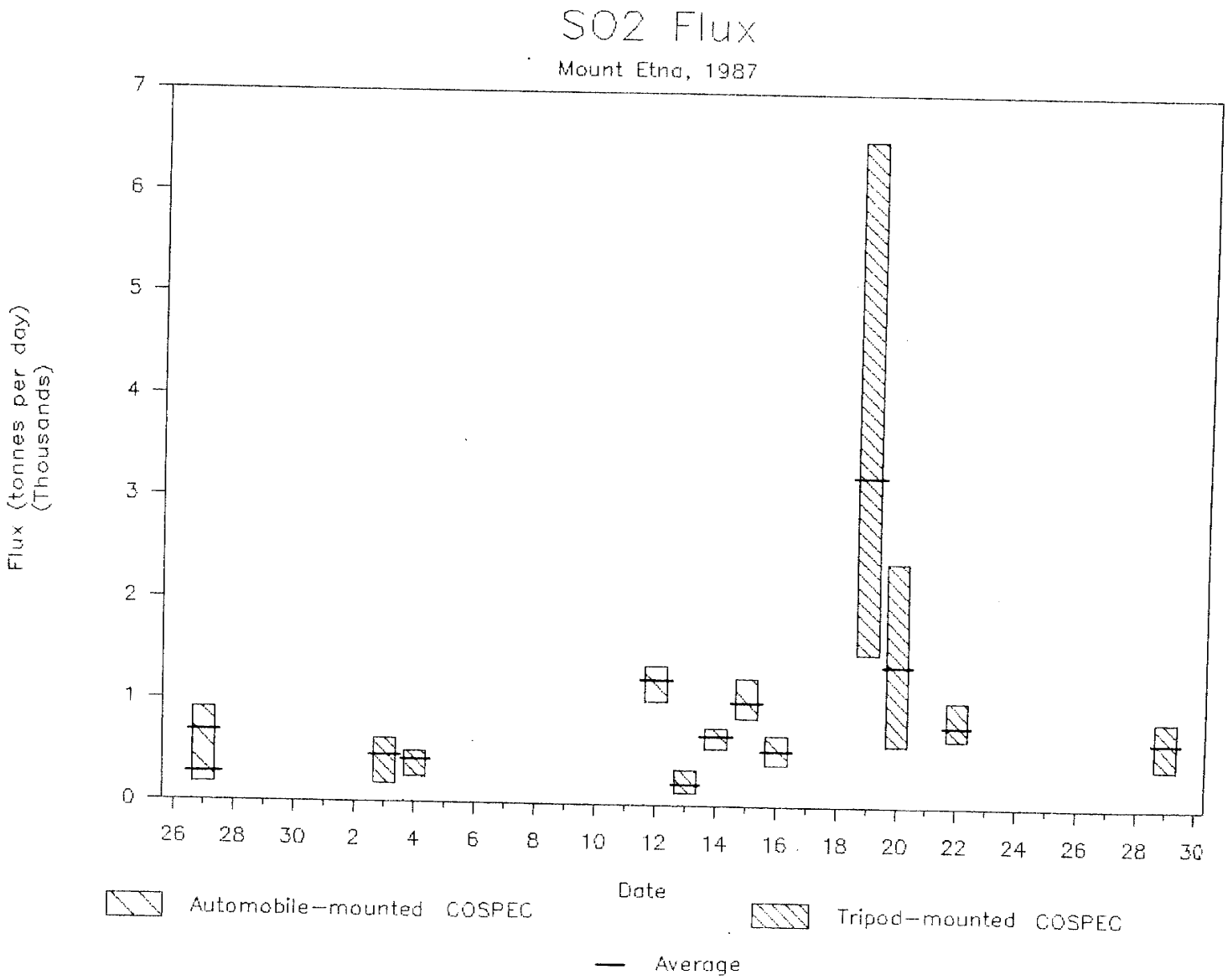
SO2 Flux
Mount Etna, 1987
Flux (tonnes per day)
(Thousands)
0
1
2
3
4
5
6
7
26
28
30
2
4
6
8
10
12
14
16
18
20
22
24
26
28
30
Date
Automobile-mounted COSPEC
Tripod-mounted COSPEC
Average

III).

The lower of the two SO_2 fluxes determined on 27 June does not fall within the 1σ range of the average system flux (Table 6). This low value corresponds to the only data taken on a road 16 to 24 kilometers from the summit vents; all of the other automobile COSPEC fluxes were taken on roads 10 to 16 kilometers from the summit vents. Both moving SO_2 plume and previously separated, ponded SO_2 were traversed during the low 27 June flux determination. The dissipated ends of the moving SO_2 plume overlapped the stagnated SO_2. The strip chart record does not distinguish between the ponded and moving SO_2. Portions of the strip chart record which contained both moving and stagnated SO_2, or only stagnated SO_2, were not included in the reported flux values. The lack of measurement of the dissipated ends of the moving SO_2 plume could be the cause of the lowest reported SO_2 fluxes.

SO_2 data taken with a tripod-mounted COSPEC show no significant variations between horizontal and vertical scans (Table 6). Fluxes measured on 19 July are significantly higher than the other tripod COSPEC data, and will be discussed later. Recalculating the statistics in Table 6 without the data for 19 July gives an average SO_2 flux of 891.60 tonnes per day (2σ equals 1104.24).

In comparison to other volcanic systems, Mount Etna is not unusual in the magnitude of its SO_2 flux. Measured,

volcanic SO_2 fluxes from various volcanoes range from tens to more than ten thousand tonnes per day. Volcanic eruptions with similar SO_2 fluxes to those measured at Mount Etna include Mount Saint Helens shortly after the large 18 May 1980 eruption (1500 to 880 tonnes per day, July to October 1980) (Casadevall et al., 1981) and the East Rift Zone eruption of Kilauea Volcano, Hawaii (1170 tonnes per day, October to November, 1986) (Andres et al., in prep.).

Particle Size Distributions and Compositions

Four QCM samples for particle analyses were collected from the summit vents. Particle size distributions are in Table 7 and Figure 13. Liquid-soaked stages are labelled but were not considered in mass fraction calculations.

Bocca Nuova's particle size distribution (Table 7) show that 58 percent of the particles collected are greater than 2 microns and 34 percent are less than 0.3 microns. No estimate was made of stage 2 (2 to 0.9 microns). In contrast, Southeast Crater data show that the majority of the particles were less than 2 microns in diameter.

Southeast Crater's particle size distributions are relatively similar to each other in all but the largest size fractions. SEM micrographs show abundant particles and liquid droplets collected on the first sampling stage of the QCM (Figure 14). The difference in size distributions can be attributed to the inhomogeneous plume and different sampling times. The longer sampling time allowed for the

Table 7. Particle size distributions determined with the QCM. Sample times are reported in minutes and mass concentrations are given in micrograms per cubic meter with the mass percentages following in parentheses. All samples were collected on 26 June 1987.

sample	time	Mass concentrations Stage 1 ≥2 μ	Stage 2 2 - 0.9 μ	Stage 3 0.9 - 0.3 μ	Stage 4 0.3 - 0.07 μ
Bocca Nuova #1	2	490.82 (58.4)	lss	67.16 (7.9)	282.21 (33.5)
Bocca Nuova #2	2.5	lss	lss	181.34	lss
Southeast Crater #1	5.5	216.24 (41.2)	107.44 (20.5)	18.00 (3.4)	183.58 (35.0)
Southeast Crater #2	3	74.83 (17.6)	124.70 (29.3)	33.69 (7.9)	192.89 (45.3)

lss = liquid-soaked stage

Figure 13. Cumulative Mass Concentrations Collected Per Stage of the QCM.

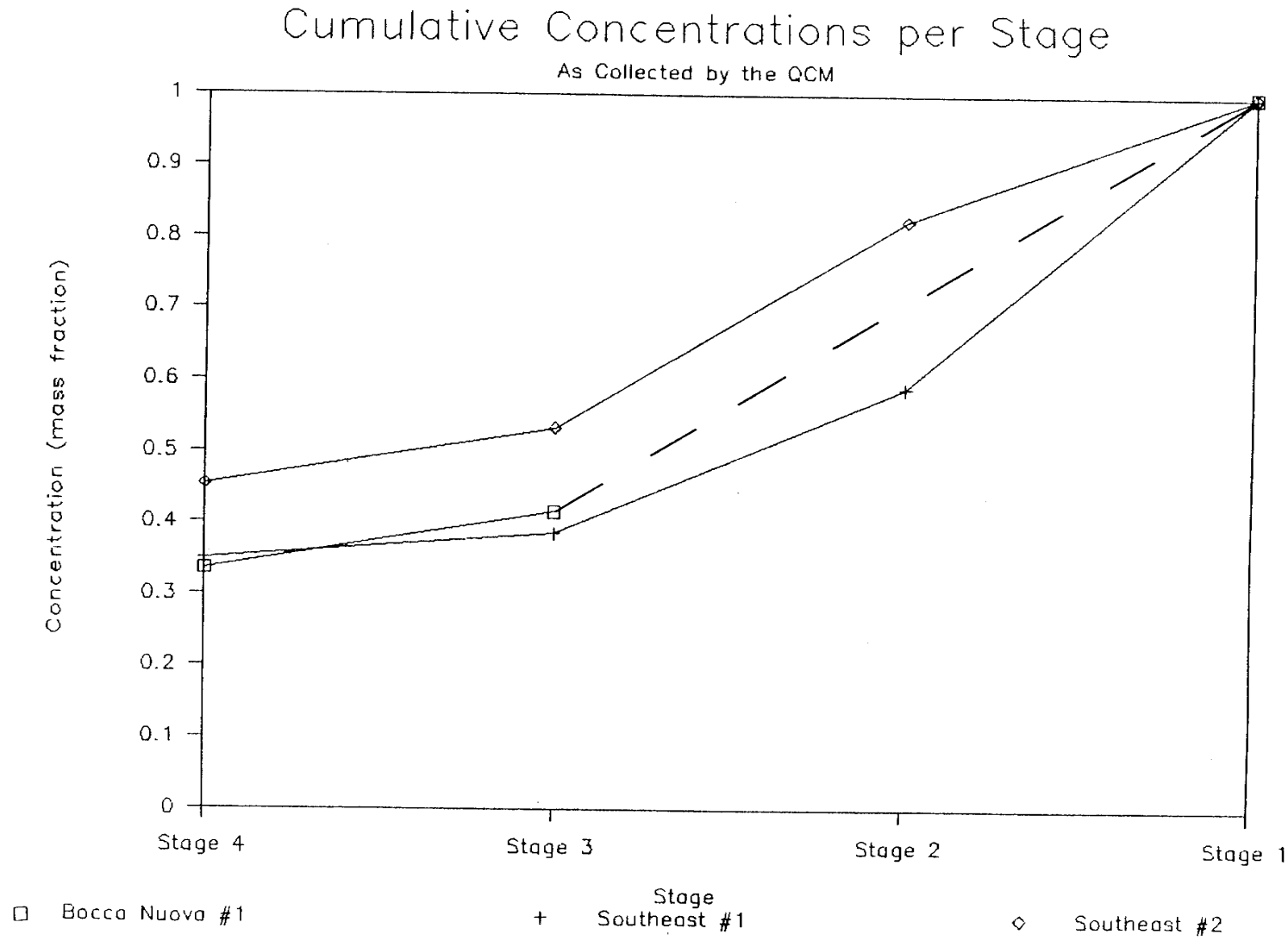
Cumulative Concentrations per Stage
As Collected by the QCM
Concentration (mass fraction)
1
0.9
0.8
0.7
0.6
0.5
0.4
0.3
0.2
0.1
0
Stage 4
Stage 3
Stage 2
Stage 1
Stage
Bocca Nuova #1
Southeast #1
Southeast #2

Figure 14. Particles and Liquid Droplets Collected on Stage 1 of the QCM. The heading to the micrographs list sample number, site, crater, and QCM stage from left to right. The footers to the micrographs list the accelerating voltage, magnification, scale in microns, and micrograph number from left to right.

A. Micrograph 273-1 shows a complex silicate covered with a dust composed of potassium and sulfur.

B. Micrograph 273-2 shows dried liquid droplets.

C. Micrograph 273-3 is an enlargement of 273-2 and shows both particles and dried liquid droplets on the first stage.

A

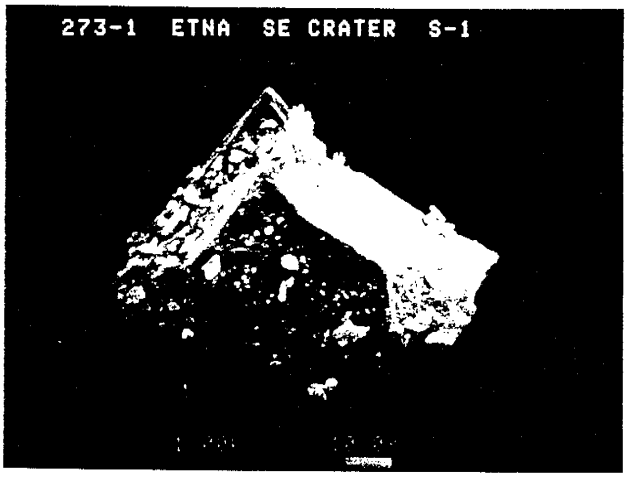

B

C

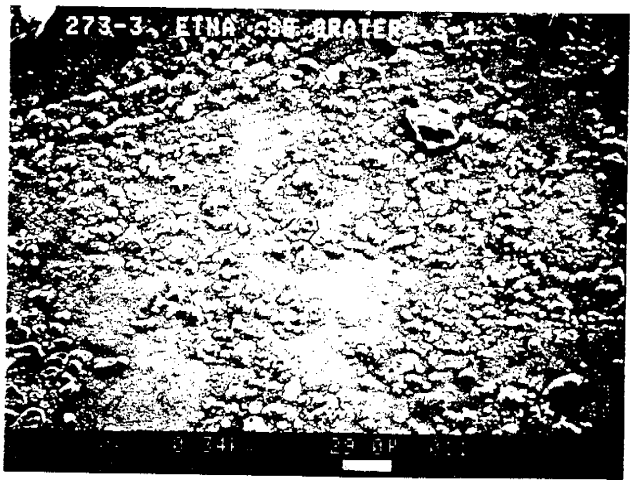

collection of unusually large particles or of liquid droplets on the first stage which skewed the mass distribution of the first Southeast Crater sample.

SEM micrographs reveal that while the largest particles were collected on stage 1, the lower stages collected smaller, single particles or particle aggregates (Figure 15). These aggregate particles are commonly composed of materials found singly on lower stages or as light dustings on larger particles (Figure 14, micrograph 273-1).

Results of EDX determinations of particles are in Table 8. Products of secondary reactions were not included in this data set. These secondary reactions included acid reactions with the thin nickel and silver platings on the stages, and possible contamination by metal shavings of unknown origin.

Suggested particle identifications (Table 8) include common phenocryst phases of the Etnean lavas such as plagioclase and pyroxenes. Other species tentatively identified include silica, chemically more complex silicates, various chlorates and chlorides, and potassium sulfites and sulfides. Most of these species have been previously identified at Mount Etna (Varekamp et al., 1986; Buat-Ménard and Arnold, 1978). The chemical compositions suggested are speculative since the methods used to identify the particles do not usually give unique solutions.

Particle chemical compositions vary with their size and

Figure 15. Particle Aggregates.

A. Micrograph 273-17 shows agglomerated silica crystals with minor amounts of an unidentified silicate.

B. Micrograph 273-37 shows intergrown potassium-sulfur crystals.

A

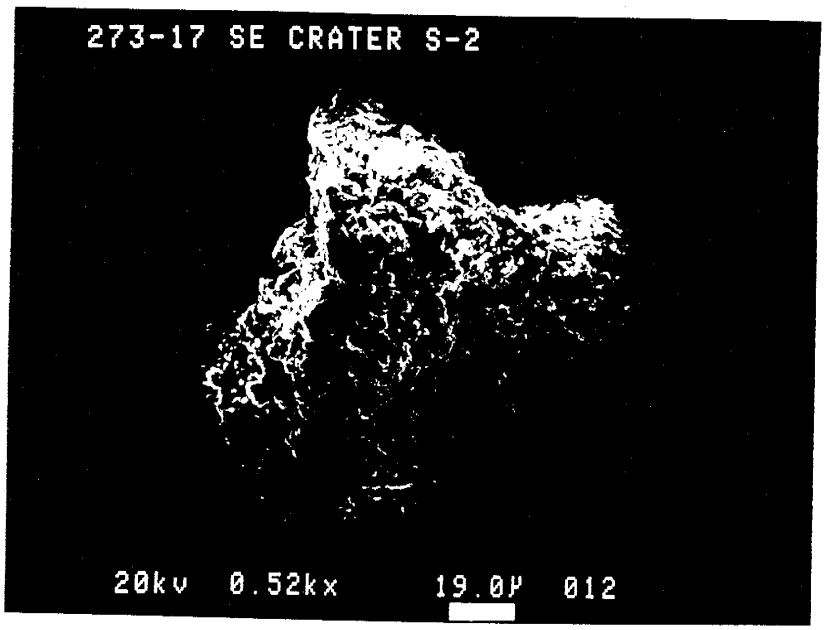
273-17 SE CRATER S-2
20kv 0.52kx 19.0µ 012

B


273-37 BOCCA NUOVA S-2
20kv 1.3kx 7.70µ 004

Table 8. Elemental summary of SEM data and suggested identifications. # refers to SEM image number (without 273-). Elements are symbolized in the top row. The identifications are suggested only and are not definite. A key for the identifications follows this table.

#	Na	Mg	Al	Si	S	Cl	K	Ca	Ti	Fe	Identification
Bocca Nuova											
Stage 1											
39	y	y	y	yy	y		y	y		y	sil; c sil; $K_2S_2O_4$
40	y		y	y	yy		y	y		y	c sil, $K_2S_2O_4$
108	y				yy		y				ind Na, S
109				y	yy						S d on ind Na, K, S
Stage 2											S on sil;
8					yy		yy				$K_2S_2O_4$
9					yy		yy				$K_2S_2O_4$
37	y				yy		yy				$K_2S_2O_4$
110				y	yy		yy				$K_2S_2O_4$; ind Na, S
Stage 3											$K_2S_2O_7$; sil
chemically identical to Stage 2 and Stage 3, particle sizes intermediate											
Stage 4											
10					yy		yy				$K_2S_2O_4$
111				yy	yy		y				sil; $K_2S_2O_4$; sa

#	Na	Mg	Al	Si	S	Cl	K	Ca	Ti	Fe	Identification
Southeast											
Stage 1											
1			y	yy	y		y	y		y	augite; $K_2S_2O_4$
2				yy	y	yy					$SiSCl_2$
22			y	yy	y	y	y	y	y	y	sil; KCl; KS d
24			y	yy	y	yy		y	y	y	dried elemental slurry
29		yy		yy							$MgSiO_3$; sil
Stage 2											
17			y	yy			y	y	y	y	sil
18		y	y	yy	y		y	y		y	sil; c sil; $MgSO_4$; KS d
20	y		y	yy	y		y	y	y	y	KS d; plg; sil
21	y		y	yy	yy		y	y		y	sa; w/o Mg, Ti
31					yy		yy				am KS d
32	y				yy		y				ind Na, K, S
33	y		yy	yy	yy		y	y		y	c sil
102				yy	y		y				$K_2S_2O_4$, sil
Stage 3											
14					y	y	y				$KClO_4$; ind K, S
104	y			y		yy					NaCl
Stage 4											
4				y	y	yy	y				$KClO_3$; indl $SiSCl_2$
6				y	y	yy	yy				ind Si, S, K, Cl
11	y				yy	y	yy				$NaClO_4$; ind K, S
12	y			y	yy	yy	yy				sa; ind K, S, Cl, Na, Si
105						y	y				sil
106	y			y		yy	y				NaCl; KCl

Key

am	amorphous
c sil	complex silicate
d	dust
ind	indeterminable composition with SEM-EDX (elements given when appropriate)
indl	ind, but likely ...
KS d	indeterminable KS (likely $K_2S_2O_4$)
plg	plagioclase
sil	silica (usually with other elements in trace amounts)
sa	stage average (average composition for all particles on stage)
w/o	sa without elements ...
y	element identified by EDX
yy	element very abundant as determined by EDX

eruptive source. The greater than 2 micron sized particles of Bocca Nuova appear to be silica and more complex silicates (Figure 16). The chemical analyses and morphological characteristics of the smaller particles on stages 2 through 4 suggest that many are potassium metasulfite platelets with trace amounts of silica and an unidentified sodium-sulfur compound (Figure 17).

Southeast Crater's particle chemistry is more complex than that of Bocca Nuova. Particles from stage 1 probably consist of silica and complex silicates with trace amounts of potassium metasulfite, potassium chloride (sylvite), and an unidentified potassium-sulfur dust. Stage 2 silicates are chemically similar to Stage 1, but particle sizes are smaller and aggregates are more prevalent. Potassium-sulfur dusts are more abundant on stage 2 than on stage 1 and chlorine is strikingly absent. Stages 3 and 4 lack silicates, but the chemistry and morphology of the particles suggest potassium chlorates and perchlorates, sodium chlorides and perchlorates, and unidentified potassium-sodium-chlorine-sulfur dusts are common.

Evidence for liquids and aerosol mists entering the QCM during sampling can be seen in the micrographs. This evidence includes cracked crusts, solution pits, and delicate crystal forms (Figures 18 and 19).

The detection of chlorine in the particles appears to be linked to the original presence of liquids and aerosols.

Figure 16. Greater Than 2 Micron-sized Particles of Bocca Nuova.

A. Micrograph 273-39 shows agglomerated silica crystals covered with smaller crystals of a complex silicate and a potassium-sulfur compound.

B. Micrograph 273-40 shows a complex silicate with smaller crystals of a potassium-sulfur compound.

A

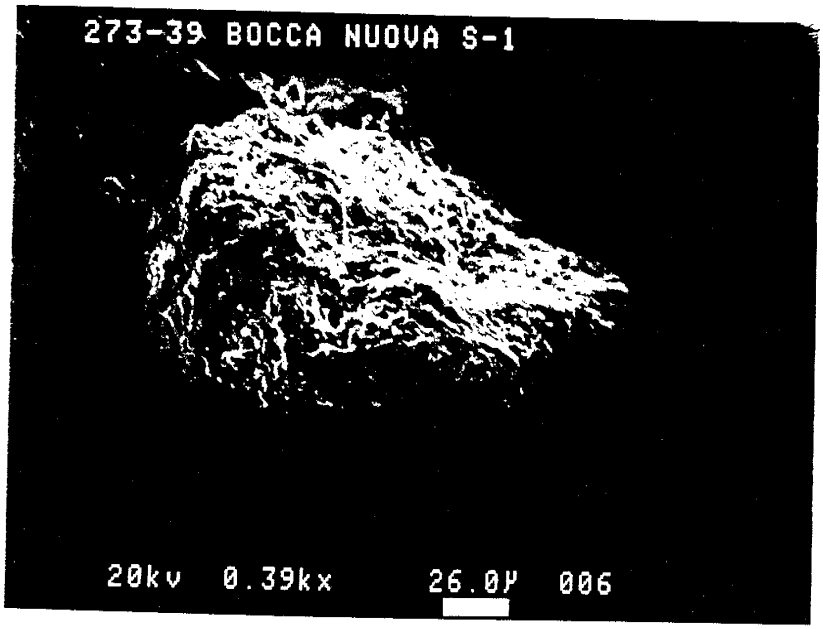
273-39 BOCCA NUOVA S-1
20kv 0.39kx 26.0μ 006

B

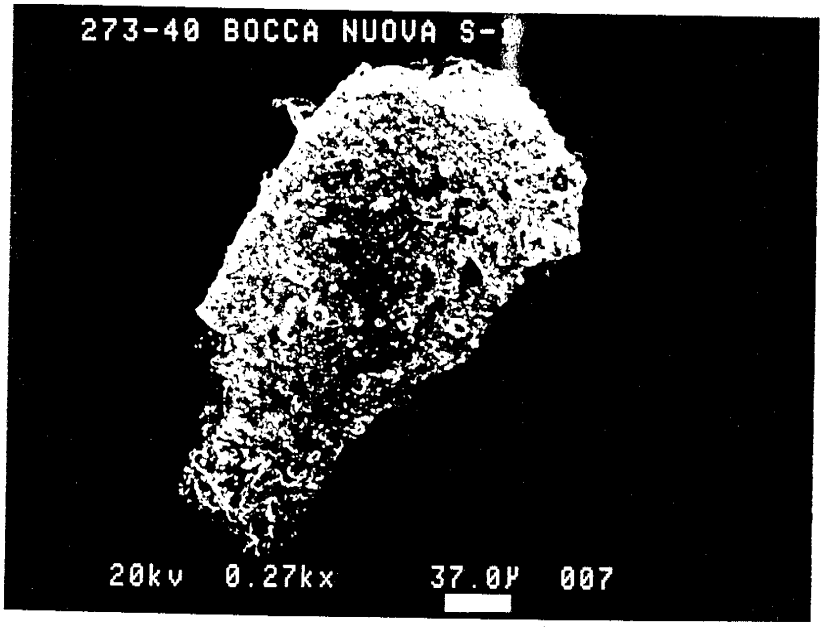
273-40 BOCCA NUOVA S-
20kv 0.27kx 37.0μ 007

Figure 17. Less Than 2 Micron-sized Particles of Bocca Nuova.

A. Micrograph 273-9 shows abundant crystals of a potassium-sulfur compound.

B. Micrograph 110 shows needles of a potassium-sulfur species and silica prisms. Micrograph 110 was shot on Bocca Nuova Stage 2 at magnification equal to 900x.

A

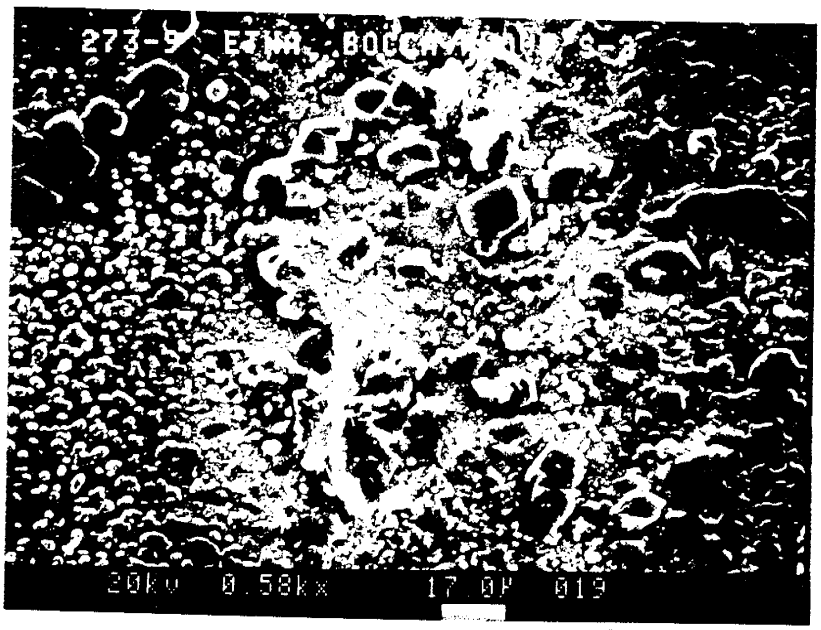

B

Figure 18. Cracking and Solution Pits.

A. Micrograph 273-13 shows cracked crusts formed from drying liquid droplets. A cracked crust can also be seen in Figure 14, micrograph 273-2.

B. Micrograph 273-31 shows a solution pit created by an acidic droplet. The nickel underplating has been remobilized out of the solution pit.

A

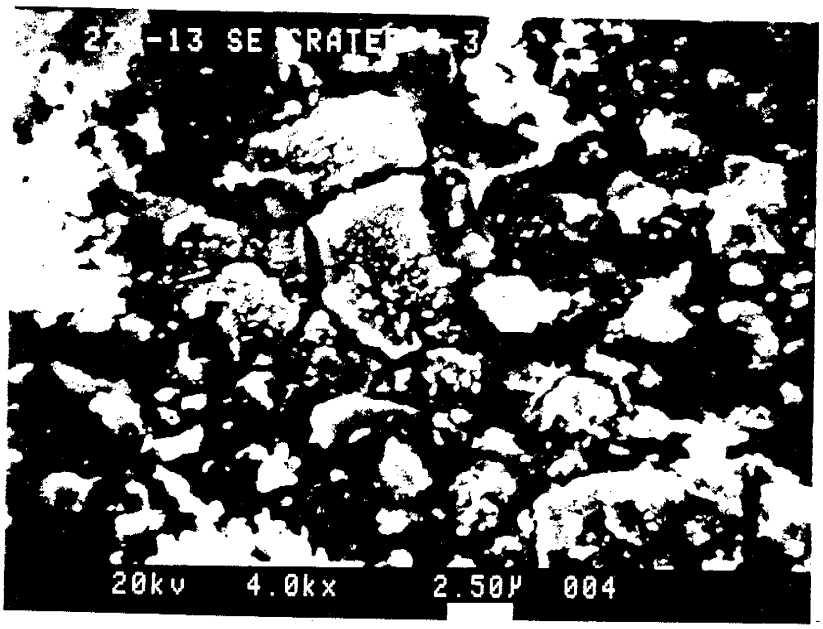
-13 SE CRATER -3
20kv 4.0kx 2.50µ 004

B

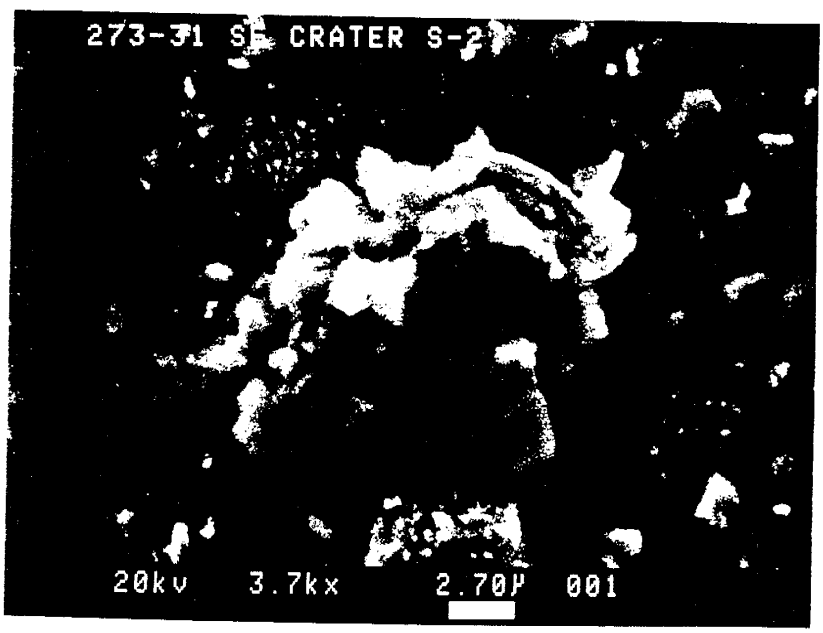
273-31 SE CRATER S-2
20kv 3.7kx 2.70µ 001

Figure 19. Crystals Formed In Liquid Droplets.

A. Micrograph 273-5 shows delicate, bladed crystals among smaller crystals of a potassium-sulfur compound.

B. Micrograph 273-10 shows crystals of a potassium-sulfur compound outlining a dried liquid pool.

C. Micrograph 273-12 shows an interlocking, delicate network of crystals which have a coralline appearance.

A

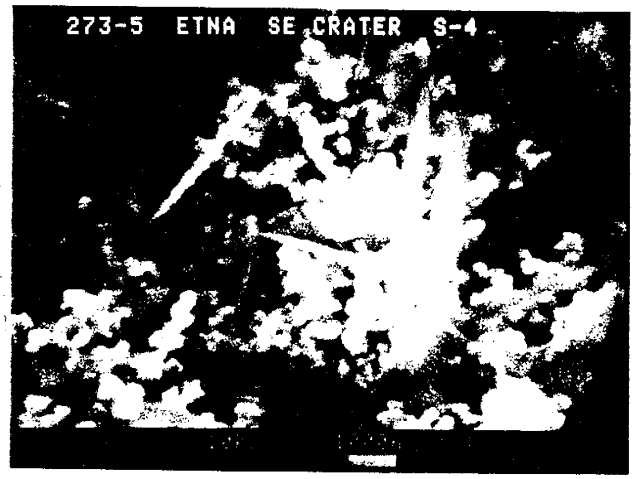
273-5 ETNA SE CRATER S-4

B

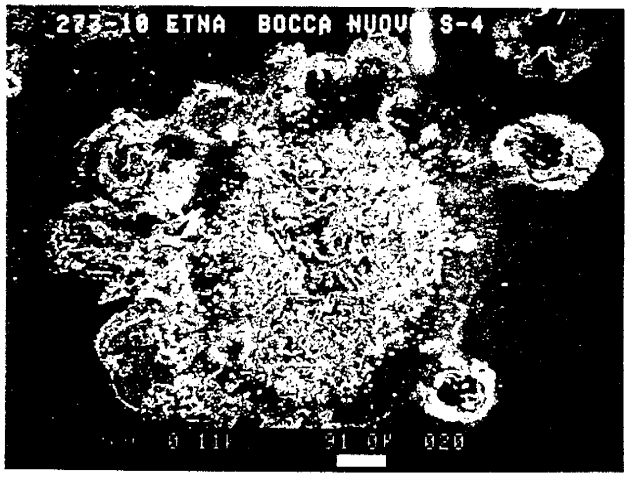
273-10 ETNA BOCCA NUOV S-4

C

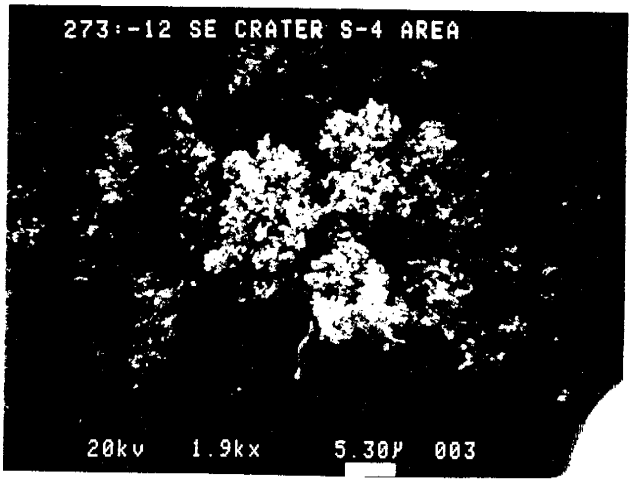
273:-12 SE CRATER S-4 AREA
20kv 1.9kx 5.30µ 003

Southeast Crater's stage 1 contains chlorine in the form of sylvite and as cracked crusts which are the remnants of dried liquid droplets. Chlorine is notably absent from stage 2, but is abundant on stages 3 and 4 where aerosols are naturally collected. This chlorine is associated with particles radially aligned (Figure 20). These particles likely formed in drying liquid droplets which were aligned by the pumped air currents passing over the stages. This suggests that the chlorine was in an aqueous form as it entered these lower stages of the QCM. Calculations show that not enough cations (as detected by INAA) were present in the plume to account for the chlorine. Therefore, the aqueous chlorine was likely in the form of HCl (hydrogen is not detected during INAA or EDX analyses).

The chlorine-rich liquids and aerosols not only reacted with volcanically derived sodium and potassium phases, but also with the nickel and silver platings. The resulting crystals are easily identified in solution pits (eroded by chlorine and sulfur-rich solutions) where the pure nickel and silver platings have formed nickel and silver chlorides and sulfides (Figure 21). Other evidence for chlorine-nickel interaction was the peeling of the nickel plating from the quartz plates (Figure 21).

Particle compositions determined by EDX qualitatively agree with aerosol filter-collected particles examined by INAA (Appendix IV). Aluminum, iron, potassium, and sodium

Figure 20. Radially-aligned Crystals Found on Stage 3 of the QCM.

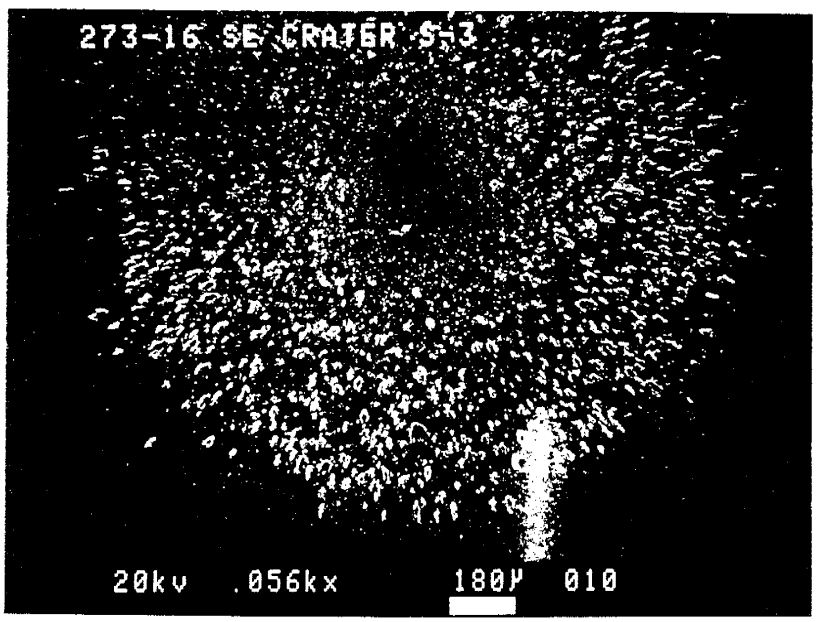
273-16 SE CRATER S-3
20kv .056kx 180µ 010

Figure 21. Nickel and Silver Secondary Reactions.

A. Micrograph 273-28 shows a peeled nickel coating exposing the underlying quartz plate. Silver sulfide crystals appear in the crack.

B. Micrograph 273-34 shows silver sulfide blades atop a cracked crust.

A

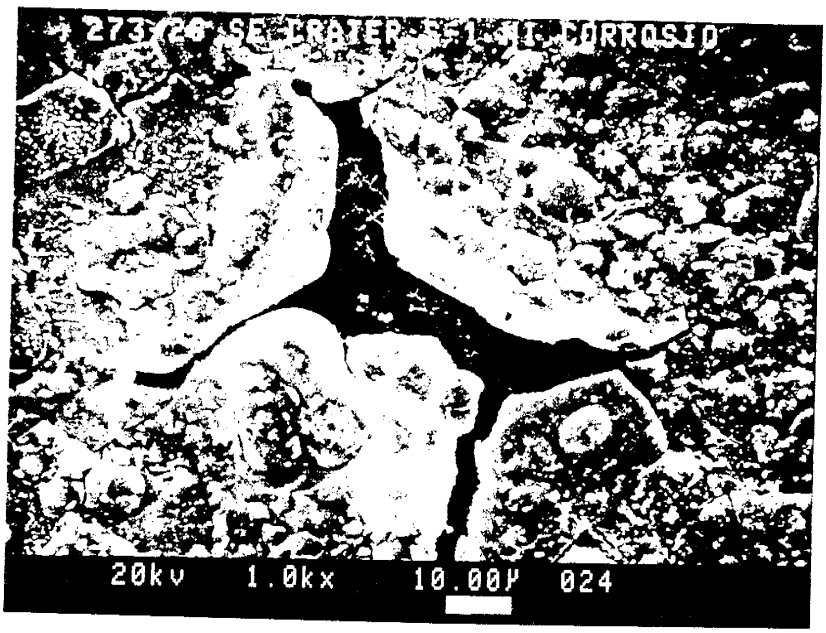

B

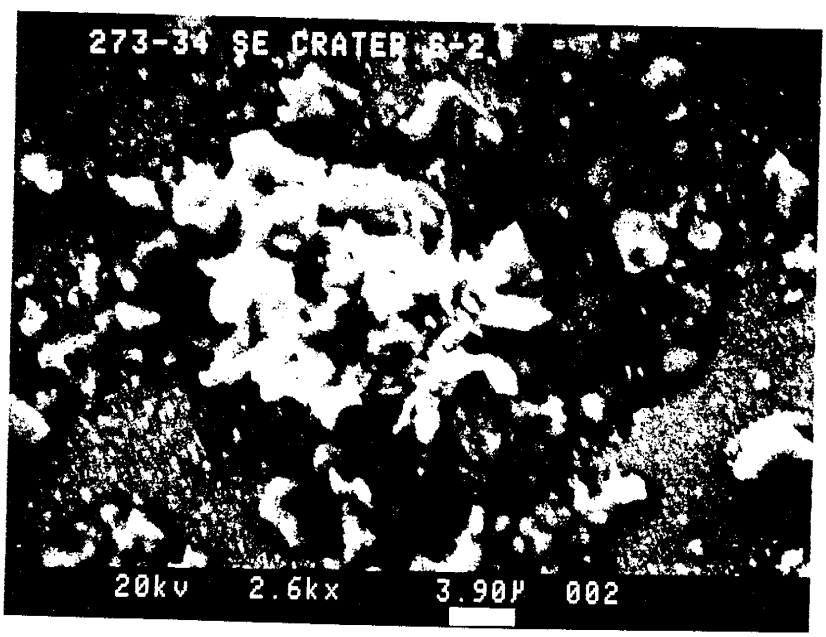

are determined by both methods to be constituents of each crater's particles. INAA also confirmed EDX analyses that chlorine is contained in Southeast Crater particles, but not in Bocca Nuova particles. EDX and INAA analyses agree on a sulfur component for Bocca Nuova particles, they do not agree for this element comprising Southeast Crater particles. The reason for this discrepancy is unresolved.

Elemental Occurrence, Enrichments, and Fluxes

The results of the three aerosol filter packs analyzed by INAA are shown in Table 9; these were compiled from the individual filter data given in Appendix IV. This data represents elemental concentrations in the portions of the plume sampled; due to plume heterogeneities, it is not representative of concentrations in the entire volcanic plume. However, the determined elemental concentrations of the two plumes partially reveal the different natures of the plumes. Two applications of the elemental concentrations will be presented later.

Qualitative examination of the data presented in Table 9 shows the plume of Bocca Nuova was chlorine-rich, but sulfur-poor as compared to the emissions of Southeast Crater. Fluorine was also a significant species in the fume from both craters. Major metals in both plumes were potassium and sodium.

Other major differences between the plumes of the two

Table 9. Summary of INAA aerosol filter results. All concentrations are reported in micrograms per cubic meter. Elements are listed in alphabetic order.

n.d. = not detected

Element	Bocca Nuova #1	Bocca Nuova #2	Southeast Crater
Al	179	76	77
As	0.49	0.45	1.2
Br	42	30	30
Cd	0.22	0.35	6.0E-1
Ce	8.6E-2	5.6E-2	n.d.
Cs	7.7E-2	5.7E-2	0.19
Cl	11191	6195	5492
Co	1.7E-2	0.17	1.3E-2
Cu	5.3	17	n.d.
Eu	1.7E-3	2.3E-3	2.4E-3
F	1186	813	1397
Au	1.2E-3	1.6E-3	2.5E-3
In	1.4E-2	3.5E-2	7.5E-2
Fe	54	33	37
La	0.10	1.2E-2	4.1E-2
Mn	0.98	0.59	0.23
Mo	1.8E-2	3.2	0.11
K	196	211	240
Re	5.7E-3	1.5E-3	9.2E-4
Rb	0.62	1.4	1.7
Sm	9.5E-3	1.3E-3	2.9E-3
Sc	2.1E-2	1.6E-3	7.6E-3
Se	9.0E-2	0.52	0.32
Na	209	241	245
S	1689	3461	13205
W	3.6E-2	3.2E-2	1.2E-2
U	n.d.	n.d.	1.3E-2
V	0.20	0.12	0.16
Yb	2.5E-3	2.9E-3	4.2E-3
Zn	34	122	156

craters was the detection of an element in one plume and not in the other. Cerium and copper are present in the Bocca Nuova samples, but not in the Southeast Crater sample. Likewise, uranium is present in the Southeast Crater sample, but not in the Bocca Nuova samples. The cause of the appearance or disappearance of these elements is unknown.

In addition to the 30 elements listed in Table 9, 10 elements were analyzed for and not detected; these elements are listed in Table 10.

One application of the aerosol filters is the determination of the enrichment factor (EF) of an element's concentration in the gaseous state relative to the magmatic state. This EF is calculated from the equation:

$$EF_{element} = \frac{element_{gas} / Y_{gas}}{element_{magma} / Y_{magma}}$$

where Y is a normalizing concentration factor (Vié le Sage, 1983). The EF data presented in this study has been normalized to bromine concentrations because it is not a major constituent of volcanic ash or the other particles collected on the filters. Therefore, these EF calculations are independent of the amount of particles collected.

Table 10. Elements analyzed for by INAA, but not detected.

antimony	chromium	mercury	osmium	tantalum
calcium	gallium	neodymium	silver	titanium

However, previous studies calculated EF's with normalizing elements which have significant concentrations in ash (e.g. aluminum and magnesium). To be comparable, the bromine-normalized data is multiplyed by 100,000 (Crowe et al., 1987). All further discussions of EF's will refer to EF's multiplied by 100,000. The magma standard ($element_{magma}$) used was the crustal average of Mason and Moore (1982) because no single Etnean analysis could be obtained for most of the elements analyzed.

Log EF's are reported in Table 11 and plotted in Figure 22. The elements were sorted by increasing log EF's for the first Bocca Nuova sample because it contained the largest number of detected elements. Log EF's close to unity indicate little elemental enrichment in the gaseous phase; these elements are usually concentrated in volcanic ash, such as iron and aluminum. Log EF's ranging from approximately two to four are associated with some elements contained in ash, such as sodium and potassium, but are generally indicative of the volatile metals. Log EF's greater than four imply significant enrichment in the gaseous phase and are typical of volatile nonmetals, such as fluorine and sulfur.

In general, the EF patterns of all three samples are very similar. The log EF's from the two Bocca Nuova samples show excellent agreement; only the log EF's for cobalt and molybdenum differ by more than one log unit. Log EF's of

Table 11. Calculated elemental enrichment factors. Dashes indicate an element not detected on the filter, and therefore an EF calculation was not performed.

Element	Bocca Nuova #1	Bocca Nuova #2	Southeast Crater
	log EF	log EF	log EF
Co	0.60	1.7	0.63
Yb	0.64	0.85	1.0
Sc	0.74	-0.23	0.47
Mn	0.79	0.71	0.31
Fe	0.80	0.73	0.79
Eu	0.91	1.2	1.2
Ce	0.93	0.88	-----
V	0.95	0.85	1.0
Sm	0.97	0.24	0.61
Al	1.1	0.88	0.90
La	1.3	0.53	1.1
Rb	1.6	2.1	2.2
U	---	---	1.8
Na	1.6	1.8	1.9
K	1.6	1.8	1.9
Mo	1.8	4.2	2.8
W	2.2	2.2	1.8
Cs	2.2	2.2	2.7
Cu	2.8	3.4	---
In	2.9	3.5	3.8
As	3.2	3.3	3.8
Au	3.2	3.5	3.7
Zn	3.5	4.2	4.3
Cd	3.8	4.2	4.4
Se	4.0	4.9	4.7
F	4.0	4.0	4.3
Re	4.5	4.1	3.9
S	4.6	5.0	5.6
Br	5.0	5.0	5.0
Cl	5.7	5.6	5.6

Figure 22. Calculated Enrichment Factors for Mount Etna. Elements are arranged by increasing EF for Bocca Nuova #1.

Enrichment Factors

Mount Etna, 1987

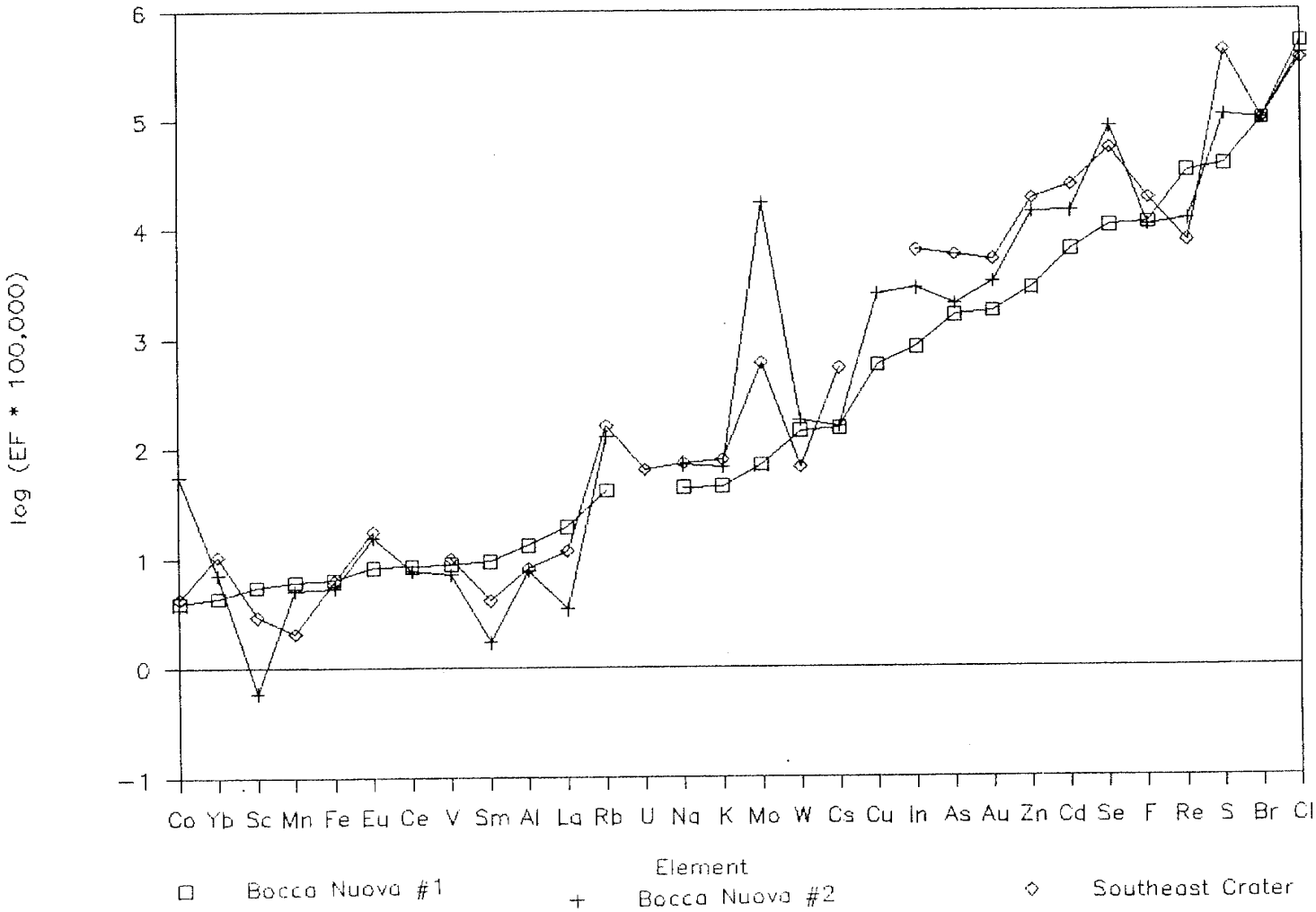

the Southeast Crater sample compare well to the two Bocca Nuova samples, except for molybdenum. Southeast Crater log EF's for cobalt and sulfur are also a log unit or greater than corresponding log EF's from one or the other Bocca Nuova samples.

Calculated EF's for Mount Etna are comparable to those for other volcanic systems (Figure 23). All Etnean EF's fall within the range or within an order of magnitude of the EF's determined for other systems, except zinc. In comparison to EF's previously determined for Mount Etna, excellent agreement is obtained except for scandium, zinc, and chlorine which are more than an order of magnitude greater than those determined by Buat-Ménard and Arnold (1978). If the new Etnean EF data is recalculated with aluminum as the normalizing element, as done by the previous workers, then EF's for these elements are less than one half of a log unit different than the previously reported values.

Another application of the elemental concentrations presented in Table 9 is the calculation of elemental fluxes to the atmosphere. These calculations assumed that all sulfur detected on the filters was emitted as SO_2 gas. This assumption was valid because minimal amounts of sulfur were detected on the particle filters except on the first Bocca Nuova sample; the majority of the sulfur was located on the treated filters which were sensitive to gaseous species only (Appendix IV). SO_2 is also the only major sulfur-bearing

Figure 23. Comparison of Enrichment Factors of Mount Etna and Other Volcanic Systems. Elements are arranged by increasing EF for Mount Etna.

Comparison of EF Data From Various Volcanic Systems

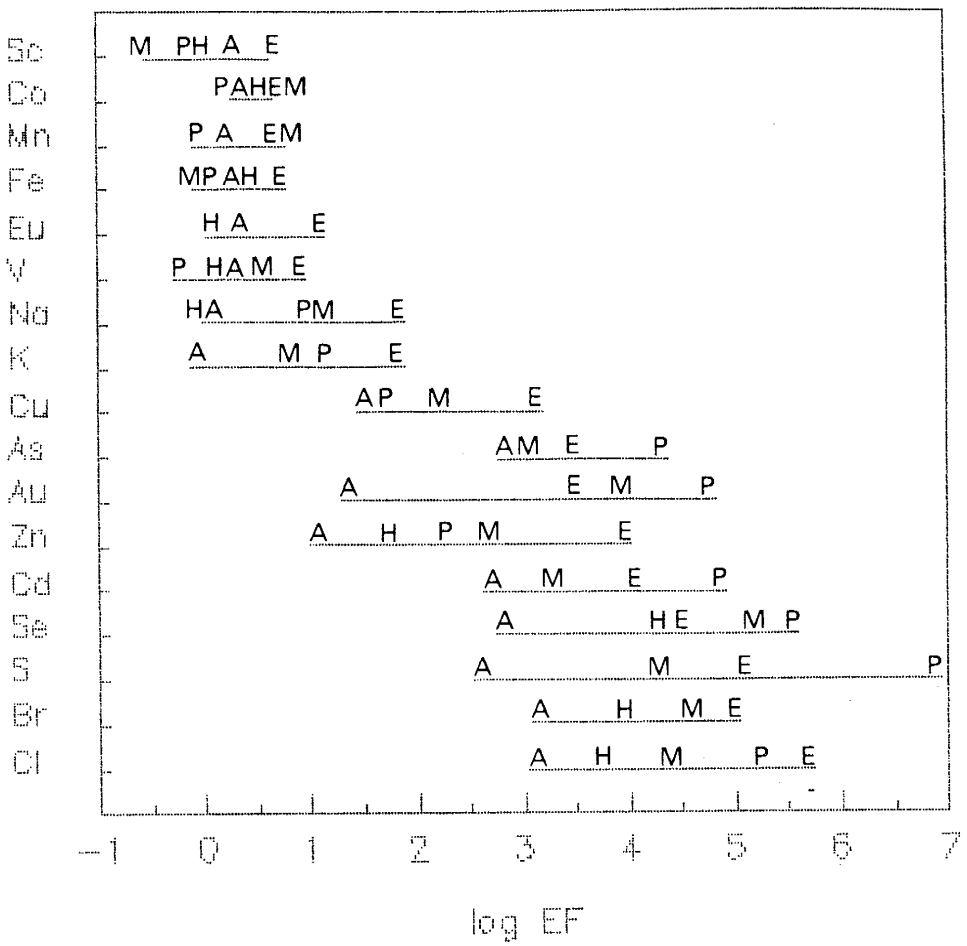

E Mount Etna, 1987 (this study)

H Heimaey, Iceland, 1973 (Mroz and Zoller, 1975)

A Augustine, Alaska, 1976 (Lepel et al., 1978)

M Mount Etna, 1976 (Buat-Menard and Arnold, 1978)

P Pu'u O'o, Hawaii, 1983-4 (Crowe et al., 1987)

gas species to be reported in Etnean emissions (Jaeschke et al., 1982). Elemental fluxes were calculated based upon Bocca Nuova exhaling 65 percent and Southeast Crater emitting 35 percent (Table 5) of the average SO_2 flux of 1056.17 tonnes per day (Table 6). Calculated elemental fluxes are in Table 12 and Figure 24. Elements are arranged in this figure and graph by increasing total fluxes.

In comparison to elemental fluxes reported by Buat-Ménard and Arnold (1978) for Mount Etna (Table 3), fluxes determined in this study are within a factor of 2 for nine of the eighteen elements analyzed in both studies. The iron flux determined in this study is twice the previously reported flux; aluminum, cesium and scandium are within a factor of 3; chlorine, zinc and manganese are within a factor of 4; and selenium and gold are within a factor of 15. The differences in fluxes can be due to differing experimental techniques or differences in vent emission chemistry. The fluxes reported in this study are a composite of fume from Bocca Nuova and Southeast Crater whereas the other calculated fluxes are not.

Table 12. Elemental fluxes emitted from Mount Etna. Plume concentrations are in micrograms per cubic meter and fluxes in tonnes per day.

Element	Plume Concentration		Flux		
	average Bocca Nuova	Southeast Crater	average Bocca Nuova	Southeast Crater	TOTAL
U	n.d.	1.3E-2	-------	1.9E-4	1.9E-4
Au	1.4E-3	2.5E-3	1.9E-4	3.5E-5	2.2E-4
Eu	2.0E-3	2.4E-3	2.6E-4	3.4E-5	3.0E-4
Yb	2.7E-3	4.2E-3	3.6E-4	5.9E-5	4.2E-4
Re	3.6E-3	9.2E-4	4.8E-4	1.3E-5	4.9E-4
Sm	5.4E-3	2.9E-3	7.2E-4	4.1E-5	7.6E-4
Sc	1.1E-2	7.6E-3	1.5E-3	1.1E-4	1.6E-3
In	2.5E-2	7.5E-2	3.3E-3	1.1E-3	4.3E-3
W	3.4E-2	1.2E-2	4.6E-3	1.7E-4	4.7E-3
La	5.5E-2	4.1E-2	7.3E-3	5.8E-4	7.9E-3
Ce	7.1E-2	n.d.	9.5E-3	-------	9.5E-3
Cs	6.7E-2	0.19	8.9E-3	2.7E-3	1.2E-2
Co	9.3E-2	1.3E-2	1.2E-2	1.8E-4	1.3E-2
V	0.16	0.16	2.1E-2	2.2E-3	2.4E-2
Se	0.31	0.32	4.1E-2	4.5E-3	4.5E-2
Cd	0.28	0.60	3.8E-2	8.3E-3	4.6E-2
As	0.47	1.2	6.3E-2	1.7E-2	8.0E-2
Mn	0.79	0.23	0.10	3.3E-3	0.11
Rb	1.0	1.7	0.13	2.4E-2	0.16
Mo	1.6	0.11	0.21	1.5E-3	0.21
Cu	11	n.d.	1.5	-------	1.5
Br	36	30	4.9	0.42	5.3
Fe	43	37	5.8	0.51	6.3
Zn	78	156	10	2.2	13
Al	127	77	17	1.1	18
K	203	240	27	3.4	30
Na	225	245	30	3.4	33
F	1000	1397	133	20	153
S	2575	13205	343	185	528
Cl	8693	5492	1159	77	1236

Figure 24. Calculated Elemental Fluxes for Mount Etna. Elements are arranged by increasing fluxes.

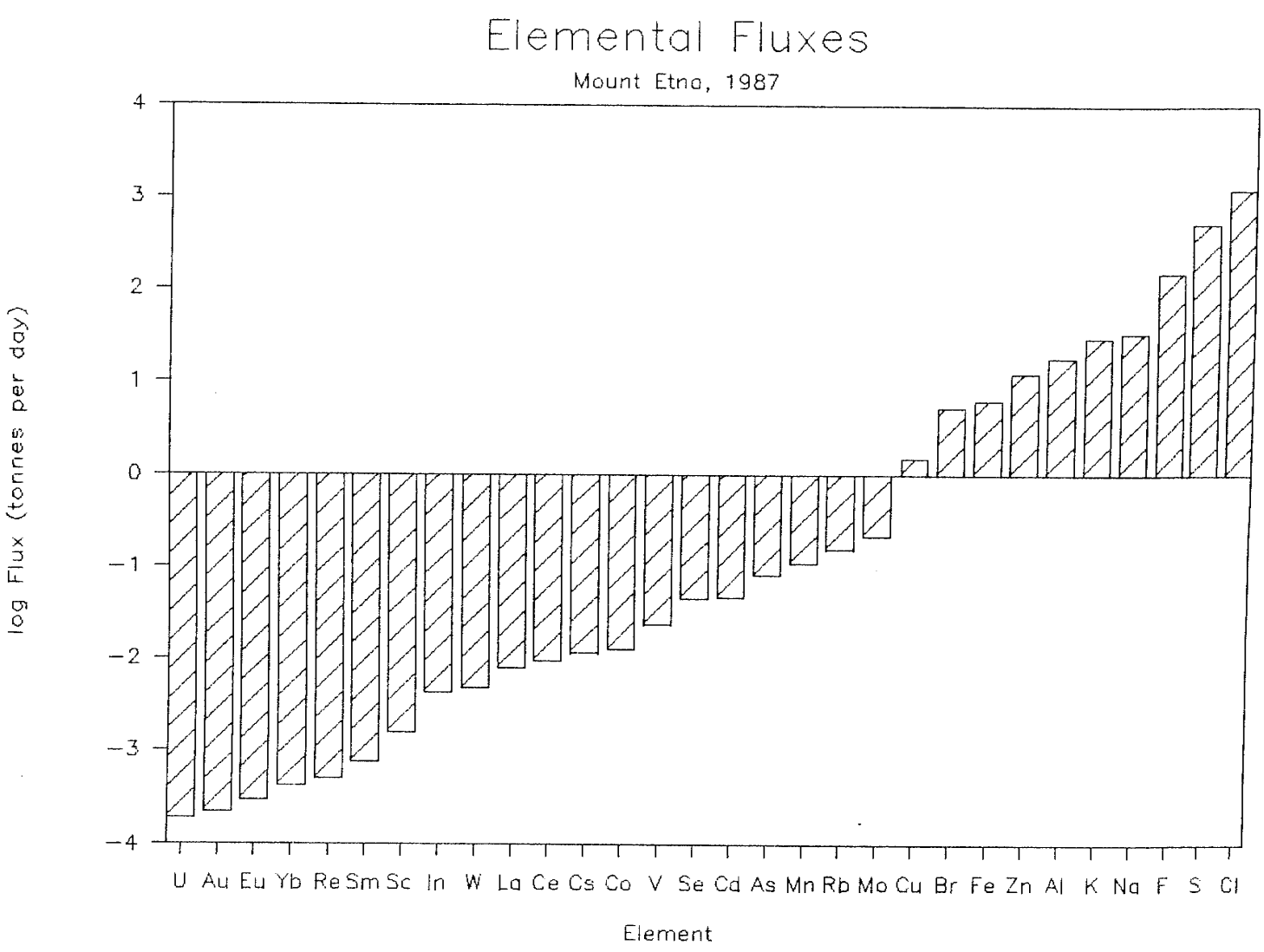
Elemental Fluxes
Mount Etna, 1987
log Flux (tonnes per day)
4
3
2
1
0
−1
−2
−3
−4
U Au Eu Yb Re Sm Sc In W La Ce Cs Co V Se Cd As Mn Rb Mo Cu Br Fe Zn Al K Na F S Cl
Element

DISCUSSION

SO_2 Emissions

Individual crater flux measurements revealed that Bocca Nuova emits almost twice as much SO_2 as Southeast Crater (Table 5). The average flux of each crater was dependent upon the amount of SO_2 available to degas in the subsurface. Since the magmas of the two craters were of similar composition, their SO_2 solubilities should be equal. So the differences in the SO_2 fluxes likely result from differing effective volumes of magma degassing underneath each crater. The "effective volume" of magma is defined as the actual volume of degassing magma in the conduit and the rate at which this magma is replaced by undegassed magma through convection processes.

The range of fluxes for each day is associated with differing eruption mechanisms and vent geometries. Although Bocca Nuova emits SO_2 in discrete Strombolian eruptions, its relatively constant SO_2 flux is caused by the persistent winds. These winds partially homogenize the air and volcanic emissions in the large crater before the SO_2 rises above the crater rim to be measured. In contrast, the interior of the small Southeast Crater vent is unaffected by winds. The emissions of Southeast Crater escape in discrete gas bursts or puffs. These puffs are not always eradicated by the wind before being monitored by the COSPEC.

The short term variations observed daily in individual

crater and system fluxes (Appendices II and III) were examined by Fourier transform calculations to determine if any intrinsic periodicity existed (Bloomfield, 1976). This investigation was exploratory in nature due to the small number of data points.

The Fourier transform calculations revealed a relatively flat spectra for the daily SO_2 flux data. This implies no dominant frequency, or random variability, existed in the daily SO_2 fluxes. The system fluxes and the individual crater fluxes also contained no frequencies which repeated daily. This suggests that if the observed SO_2 fluxes were dependent upon magma convection, then the magma movement was randomly variable, or that the dependent frequency was longer than the collection intervals of SO_2 flux data.

The SO_2 periodicity results were compared to similar Fourier transform calculations of contemporaneous Mount Etna surface tremor data. Volcanic surface tremors occur in the 0.15 to 10 hertz range of seismometer-detected energy spectra. Tremor data was obtained from the Istituto di Scienze Della Terra, Catania, Italy. Hypotheses for the tremor mechanism include magma-solid interactions (Chouet et al., 1987; Ferrazzini and Aki, 1987; Ferrick et al., 1982) and gas-magma interactions (Chouet, 1985; Schick et al., 1982; Aki and Koyanagi, 1981; Del Pezzo et al., 1974; Lo Bascio et al., 1973). The gas-magma interaction hypotheses are based upon the positive correlation between gas-rich

Strombolian eruptions and tremor frequency. The calculations of tremor data showed fundamental frequencies not seen in the SO_2 data. This suggests that Mount Etna SO_2 fluxes are not correlative with surface tremors; however, this does not prove or disprove hypotheses for tremor mechanisms. Only SO_2 gases were examined in this study and the emission fluxes of other gas species not monitored may show positive correlations with surface tremor frequencies.

Individual crater fluxes were also compared to timings of crater eruptions and degassing bursts (Appendix I) by Fourier transform calculations. The frequency spectra for the activities of the two craters differed from corresponding SO_2 flux spectra. However, data allowed only comparisons of activity and SO_2 data measured on different days, and therefore the comparisons may be invalid.

Total system SO_2 fluxes obtained in this study (Figure 12) reveal a fairly flat baseline with a prominent spike on 19 July 1987. An examination of COSPEC scan types and associated fluxes (Table 6) revealed no correlation.

The quiet degassing nature of Mount Etna observed during the study period is consistent with the constant SO_2 flux. The average SO_2 flux of 1000 tonnes per day is the approximate baseline value and agrees well with Malinconico (1979) (Figure 5). Malinconico observed summit eruptions after SO_2 fluxes peaked at greater than 5000 tonnes per day and a lava flow after SO_2 fluxes receded from 4000 tonnes per day. SO_2 fluxes on 19 July 1987 averaged 3000 tonnes

per day, but no departure from baseline activity was observed.

Malinconico (1987) proposes SO_2 flux measurements can be used to predict volcanic eruptions. His proposal assumes (but does not state) that the magma composition and the plumbing system of a volcano remain constant over long time periods. These assumptions are invalid for most volcanoes, particularly for Mount Etna, because variations in Etnean lavas are known (Cristofolini and Romano, 1982) and changes in the plumbing system are evidenced by eruptions occurring from various craters (Romano and Sturiale, 1982). Malinconico interprets increasing SO_2 fluxes as a result of rising magma levels in the volcanic conduit. This is a simplistic view of the situation; increasing SO_2 fluxes signify a greater effective volume of degassing magma which is supersaturated with respect to sulfur. Gerlach (1986) empirically determined for Hawaiian tholeiites that most sulfur exsolves from the magma at 100 to 150 meters depth; similar exsolution depths should apply to Etnean magmas based on their similar composition to Hawaiian magmas. Although shallow magmas exsolve SO_2, this degassing is independent of whether the magmas erupt. To equate increasing SO_2 fluxes with pending eruptive activity is a fallacy. To the best of my knowledge, no successful predictions of volcanic eruptions have ever been made based solely on SO_2 flux data.

Although the sharp increase in SO_2 flux did not

coincide with extrusive activity, it may still have been a function of changing levels of magma in the Southeast Crater vent. The relative level of magma in the vent can be qualitatively assessed during night observation. The vent walls were near vertical and channelled the emitted light upwards. This light was reflected by co-escaping vapors and could be clearly seen from a distance of one kilometer. The intensity of the vent's reflected light was a function of the concentration of vapors and moisture in the air above the vent.

On 18 July, no SO_2 measurements were possible, but the crater glow was unusually intense. SO_2 emissions spiked on 19 July, but no crater glow observations were obtained that night. On 20 July, the crater glow was normal and SO_2 fluxes decreased sharply. The change in crater glow could reflect changing humidity although the dramatic changes observed in nighttime glow were not repeated even though humidity varied greatly throughout the study period. Another explanation for the changing crater glow and SO_2 increase is a rising of the level of magma in the Southeast Crater vent. A higher magma level would allow for more light to be observed because the area of exposed, light absorbing, crater walls was decreased. The higher magma level might also have allowed for a larger effective volume of magma to degas and increase SO_2 fluxes.

Another hypothesis for the observed SO_2 peak is flow of a relatively undegassed batch of magma into the Southeast

Crater conduit. This has been suggested by others for similar SO_2 increases in volcanic gas emissions (Casadevall et al., 1984; Malinconico, 1979). The undegassed magma would have circulated from the conduit into one of Mount Etna's rifts for later flank eruption or dike intrusion. The residence time in the conduit would be represented by a peak in SO_2 emissions. Some evidence exists to support this hypothesis. Decreasing Southeast Crater SO_2 fluxes on 20 and 22 July (Table 5) would represent the migration of magma out of the conduit. Very warm ground was detected east of the crater (Figure 1c) and may be the result of magma flow into a rift. Inflation and deformation of the eastern flank of Mount Etna during the 1987 summer (Murray, 1987) could also have been the result of magma movement. The relatively undegassed batch of magma hypothesis is compatible with the rising magma level hypothesis to account for increased SO_2 fluxes and crater glow.

Another aspect of Etnean gaseous emissions was the noticeable parting of the volcanic plume into a visible steam plume and a nearly-transparent SO_2 plume (Figure 25). This occurred during periods of moderate to high wind velocities. The natural slow rate of the volcanic plume's rise relative to the high wind velocities caused turbulent eddies to break up the plume (Moffat and Millán, 1971). Differential cooling in the volcanic plume occurred because SO_2 has a lower heat capacity than the steam. As the SO_2 cooled, it gravitationally sank and separated from the

Figure 25. Separation Mechanism of SO_2 Plume from the Steam Plume. Heat capacities and densities from CRC (1986) and air + plume temperature measured on site by thermometer and thermocouple.

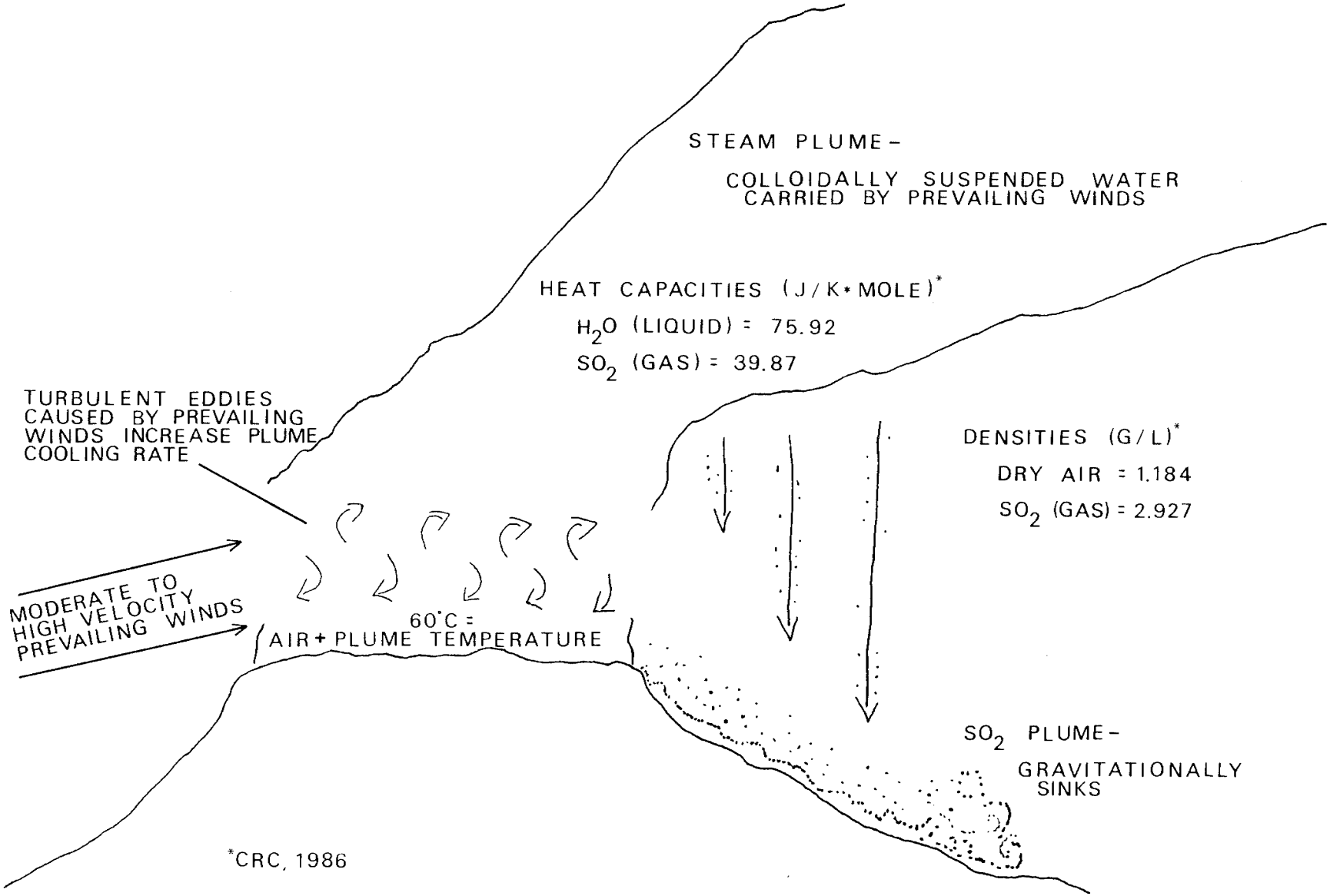
STEAM PLUME –
COLLOIDALLY SUSPENDED WATER CARRIED BY PREVAILING WINDS
HEAT CAPACITIES (J/K*MOLE)*
H_2O (LIQUID) = 75.92
SO_2 (GAS) = 39.87
TURBULENT EDDIES CAUSED BY PREVAILING WINDS INCREASE PLUME COOLING RATE
DENSITIES (G/L)*
DRY AIR = 1.184
SO_2 (GAS) = 2.927
MODERATE TO HIGH VELOCITY PREVAILING WINDS
60°C = AIR + PLUME TEMPERATURE
SO_2 PLUME –
GRAVITATIONALLY SINKS
*CRC, 1986

rising plume. While the SO_2 travelled down slope near the ground surface, the steam was carried away by the prevailing winds.

Field evidence verified the SO_2 separation from the volcanic plume. Frequently, a visible plume was seen overhead with a weak, COSPEC-measured, SO_2 signal. Concurrently, the COSPEC measured a strong SO_2 signal in winds blowing nearer the ground. The smell of the separated SO_2 gas moving at ground level was sometimes overwhelming. COSPEC measurements indicated that 20 to 80 percent of the Etnean SO_2 emissions escaped the volcanic plume and travelled as a separate plume during periods of moderate to high winds. Similar plume separations have also been observed at Mount Etna (Malinconico, personal communication); Kilauea, Hawaii (Andres et al., in prep.); Mount Erebus, Antarctica (Kyle and others, unpublished data); and Fuego, Guatemala (Stoiber et al., 1983).

The existence of SO_2 plume separation can have severe consequences for COSPEC-obtained SO_2 flux data. Wind speed and distance to the plume are factors in calculating SO_2 fluxes. Substitution of steam plume parameters for the true SO_2 plume parameters can lead to significant errors in the SO_2 flux calculations. These errors were avoided during this study of Mount Etna because the SO_2 plume separation was recognized and SO_2 plume parameters were noted.

The separated SO_2 plume can also be absorbed by or

deposited on soils, plants, and surface waters as the plume travels over the ground surface. Absorption and deposition will decrease the amount of SO_2 and thus result in measurement of lower SO_2 fluxes than the vent-emitted fluxes.

Particle Emissions

Varekamp et al. (1986) compared volcanic particle compositions as a function of fluorine-chlorine ratios (F/Cl) in the volcanic fume. They proposed the F/Cl controlled particle chemistry by determining whether fluorine or chlorine compounds carried the co-emitted metals. They concluded that low F/Cl plumes contained greater concentrations of potassium, sodium, and zinc and lower concentrations of aluminum and calcium than high F/Cl plumes. At Mount Etna, Bocca Nuova emitted a lower F/Cl plume (F/Cl range of 0.11 to 0.13) whereas Southeast Crater emitted a higher F/Cl plume (F/Cl of 0.25). Particle chemistry presented in Table 8 qualitatively agrees for aluminum and calcium, but is inconclusive for potassium and sodium; zinc was not detected in EDX analyses. INAA data for particles collected on the particle filters (Appendix IV) disagree with Varekamp et al. (1986) for sodium and aluminum; these data are inconclusive for potassium and zinc.

The absence of chlorine from Bocca Nuova particles (Table 8) is explained by the high volatility of chlorine

and chlorine compounds (Krauskopf, 1979). The abundance of volatile chlorine was corroborated by aerosol filters. Southeast Crater's chlorine-rich particles resulted from sublimation or crystallization. The same processes were undoubtedly occurred at Bocca Nuova, but the chlorine contained in aerosols was likely adhering to ash particles created by the crater's Strombolian eruptions. The adherence of liquids to the ash particles prevented them from rising 400 meters to clear the crater rim. Instead, they sank back into the crater and could not be sampled. Similar fallout of liquid coated particles has been suggested by Varekamp et al. (1986) and Finlayson-Pitts and Pitts (1986). Gaseous chlorine species which escaped the crater were not retained by the QCM and thus passed through the instrument without detection.

Volcanic Versus Atmospheric Fluxes

Table 13 compares the absolute Etnean fluxes to the anthropogenic fluxes of the Mediterranean region. Sources for global anthropogenic fluxes are listed in Table 13. Calculation of local anthropogenic fluxes in the Mediterranean region was after Buat-Ménard and Arnold (1978) and depended upon the proportion of the Mediterranean area's industrialized output relative to the world's industrialized output. Goldberg (1976) has shown the validity of this approximation.

Mount Etna's chlorine and fluorine emissions were among

Table 13. Anthropogenic and volcanic flux comparison. All fluxes are reported in tonnes per day. "Local" refers to the Mediterranean region.

Element	Mt. Etna Total (1)	Anthropogenic Local (2)	Ratio (2/1)
F[1]	153	10	0.07
Cl[1]	1236	242	0.20
Br[1]	5.3	24	4.6
Zn[2]	13	115	9.1
Cd[2]	4.6E-02	0.75	16
S[1]	528	8907	17
Cu[2]	1.5	36	24
Mo[2]	0.21	7.0	32
Se[2]	4.5E-02	1.9	42
Co[2]	1.3E-02	0.60	48
Al[2]	18	986	55
As[2]	8.0E-02	11	133
Sm[2]	7.6E-04	0.16	216
Fe[2]	6.3	1465	233
Mn[2]	0.11	43	400
V[2]	2.4E-02	29	1222

Sources: [1]Cadle, 1980.
[2]Lantzy and Mackenzie, 1979

==========

the volcano's largest elemental contributions to the atmosphere. They are also 15 and 5 times greater than Mediterranean region's anthropogenic emissions, respectively. Sulfur, the element with the second largest Etnean elemental flux, is 17 times less than the region's anthropogenic emission. For the other elements reported, anthropogenic emissions are 4 to over 1000 times larger than Etnean emissions.

Based on the volcanic-anthropogenic comparison, Mount Etna's emissions of summer 1987 had no measureable effect on the world's atmosphere, except for possible additions of fluorine and chlorine. Volcanic emissions can affect

climatic changes when eruption products penetrate the stratosphere; these eruptions usually result in hemispheric cooling (Self and Rampino, 1988; Sigurdsson, 1982; Pollack et al., 1976). Mount Etna's activity was non-explosive during the study period and there was no measured input to the stratosphere.

Mount Etna's emissions in the summer of 1987 had no measureable effect on the Mediterranean region, but did have a limited, local effect. Through the processes of wet and dry deposition (Finlayson-Pitts and Pitts, 1986), metals and acids emitted from the summit craters were deposited on the summit and flanks of Etna. The deposition of these acids lowers the pH of local waters and soils. Studies by Martin et al. (1984) indicate that within 100 kilometers, SO_2 concentrations are reduced by several orders of magnitude through processes of deposition and conversion of SO_2 to sulfate. More soluble acids, such as HCl, will undergo similar concentration decreases in shorter travel distances. A thorough study of the local climatic impact of Etnean emissions is complicated by the proximity of anthropogenic sources from the heavily populated, lower slopes of Mount Etna.

SUMMARY AND CONCLUSIONS

The sulfur dioxide and particle emissions of Mount Etna were sampled from June to August 1987. Only two of the four summit craters were active at that time. Data was collected to calculate fluxes of SO_2, particles, and elements. SO_2 fluxes for the entire system were remarkably constant throughout the study except for a four day period with relatively large fluxes. The constant SO_2 emissions correlate well with the constant, low-level, volcanic activity during the study period. The short duration increase in SO_2 flux may be related to changing magma levels, or passage of undegassed magma through a crater to one of the rifts. The absence of increased volcanic activity during the SO_2 increase highlights the non-predictive nature of SO_2 monitoring. Differences between SO_2 fluxes for the two, active craters are best explained by differing magma volumes degassing beneath each crater. Disagreements between particle and elemental fluxes for each crater are explained by varying dilutions of the sampled plume by the winds common to the summit. Similar elemental enrichment factors were calculated for most elements from each crater; this testifies to the homogeneous composition of the common magma source for each crater. Differences observed in particle compositions and size distributions for each crater are likely due to the differing eruption style

of each crater. Atmospheric implications of Etnean emissions were negligible compared to the region's anthropogenic sources.

Appendix I. Repose Time Between Bocca Nuova Eruptions and Southest Crater Degassing Bursts. Time is reported in hours:minutes:seconds. In the statistics:

events = number of events timed
max = maximum repose time
min = minimum repose time
avg = average repose time
std dev = standard deviation computed at the 95% confidence interval.

Bocca Nuova eruptions

21 Jul 87		22 Jul 87	
event time	repose time	event time	repose time
10:57:19	--------	11:16:04	--------
11:00:22	00:03:03	11:16:56	00:00:52
11:04:41	00:04:19	11:18:06	00:01:10
11:05:28	00:00:47	11:19:31	00:01:25
11:06:36	00:01:08	11:19:40	00:00:09
11:07:50	00:01:14	11:21:46	00:02:06
11:08:22	00:00:32	11:26:10	00:04:24
11:13:21	00:04:59	11:31:00	00:04:50
11:14:32	00:01:11	11:36:13	00:05:13
11:16:55	00:02:23	11:36:37	00:00:24
11:18:11	00:01:16	11:38:17	00:01:40
11:18:54	00:00:43	11:40:07	00:01:50
11:19:13	00:00:19	11:40:16	00:00:09
11:23:07	00:03:54	11:42:16	00:02:00
11:25:05	00:01:58	11:47:55	00:05:39
11:26:24	00:01:19	11:48:56	00:01:01
11:28:20	00:01:56	11:54:24	00:05:28
11:32:55	00:04:35	11:56:37	00:02:13
11:33:56	00:01:01	11:58:37	00:02:00
11:34:24	00:00:28	11:59:16	00:00:39
11:34:56	00:00:32	12:00:01	00:00:45
11:36:10	00:01:14	12:02:19	00:02:18
11:39:08	00:02:58	12:04:52	00:02:33
11:41:20	00:02:12	12:07:14	00:02:22
11:42:35	00:01:15	12:07:26	00:00:12
11:43:38	00:01:03	12:12:24	00:04:58
11:47:55	00:04:17	12:13:21	00:00:57
11:48:12	00:00:17	12:15:28	00:02:07
11:52:21	00:04:09		
11:55:28	00:03:07		
11:59:46	00:04:18		
events =	30	events =	27
max =	00:04:59	max =	00:05:39
min =	00:00:17	min =	00:00:09
avg =	00:02:05	avg =	00:02:12
std dev =	00:02:56	std dev =	00:03:24

Southeast Crater degassing bursts

9 Jul 87		21 Jul 87	
event time	repose time	event time	repose time
08:50:02	--------	12:38:25	--------
08:50:08	00:00:06	12:39:36	00:01:11
08:50:42	00:00:34	12:41:06	00:01:30
08:50:45	00:00:03	12:41:30	00:00:24
08:50:47	00:00:02	12:41:58	00:00:28
08:51:31	00:00:44	12:42:42	00:00:44
08:52:00	00:00:29	12:42:44	00:00:02
08:52:04	00:00:04	12:43:20	00:00:36
08:52:07	00:00:03	12:44:01	00:00:41
08:52:09	00:00:02	12:44:25	00:00:24
08:52:14	00:00:05	12:44:36	00:00:11
08:53:00	00:00:46	12:44:38	00:00:02
08:53:27	00:00:27	12:44:49	00:00:11
08:54:00	00:00:33	12:45:05	00:00:16
08:54:34	00:00:34	12:45:13	00:00:08
08:54:37	00:00:03	12:45:16	00:00:03
08:54:40	00:00:03	12:45:18	00:00:02
08:55:12	00:00:32	12:46:37	00:01:19
08:55:28	00:00:16	12:46:58	00:00:21
08:56:09	00:00:41	12:48:31	00:01:33
08:56:29	00:00:20	12:49:10	00:00:39
08:56:38	00:00:09	12:49:30	00:00:20
08:56:41	00:00:03	12:49:51	00:00:21
08:57:10	00:00:29	12:49:58	00:00:07
08:57:42	00:00:32	12:51:39	00:01:41
08:57:44	00:00:02	12:52:01	00:00:22
08:58:21	00:00:37	12:52:06	00:00:05
08:58:32	00:00:11	12:53:23	00:01:17
08:59:10	00:00:38	12:53:28	00:00:05
08:59:14	00:00:04	12:53:39	00:00:11
08:59:25	00:00:11	12:53:58	00:00:19
08:59:41	00:00:16	12:54:58	00:01:00
08:59:51	00:00:10	12:55:00	00:00:02
09:00:02	00:00:11	12:55:22	00:00:22
09:00:21	00:00:19	12:57:02	00:01:40
09:00:35	00:00:14	12:57:07	00:00:05
09:00:41	00:00:06	12:57:09	00:00:02
09:00:53	00:00:12	12:57:26	00:00:17
09:01:01	00:00:08	12:58:17	00:00:51
09:02:22	00:01:21	12:58:28	00:00:11
09:02:24	00:00:02	12:58:50	00:00:22
09:02:27	00:00:03	12:59:13	00:00:23
09:02:31	00:00:04	12:59:20	00:00:07
09:03:08	00:00:37	12:59:23	00:00:03
09:03:12	00:00:04	13:00:17	00:00:54
09:04:06	00:00:54		

09:04:12	00:00:06
09:04:57	00:00:45
09:05:33	00:00:36
09:06:06	00:00:33
09:06:08	00:00:02
09:06:27	00:00:19
09:07:00	00:00:33
09:07:45	00:00:45
09:07:47	00:00:02
09:08:21	00:00:34
09:08:23	00:00:02
09:08:36	00:00:13
09:09:14	00:00:38
09:09:31	00:00:17
09:09:36	00:00:05
09:09:48	00:00:12
09:09:49	00:00:01
09:10:21	00:00:32
09:10:36	00:00:15
09:10:46	00:00:10
09:11:07	00:00:21
09:11:42	00:00:35
09:11:54	00:00:12
09:12:05	00:00:11
09:12:34	00:00:29

events	= 70	events	= 44
max	= 00:01:21	max	= 00:01:41
min	= 00:00:01	min	= 00:00:02
avg	= 00:00:19	avg	= 00:00:30
std dev	= 00:00:33	std dev	= 00:00:58

Geoscience Department
N. M. I. M. T.
Socorro, N. M. 87801

Appendix II. Individual Crater SO_2 Fluxes. The date, type of COSPEC scan and scan site heads each page. Time of measurement is reported in hours, minutes, and seconds (HH:MM:SS); SO_2 fluxes in tonnes per day (tpd); and rise rates in meters per second (m/s). Blank fluxes correspond to runs during which an individual crater flux was not determined. Standard deviation computed to 95 percent confidence interval. Graphs plotted with identical axes.

---

19 July 1987

Tripod-mounted COSPEC, horizontal scans (summit)

Run	Time (HH:MM:SS)	Flux (tpd) Bocca Nuova	Flux (tpd) Southeast Crater	Rise Rate (m/s)
1	15:06:00	927.27	692.92	*
2	15:10:00	879.75		*
3	15:12:00	691.18		*
4	15:14:00	2038.49		*
5	15:15:00	1967.49	1386.72	*
6	15:17:00	3898.33	1732.71	*
7	15:18:00	2219.83	1441.96	*
8	15:20:00	2084.76	871.83	*
10	15:24:00	2739.23		*
11	15:25:00	3450.37		*
12	15:26:00	1305.46	5229.31	*
13	15:29:00	3392.91		*
14	15:31:00	638.98	851.61	*
15	15:33:00	1231.27	427.47	*
16	15:34:00	732.35	1119.74	*
17	15:35:00	392.65		*
18	15:36:00	739.12		*
19	15:37:00	482.48		*
20	15:38:00	399.14		*
	Minimum	392.65	427.47	
	Average	1590.06	1528.25	
	Maximum	3898.33	5229.31	
	Std Dev	2188.45	2727.00	

* Rise rates for Bocca Nuova and Southeast Crater were 7.61 and 9.68 meters per second respectively.

20 July 1987

Tripod-mounted COSPEC, horizontal scans (summit)

Run	Time (HH:MM:SS)	Flux (tpd) Bocca Nuova	Flux (tpd) Southeast Crater	Rise Rate (m/s)
8	08:49:00	622.28	165.33	*
9	08:51:00	339.14	410.69	*
11	08:55:00	556.07	207.01	*
12	08:57:00	652.75	380.40	*
13	08:59:00	277.60	463.79	*
14	09:04:00	815.16	583.81	*
15	09:06:00	547.54	771.49	*
16	09:08:00	681.32	584.90	*
17	09:10:00	1456.96	581.10	*
18	09:12:00	1751.03	636.26	*
19	09:14:00	1095.37	637.99	*
20	09:16:00	575.68	419.05	*
21	09:18:00	878.95	259.49	*
22	09:20:00	1357.17	276.97	*
23	09:22:00	1444.06	281.65	*
24	09:24:00	1449.01	489.29	*
25	09:26:00	1581.62		*
26	09:28:00	1239.88		*
27	09:30:00	1158.80	325.43	*
28	09:32:00	1342.53	734.98	*
29	09:34:00	1272.16	324.74	*
30	09:36:00	838.06	737.80	*
31	09:38:00	1054.60	398.56	*
32	09:40:00	776.59	316.85	*
33	09:42:00	500.07	278.13	*
34	09:44:00	651.49	230.43	*
35	09:46:00	697.95	731.63	*
36	09:48:00	523.28	586.18	*
37	09:50:00	498.56	702.46	*
38	09:52:00	743.24	465.36	*
40	09:56:00	1257.86	362.65	*
41	09:58:00	1046.73	386.72	*
42	10:00:00	1175.99	448.39	*
43	10:02:00	1468.05	300.65	*
44	10:04:00	1063.23	323.67	*
45	10:06:00	1076.60	357.35	*
46	10:08:00	947.07	359.80	*
47	10:10:00	1232.77	172.89	*
48	10:12:00	1245.87	321.97	*
49	10:14:00	1537.12	264.01	*
50	10:16:00	1088.56	394.78	*
51	10:18:00	1255.52		*
52	10:20:00	1077.40		*
53	10:22:00	1139.78		*

Minimum	277.60	165.33
Average	999.81	427.56
Maximum	1751.03	771.49
Std Dev	725.78	336.41

* Rise rates for Bocca Nuova and Southeast Crater were 11.03 and 9.35 meters per second respectively.

---

22 July 1987

Tripod-mounted COSPEC, horizontal scans (summit)

Run	Time (HH:MM:SS)	Flux (tpd) Bocca Nuova	Flux (tpd) Southeast Crater	Rise Rate (m/s)
3	13:39:00	433.99	217.02	*

* Rise rates for Bocca Nuova and Southeast Crater were 8.03 and 8.77 meters per second respectively

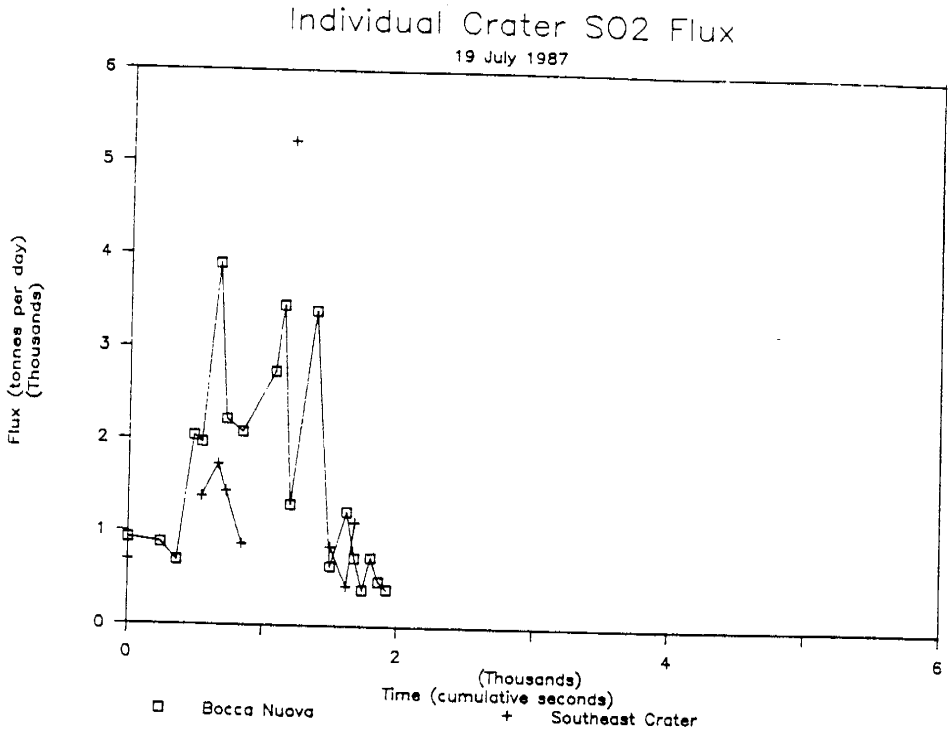
Individual Crater SO2 Flux
19 July 1987
Flux (tonnes per day)
(Thousands)
0
1
2
3
4
5
6
0
2
4
6
(Thousands)
Time (cumulative seconds)
Bocca Nuova
Southeast Crater

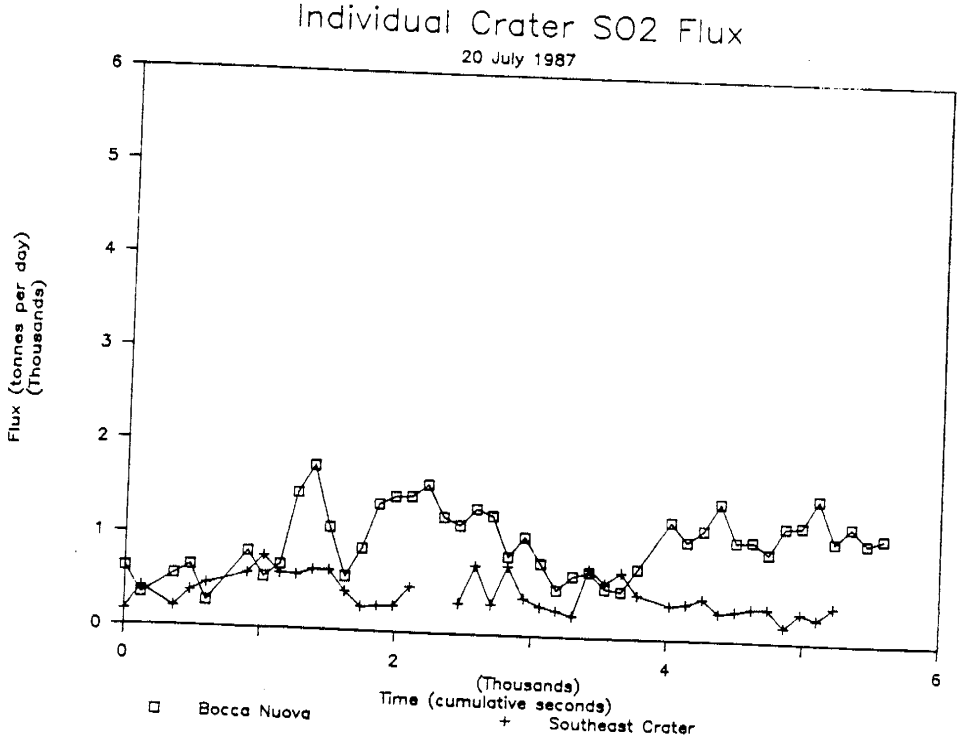
Individual Crater SO2 Flux
20 July 1987
Flux (tonnes per day)
(Thousands)
0
1
2
3
4
5
6
0
2
4
6
(Thousands)
Time (cumulative seconds)
Bocca Nuova
Southeast Crater

Appendix III. Total System SO_2 Fluxes. The date, type of COSPEC scan and scan site heads each page. Time of measurement is reported in hours, minutes, and seconds (HH:MM:SS); SO_2 fluxes in tonnes per day (tpd); and rise rates or wind speeds in meters per second (m/s). Standard deviation computed to 95 percent confidence interval. Graphs plotted with identical axes.

---

27 June 1987

Automobile-mounted COSPEC (Catania-Taormina)

Run	Time (HH:MM:SS)	Flux (tpd)	Wind Speed (m/s)
1	13:00:00	273.98	2
2	13:45:00	176.09	2
	Minimum	176.09	
	Average	225.04	
	Maximum	273.98	
	Std Dev	97.89	

---

27 June 1987

Automobile-mounted COSPEC (Fornazzo-Vena)

Run	Time (HH:MM:SS)	Flux (tpd)	Wind Speed (m/s)
1	14:43:30	909.11	2
2	15:06:00	917.06	2
3	15:26:00	620.03	2
4	15:33:06	531.21	2
5	16:21:00	679.43	2
	Minimum	531.21	
	Average	731.37	
	Maximum	917.06	
	Std Dev	311.42	

3 July 1987

Tripod-mounted COSPEC, horizontal scans (summit)

Run	Time (HH:MM:SS)	Flux (tpd)	Rise Rate (m/s)
1	14:27:30	459.87	8
2	14:32:00	373.39	8
3	14:38:00	245.57	8
4	16:44:30	453.33	8
5	16:48:00	366.17	8
6	16:51:00	621.84	8
7	16:55:30	273.87	8
8	17:00:00	177.90	8
	Minimum	177.90	
	Average	371.49	
	Maximum	621.84	
	Std Dev	264.65	

---

4 July 1987

Tripod-mounted COSPEC, horizontal scans (summit)

Run	Time (HH:MM:SS)	Flux (tpd)	Rise Rate (m/s)
1	07:12:50	311.29	7.5
2	07:19:30	271.96	7.5
3	07:22:30	336.67	7.5
4	07:25:30	316.78	7.5
5	07:28:30	324.96	7.5
6	07:31:30	267.39	7.5
7	07:34:30	362.65	7.5
8	07:37:30	441.68	7.5
9	07:40:30	250.10	7.5
10	07:43:30	337.55	7.5
11	07:46:30	290.46	7.5
12	07:49:30	396.97	7.5
13	07:52:30	494.51	7.5
14	07:55:30	443.09	7.5
15	08:01:00	351.71	7.5
	Minimum	250.10	
	Average	346.52	
	Maximum	494.51	
	Std Dev	136.77	

12 July 1987

Automobile-mounted COSPEC (Ragalna-Tardaria)

Run	Time (HH:MM:SS)	Flux (tpd)	Wind Speed (m/s)
1	08:20:00	1015.09	1
2	09:00:00	1362.63	1
	Minimum	1015.09	
	Average	1188.86	
	Maximum	1362.63	
	Std Dev	347.54	

---

13 July 1987

Tripod-mounted COSPEC, horizontal scans (Orchard Site)

Run	Time (HH:MM:SS)	Flux (tpd)	Rise Rate (m/s)
1	08:13:00	138.98	3
2	08:20:00	127.73	3
3	08:23:00	117.93	3
4	08:26:00	134.49	3
5	08:42:00	235.81	3
6	08:44:00	207.44	3
7	08:49:00	343.34	3
	Minimum	117.93	
	Average	186.53	
	Maximum	343.34	
	Std Dev	152.29	

14 July 1987

Automobile-mounted COSPEC (Fornazzo-Monterosso)

Run	Time (HH:MM:SS)	Flux (tpd)	Wind Speed (m/s)
1	08:24:00	556.16	1.5
2	08:39:00	751.47	1.5
3	09:01:00	737.24	1.5
	Minimum	556.16	
	Average	681.62	
	Maximum	751.47	
	Std Dev	177.81	

---

15 July 1987

Automobile-mounted COSPEC (Nicolosi-Trecastagni)

Run	Time (HH:MM:SS)	Flux (tpd)	Wind Speed (m/s)
1	07:51:00	1247.25	5
2	08:16:00	859.26	5
3	08:43:00	925.08	5
	Minimum	859.26	
	Average	1010.53	
	Maximum	1247.25	
	Std Dev	339.06	

---

16 July 1987

Automobile-mounted COSPEC (Nicolosi-Fleri)

Run	Time (HH:MM:SS)	Flux (tpd)	Wind Speed (m/s)
1	07:22:00	422.26	1.5
2	07:46:00	534.66	1.5
3	08:23:00	391.53	1.5
4	08:37:00	684.66	1.5
5	08:53:00	551.36	1.5
	Minimum	391.53	
	Average	516.89	
	Maximum	684.66	
	Std Dev	208.46	

19 July 1987

Tripod-mounted COSPEC, horizontal scans (summit)

Run	Time (HH:MM:SS)	Flux (tpd)	Rise Rate (m/s)
1	15:06:00	1620.19	*
5	15:15:00	3354.21	*
6	15:17:00	5631.04	*
7	15:18:00	3661.78	*
8	15:20:00	2956.59	*
12	15:26:00	6534.77	*
14	15:31:00	1490.60	*
15	15:33:00	1658.74	*
16	15:34:00	1852.09	*
	Minimum	1490.60	
	Average	3195.56	
	Maximum	6534.77	
	Std Dev	3460.06	

* Different rise rate for each crater, see Appendix III

---

20 July 1987

Tripod-mounted COSPEC, horizontal scans (summit)

Run	Time (HH:MM:SS)	Flux (tpd)	Rise Rate (m/s)
1	08:35:00	1602.72	10.19
2	08:37:00	2136.70	10.19
3	08:39:00	2295.20	10.19
4	08:41:00	1315.56	10.19
5	08:43:00	2116.01	10.19
6	08:45:00	1289.26	10.19
7	08:47:00	1022.05	10.19
8	08:49:00	787.61	*
9	08:51:00	749.82	*
10	08:53:00	598.72	10.19
11	08:55:00	763.08	*
12	08:57:00	1033.15	*
13	08:59:00	741.39	*
14	09:04:00	1398.97	*
15	09:06:00	1319.03	*
16	09:08:00	1266.21	*
17	09:10:00	2038.06	*
18	09:12:00	2387.29	*
19	09:14:00	1733.36	*
20	09:16:00	994.73	*

21	09:18:00	1138.44	*
22	09:20:00	1634.14	*
23	09:22:00	1725.71	*
24	09:24:00	1938.30	*
27	09:30:00	1484.24	*
28	09:32:00	2077.51	*
29	09:34:00	1596.90	*
30	09:36:00	1575.86	*
31	09:38:00	1453.16	*
32	09:40:00	1093.44	*
33	09:42:00	778.20	*
34	09:44:00	881.93	*
35	09:46:00	1429.58	*
36	09:48:00	1109.46	*
37	09:50:00	1201.02	*
38	09:52:00	1208.59	*
39	09:54:00	1002.45	10.19
40	09:56:00	1620.52	*
41	09:58:00	1433.45	*
42	10:00:00	1624.38	*
43	10:02:00	1768.70	*
44	10:04:00	1386.89	*
45	10:06:00	1433.95	*
46	10:08:00	1306.87	*
47	10:10:00	1405.66	*
48	10:12:00	1567.84	*
49	10:14:00	1801.12	*
50	10:16:00	1483.34	*

Minimum	598.72
Average	1411.47
Maximum	2387.29
Std Dev	852.33

* Different rise rate for each crater, see Appendix III

22 July 1987

Tripod-mounted COSPEC, horizontal scans (summit)

Run	Time (HH:MM:SS)	Flux (tpd)	Rise Rate (m/s)
1	13:37:00	763.52	8.4
2	13:39:00	725.59	8.4
3	13:41:00	651.01	*
4	13:43:00	696.45	8.4
5	13:45:00	1026.95	8.4
	Minimum	651.01	
	Average	772.70	
	Maximum	1026.95	
	Std Dev	264.68	

* Different rise rate for each crater, see Appendix III

---

29 July 1987

Tripod-mounted COSPEC, vertical scans (summit)

Run	Time (HH:MM:SS)	Flux (tpd)	Rise Rate (m/s)
1	10:33:00	384.49	3.5
2	10:35:00	609.46	3.5
3	10:37:00	468.70	3.5
4	10:39:00	572.11	3.5
5	10:41:00	683.36	3.5
6	10:43:00	618.52	3.5
7	10:45:00	679.31	3.5
8	10:47:00	581.67	3.5
9	10:49:00	826.57	3.5
10	10:51:00	641.91	3.5
11	10:53:00	783.65	3.5
12	10:55:00	638.38	3.5
13	10:57:00	734.75	3.5
14	10:59:00	859.46	3.5
	Minimum	384.49	
	Average	648.74	
	Maximum	859.46	
	Std Dev	250.13	

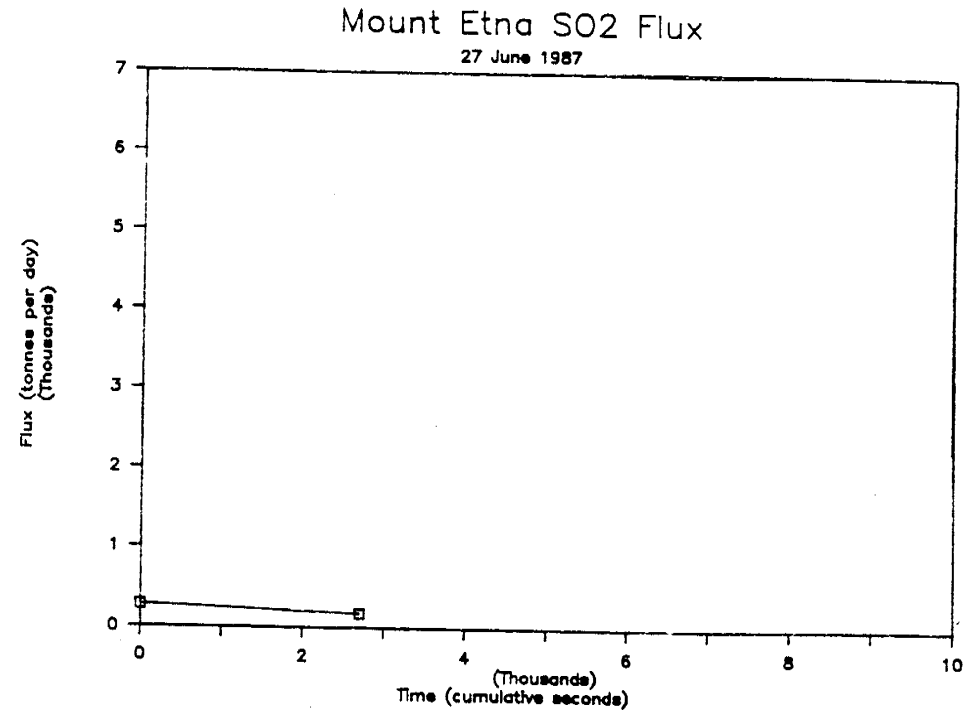
Mount Etna SO2 Flux
27 June 1987
Flux (tonnes per day)
(Thousands)
7
6
5
4
3
2
1
0
0
2
4
6
8
10
(Thousands)
Time (cumulative seconds)

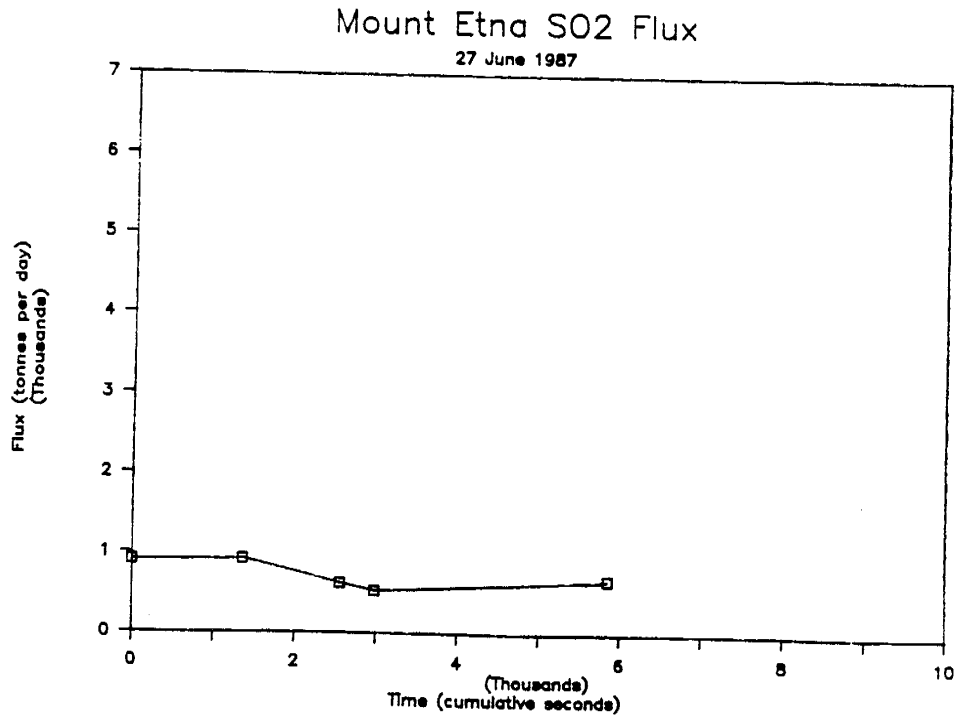
Mount Etna SO2 Flux
27 June 1987
Flux (tonnes per day)
(Thousands)
7
6
5
4
3
2
1
0
0
2
4
6
8
10
(Thousands)
Time (cumulative seconds)

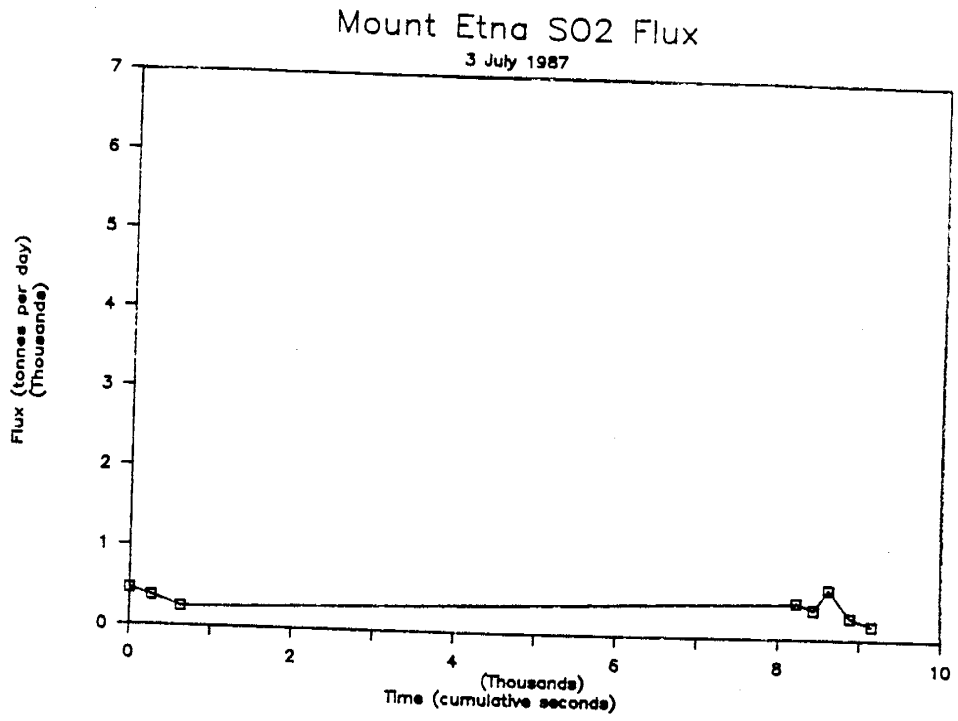
Mount Etna SO2 Flux
3 July 1987
Flux (tonnes per day)
(Thousands)
0
1
2
3
4
5
6
7
0
2
4
6
8
10
(Thousands)
Time (cumulative seconds)

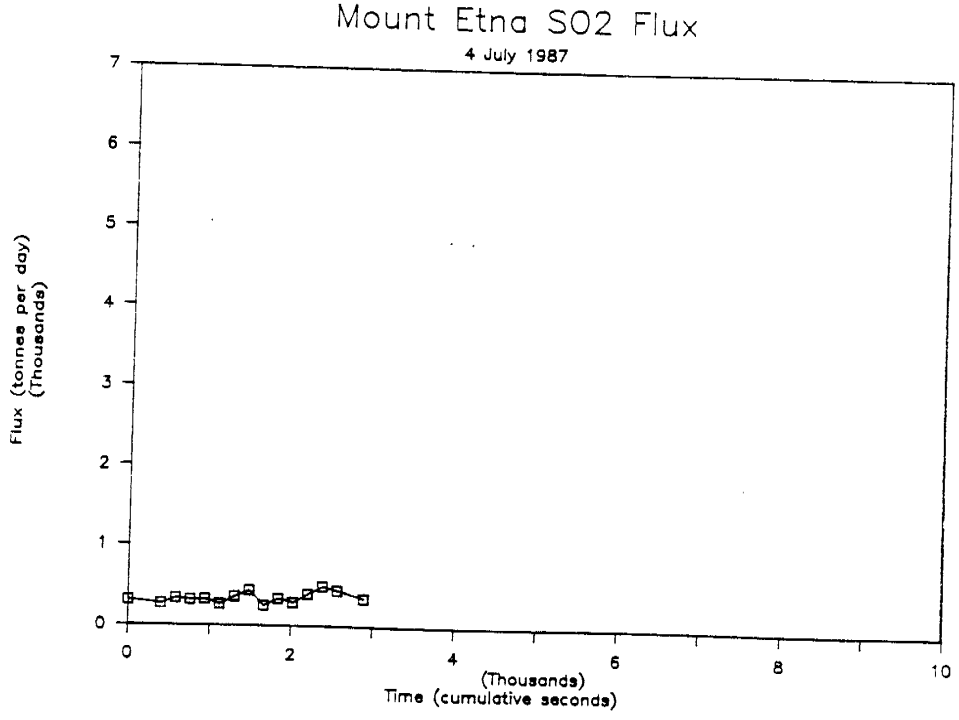
Mount Etna SO2 Flux
4 July 1987
Flux (tonnes per day)
(Thousands)
0
1
2
3
4
5
6
7
0
2
4
6
8
10
(Thousands)
Time (cumulative seconds)

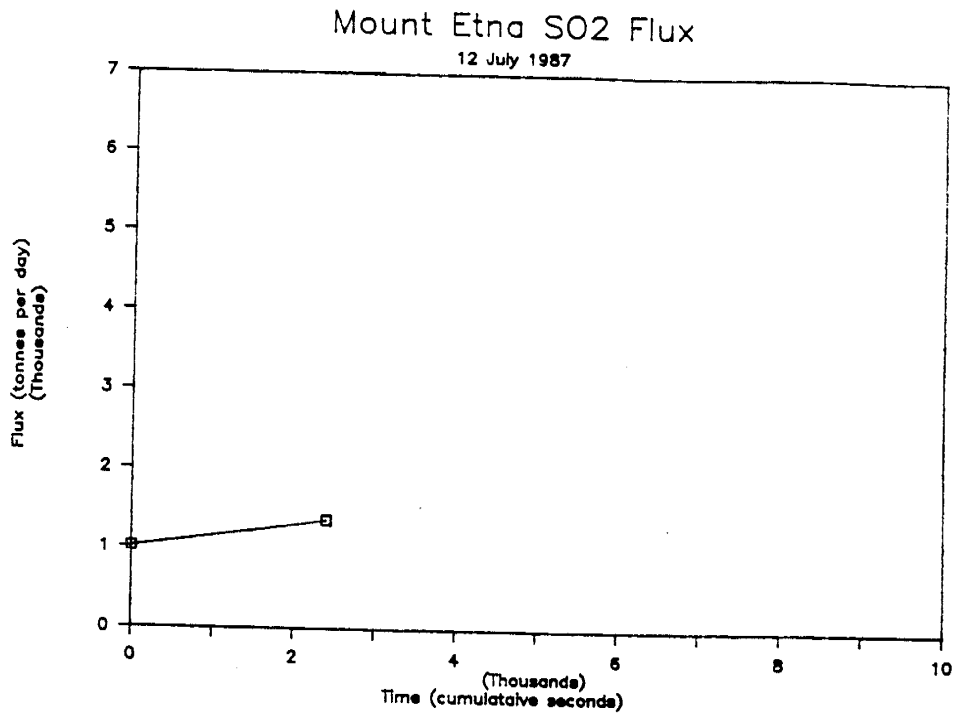
Mount Etna SO2 Flux
12 July 1987
Flux (tonnes per day)
(Thousands)
0
1
2
3
4
5
6
7
0
2
4
6
8
10
(Thousands)
Time (cumulatalve seconds)

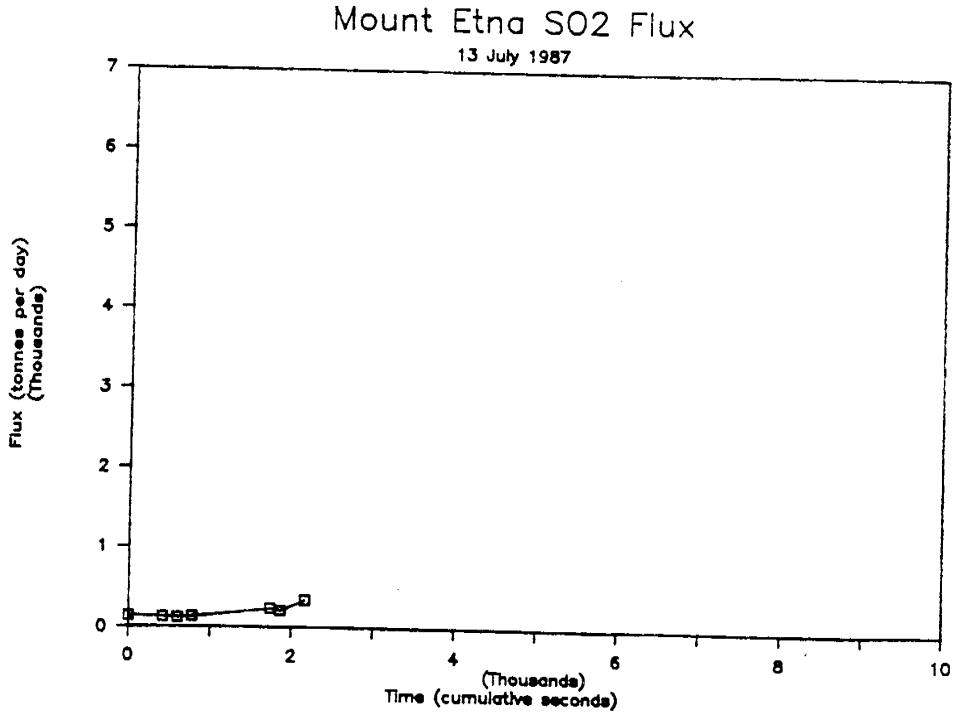
Mount Etna SO2 Flux
13 July 1987
Flux (tonnes per day)
(Thousands)
0
1
2
3
4
5
6
7
0
2
4
6
8
10
(Thousands)
Time (cumulative seconds)

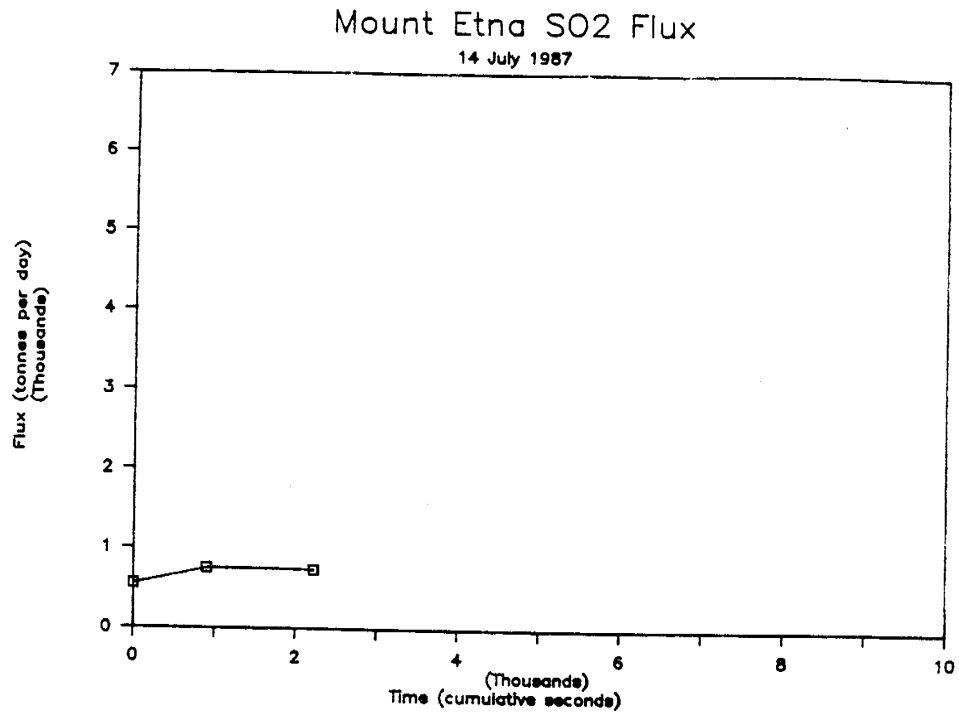
Mount Etna SO2 Flux
14 July 1987
Flux (tonnes per day)
(Thousands)
7
6
5
4
3
2
1
0
0
2
4
6
8
10
(Thousands)
Time (cumulative seconds)

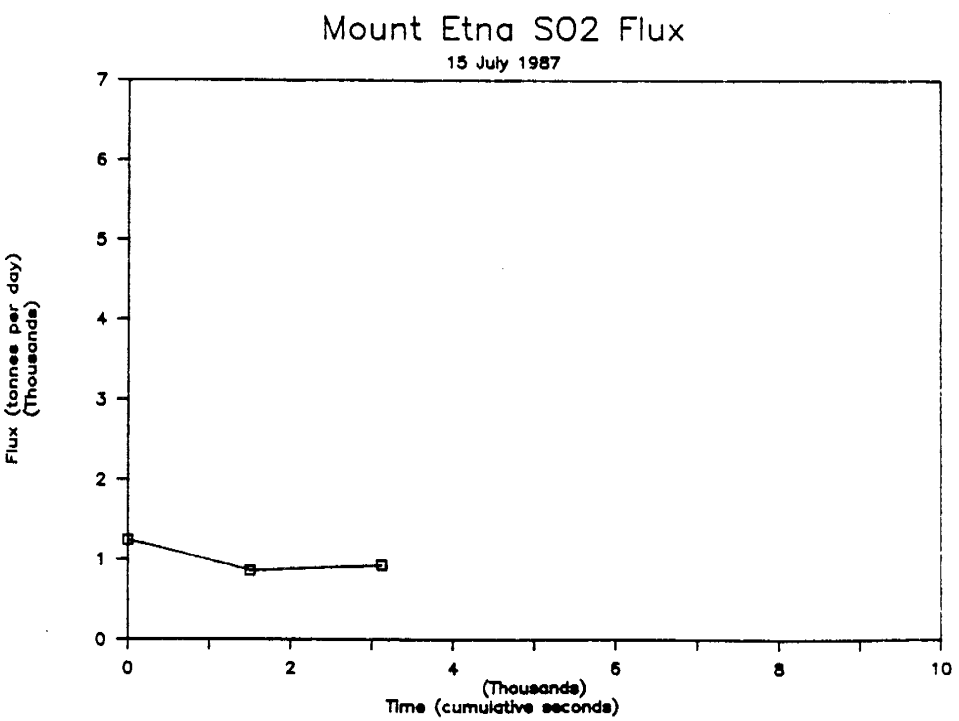
Mount Etna SO2 Flux
15 July 1987
Flux (tonnes per day)
(Thousands)
7
6
5
4
3
2
1
0
0
2
4
6
8
10
(Thousands)
Time (cumulative seconds)

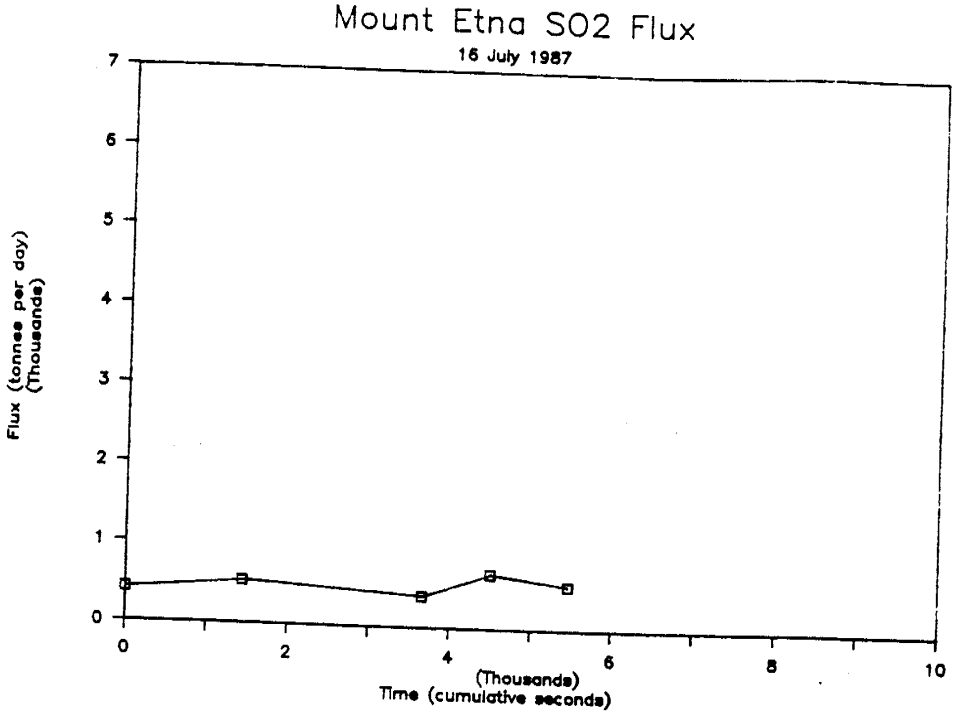
Mount Etna SO2 Flux
16 July 1987
Flux (tonnes per day)
(Thousands)
0
1
2
3
4
5
6
7
0
2
4
6
8
10
(Thousands)
Time (cumulative seconds)

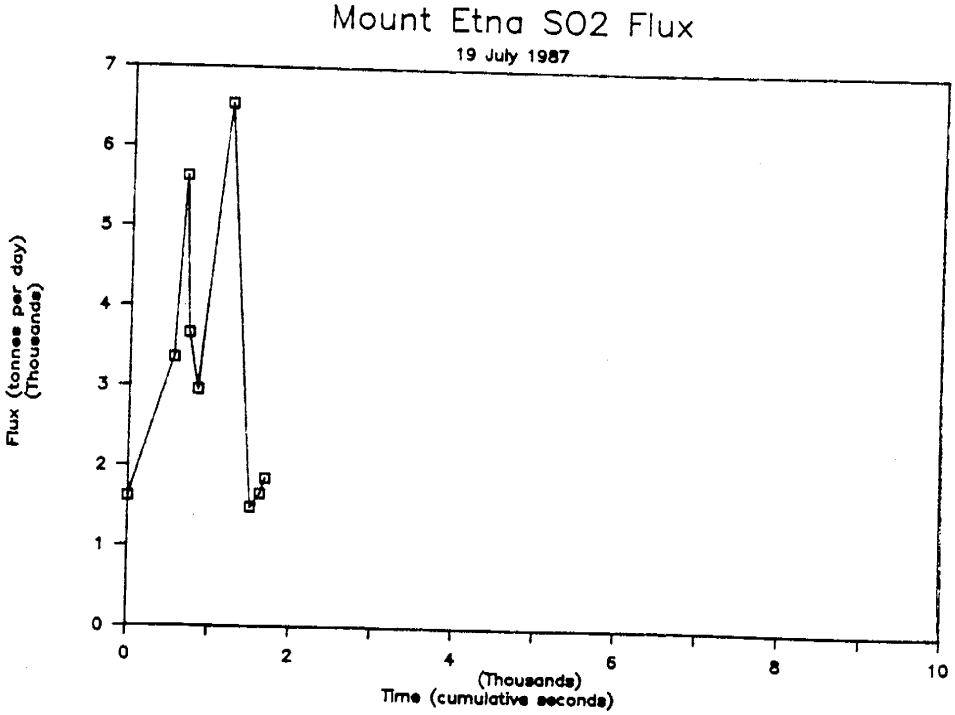
Mount Etna SO2 Flux
19 July 1987
Flux (tonnes per day)
(Thousands)
0
1
2
3
4
5
6
7
0
2
4
6
8
10
(Thousands)
Time (cumulative seconds)

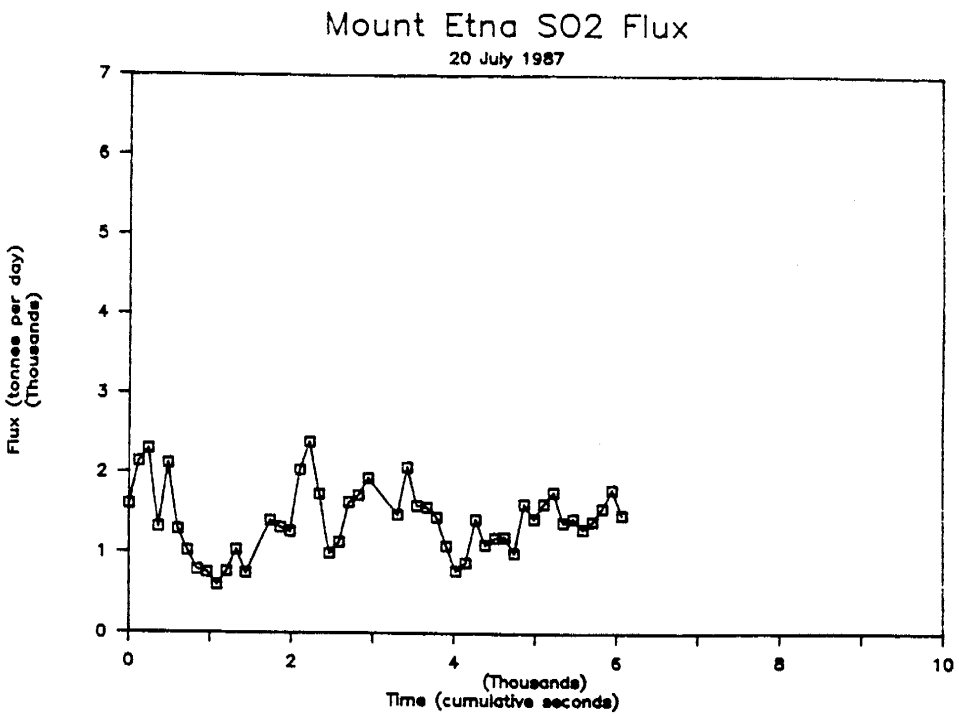
Mount Etna SO2 Flux
20 July 1987
Flux (tonnes per day)
(Thousands)
0
1
2
3
4
5
6
7
0
2
4
6
8
10
(Thousands)
Time (cumulative seconds)

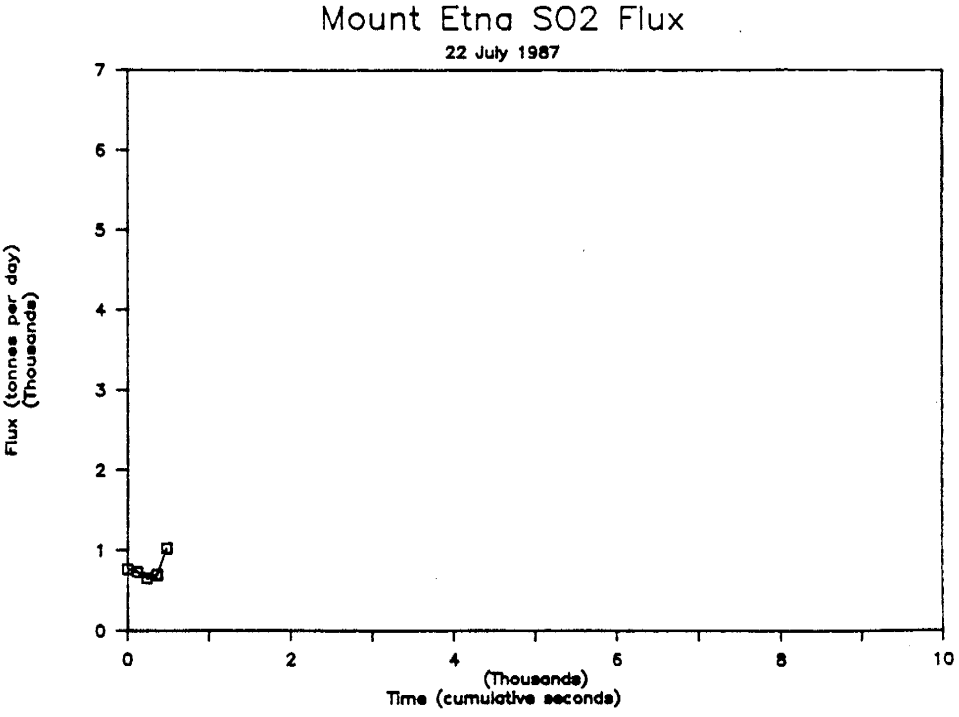
Mount Etna SO2 Flux
22 July 1987
Flux (tonnes per day)
(Thousands)
0
1
2
3
4
5
6
7
0
2
4
6
8
10
(Thousands)
Time (cumulative seconds)

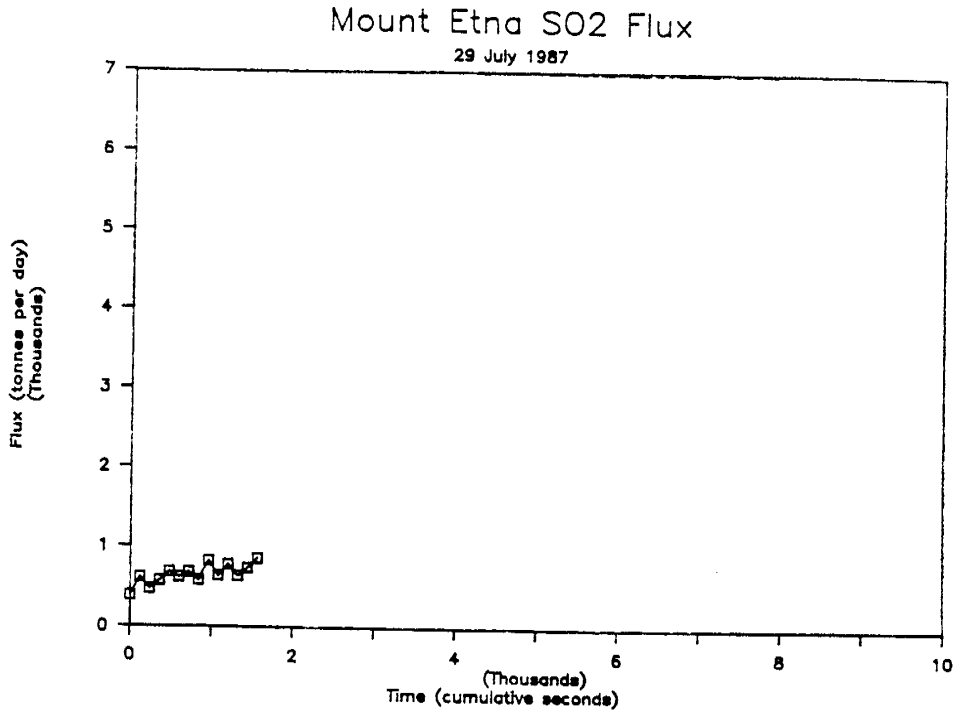
Mount Etna SO2 Flux
29 July 1987
Flux (tonnes per day)
(Thousands)
0
1
2
3
4
5
6
7
0
2
4
6
8
10
(Thousands)
Time (cumulative seconds)

Appendix IV. Elemental Concentrations Determined by INAA. All values reported in micrograms per cubic meter. The 1, 2, 3 denote Bocca Nuova samples #1, #2, and the Southeast Crater sample respectively. The letter "a" denotes the particle filter and "b - e" the ^{7}LiOH treated filters. Filter totals may not equal summation of individual filter data due to rounding.

n.d. = not detected

filter	Al	As	Br	Cd	Ce	Cs
1a	50	0.20	1.1	0.22	5.6E-02	6.5E-02
1b	26	8.4E-02	16	n.d.	3.0E-02	1.1E-02
1c	26	1.6E-03	1.2	n.d.	n.d.	n.d.
1d	38	6.3E-02	10	n.d.	n.d.	n.d.
1e	40	0.15	14	n.d.	n.d.	n.d.
2a	14	0.34	1.5	0.35	n.d.	5.7E-02
2b	8.2	0.11	25	n.d.	5.6E-02	n.d.
2c	17	3.3E-04	3.7	n.d.	n.d.	n.d.
2d	20	n.d.	n.d.	n.d.	n.d.	n.d.
2e	16	n.d.	n.d.	n.d.	n.d.	n.d.
3a	14	0.47	20	0.60	n.d.	0.19
3b	12	0.75	7.4	n.d.	n.d.	n.d.
3c	16	4.4E-03	0.40	n.d.	n.d.	n.d.
3d	5.6	n.d.	0.25	n.d.	n.d.	n.d.
3e	29	n.d.	2.1	n.d.	n.d.	n.d.

	Cl	Co	Cu	Eu	F	Au
1a	n.d.	1.3E-02	5.3	1.7E-03	11	1.2E-03
1b	3890	3.4E-03	n.d.	n.d.	507	n.d.
1c	57	n.d.	n.d.	n.d.	14	n.d.
1d	2579	n.d.	n.d.	n.d.	237	n.d.
1e	4666	n.d.	n.d.	n.d.	417	n.d.
2a	n.d.	2.9E-02	17	2.2E-03	n.d.	1.6E-03
2b	6005	3.4E-02	n.d.	9.9E-05	753	n.d.
2c	127	4.9E-02	n.d.	n.d.	33	n.d.
2d	63	1.1E-02	n.d.	n.d.	17	n.d.
2e	n.d.	4.5E-02	n.d.	n.d.	11	n.d.
3a	302	1.1E-02	n.d.	n.d.	111	2.5E-03
3b	4660	1.8E-03	n.d.	2.4E-03	1286	n.d.
3c	88	n.d.	n.d.	n.d.	n.d.	n.d.
3d	74	n.d.	n.d.	n.d.	n.d.	n.d.
3e	369	n.d.	n.d.	n.d.	n.d.	n.d.

	In	Fe	La	Mn	Mo	K
1a	1.4E-02	53	3.3E-02	0.98	1.8E-02	196
1b	n.d.	1.3	9.0E-03	n.d.	n.d.	n.d.
1c	n.d.	n.d.	1.8E-03	n.d.	n.d.	n.d.
1d	n.d.	n.d.	3.1E-02	n.d.	n.d.	n.d.
1e	n.d.	n.d.	2.3E-02	n.d.	n.d.	n.d.
2a	3.5E-02	33	1.2E-02	0.59	3.2	211
2b	n.d.	n.d.	n.d.	n.d.	n.d.	n.d.
2c	n.d.	n.d.	n.d.	n.d.	n.d.	n.d.
2d	n.d.	n.d.	n.d.	n.d.	n.d.	n.d.
2e	n.d.	n.d.	n.d.	n.d.	n.d.	n.d.
3a	7.5E-02	30	n.d.	0.23	0.11	240
3b	n.d.	3.1	1.2E-02	n.d.	n.d.	n.d.
3c	n.d.	4.1	1.4E-02	n.d.	n.d.	n.d.
3d	n.d.	n.d.	1.9E-03	n.d.	n.d.	n.d.
3e	n.d.	n.d.	1.3E-02	n.d.	n.d.	n.d.

	Re	Rb	Sm	Sc	Se	Na
1a	4.2E-03	0.62	4.4E-03	7.0E-03	8.0E-02	179
1b	1.5E-03	n.d.	7.3E-04	2.7E-03	1.0E-02	3.3
1c	n.d.	n.d.	1.7E-04	1.3E-03	n.d.	4.6
1d	n.d.	n.d.	1.6E-03	3.6E-03	n.d.	8.1
1e	n.d.	n.d.	2.6E-03	5.9E-03	n.d.	14
2a	n.d.	1.4	1.3E-03	1.6E-03	0.50	237
2b	1.5E-03	n.d.	n.d.	n.d.	2.0E-02	0.11
2c	n.d.	n.d.	n.d.	n.d.	n.d.	1.0
2d	n.d.	n.d.	n.d.	n.d.	n.d.	2.9
2e	n.d.	n.d.	n.d.	n.d.	n.d.	0.71
3a	n.d.	1.7	n.d.	9.0E-04	0.25	245
3b	9.2E-04	n.d.	9.8E-04	3.2E-03	3.6E-02	n.d.
3c	n.d.	n.d.	1.9E-03	3.5E-03	1.1E-02	n.d.
3d	n.d.	n.d.	n.d.	n.d.	8.7E-03	n.d.
3e	n.d.	n.d.	n.d.	n.d.	1.7E-02	n.d.

	S	W	U	V	Yb	Zn
1a	679	n.d.	n.d.	0.20	2.5E-03	1.4
1b	n.d.	8.1E-03	n.d.	n.d.	n.d.	22
1c	1011	4.4E-03	n.d.	n.d.	n.d.	4.2
1d	n.d.	2.4E-02	n.d.	n.d.	n.d.	3.2
1e	n.d.	n.d.	n.d.	n.d.	n.d.	2.6
2a	n.d.	n.d.	n.d.	0.12	2.9E-03	3.5
2b	n.d.	1.0E-02	n.d.	n.d.	n.d.	31
2c	1906	2.2E-02	n.d.	n.d.	n.d.	37
2d	1555	n.d.	n.d.	n.d.	n.d.	27
2e	n.d.	n.d.	n.d.	n.d.	n.d.	23
3a	n.d.	n.d.	n.d.	0.11	4.2E-03	7.0
3b	4188	n.d.	6.2E-03	4.6E-02	n.d.	25
3c	5196	1.2E-02	7.2E-03	n.d.	n.d.	45
3d	3820	n.d.	n.d.	n.d.	n.d.	27
3e	n.d.	n.d.	n.d.	n.d.	n.d.	52

TOTALS

Element	1	2	3	Error*
Al	179	76	77	5
As	0.49	0.45	1.2	5
Br	42	30	30	1
Cd	0.22	0.35	6.0E-1	24
Ce	8.6E-2	5.6E-2	n.d.	8
Cs	7.7E-2	5.7E-2	0.19	7
Cl	11191	6195	5492	8
Co	1.7E-2	0.17	1.3E-2	13
Cu	5.3	17	n.d.	29
Eu	1.7E-3	2.3E-3	2.4E-3	24
F	1186	813	1397	13
Au	1.2E-3	1.6E-3	2.5E-3	4
In	1.4E-2	3.5E-2	7.5E-2	18
Fe	54	33	37	16
La	0.10	1.2E-2	4.1E-2	11
Mn	0.98	0.59	0.23	29
Mo	1.8E-2	3.2	0.11	8
K	196	211	240	14
Re	5.7E-3	1.5E-3	9.2E-4	11
Rb	0.62	1.4	1.7	8
Sm	9.5E-3	1.3E-3	2.9E-3	3
Sc	2.1E-2	1.6E-3	7.6E-3	7
Se	9.0E-2	0.52	0.32	17
Na	209	241	245	5
S	1689	3461	13205	14
W	3.6E-2	3.2E-2	1.2E-2	24
U	n.d.	n.d.	1.3E-2	20
V	0.20	0.12	0.16	7
Yb	2.5E-3	2.9E-3	4.2E-3	16
Zn	34	122	156	2
Pump Time (MM:SS)	30:00	37:50	20:00	

* Analytical errors estimated by Meeker, personal communication.

Fraction of Elemental concentration Located on Particle Filter.

Element	1	2	3
Al	0.28	0.19	0.19
As	0.40	0.76	0.39
Br	0.03	0.05	0.66
Cd	1.00	1.00	1.00
Ce	0.66	0.00	-----
Cs	0.85	1.00	1.00
Cl	0.00	0.00	0.05
Co	0.79	0.17	0.86
Cu	1.00	1.00	-----
Eu	1.00	0.96	0.00
F	0.01	0.00	0.08
Au	1.00	1.00	1.00
In	1.00	1.00	1.00
Fe	0.98	1.00	0.81
La	0.33	1.00	0.00
Mn	1.00	1.00	1.00
Mo	1.00	1.00	1.00
K	1.00	1.00	1.00
Re	0.74	0.00	0.00
Rb	1.00	1.00	1.00
Sm	0.46	1.00	0.00
Sc	0.34	1.00	0.12
Se	0.88	0.96	0.78
Na	0.86	0.98	1.00
S	0.40	0.00	0.00
W	0.00	0.00	0.00
U	-----	-----	0.00
V	1.00	1.00	0.71
Yb	1.00	1.00	1.00
Zn	0.04	0.03	0.05

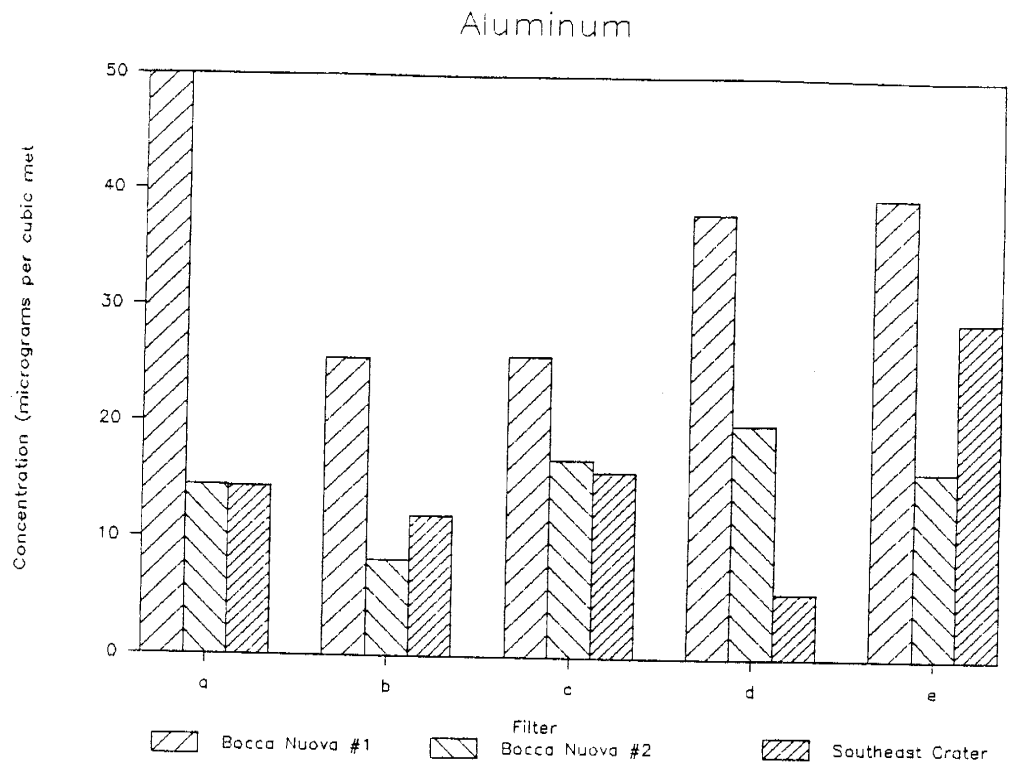
Aluminum
Concentration (micrograms per cubic met
50
40
30
20
10
0
a
b
c
d
e
Filter
Bocca Nuova #1
Bocca Nuova #2
Southeast Crater

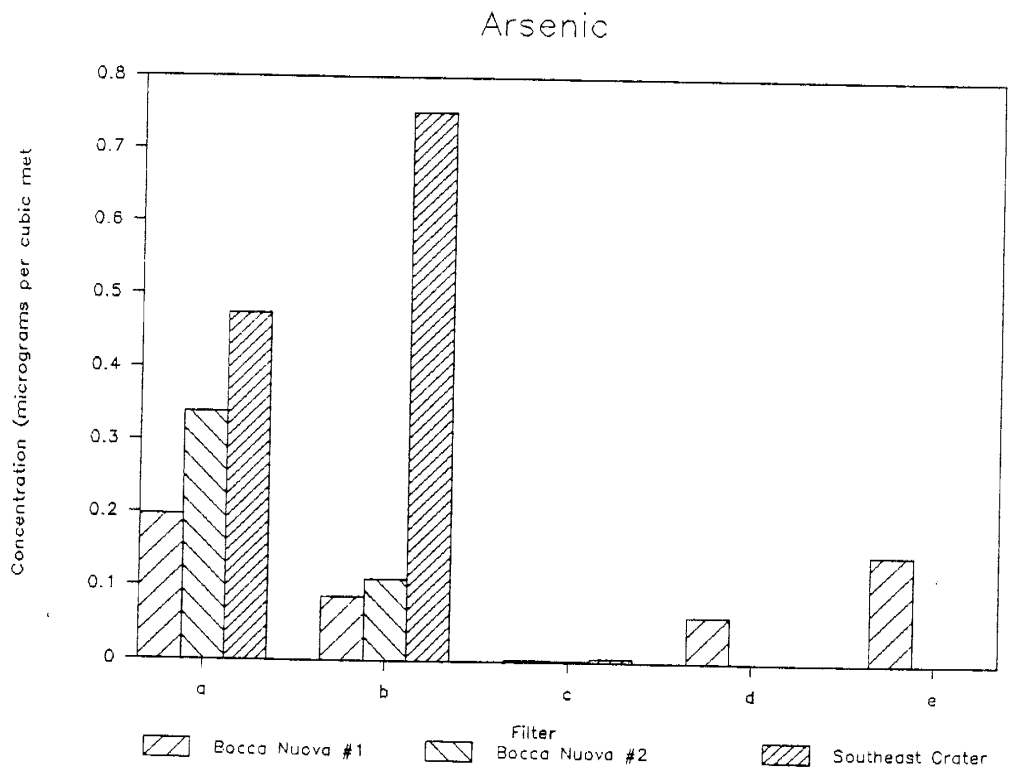
Arsenic
Concentration (micrograms per cubic met
0.8
0.7
0.6
0.5
0.4
0.3
0.2
0.1
0
a
b
c
d
e
Filter
Bocca Nuova #1
Bocca Nuova #2
Southeast Crater

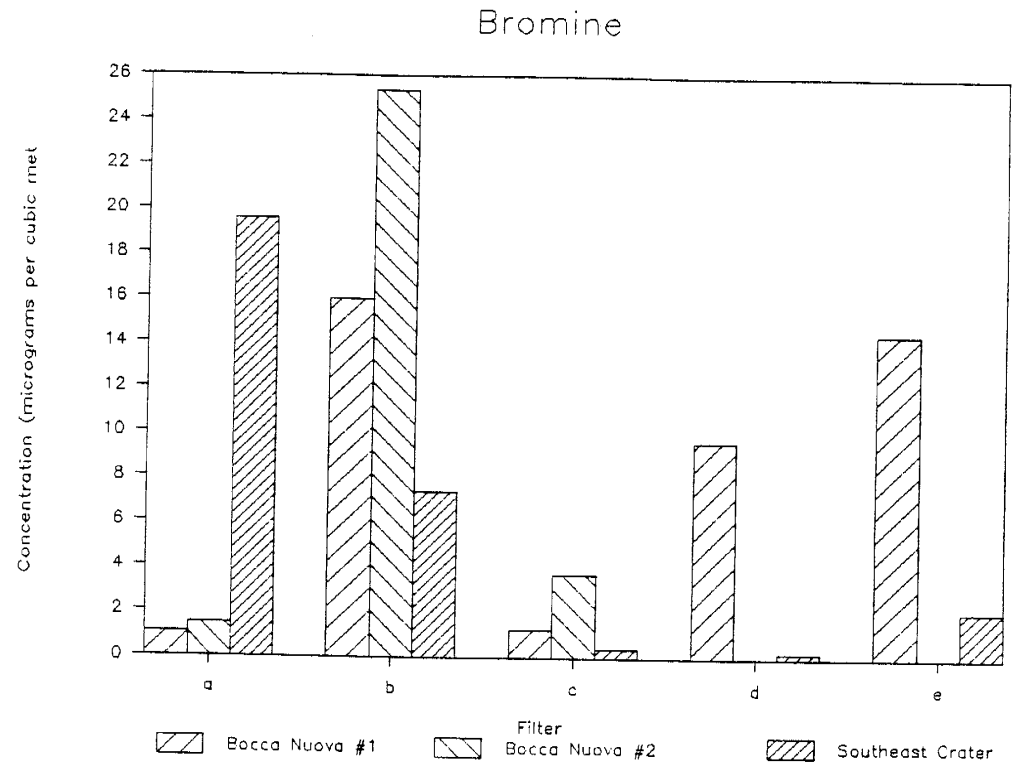
Bromine
Concentration (micrograms per cubic met
26
24
22
20
18
16
14
12
10
8
6
4
2
0
a
b
c
d
e
Filter
Bocca Nuova #1
Bocca Nuova #2
Southeast Crater

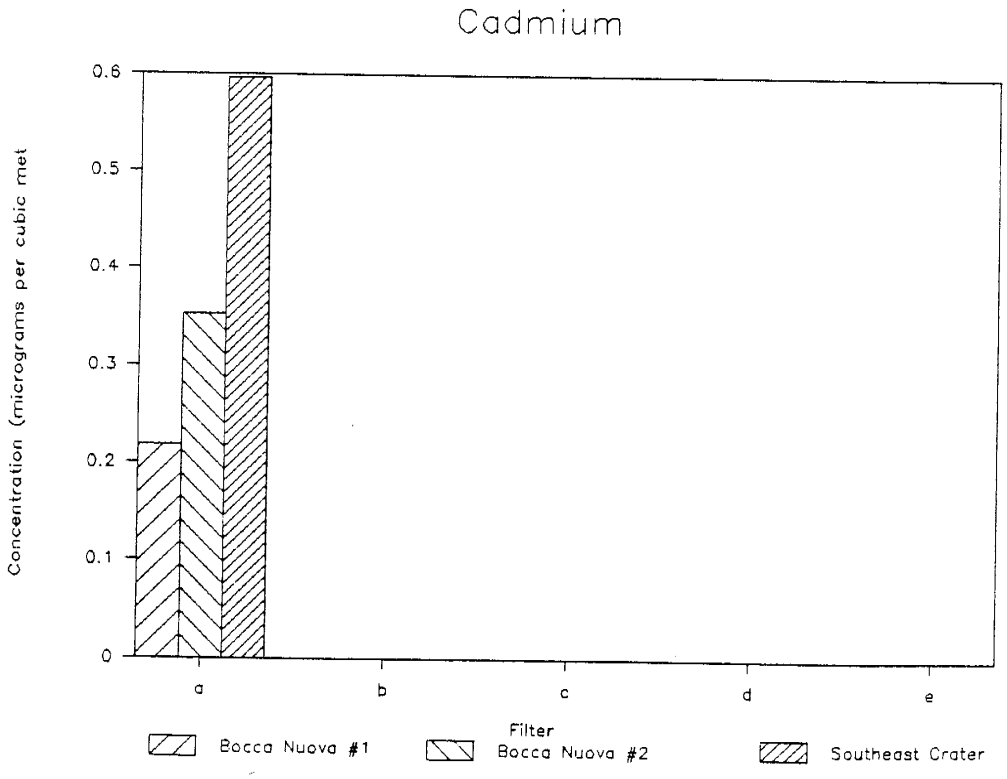
Cadmium
Concentration (micrograms per cubic met
0.6
0.5
0.4
0.3
0.2
0.1
0
a
b
c
d
e
Filter
Bocca Nuova #1
Bocca Nuova #2
Southeast Crater

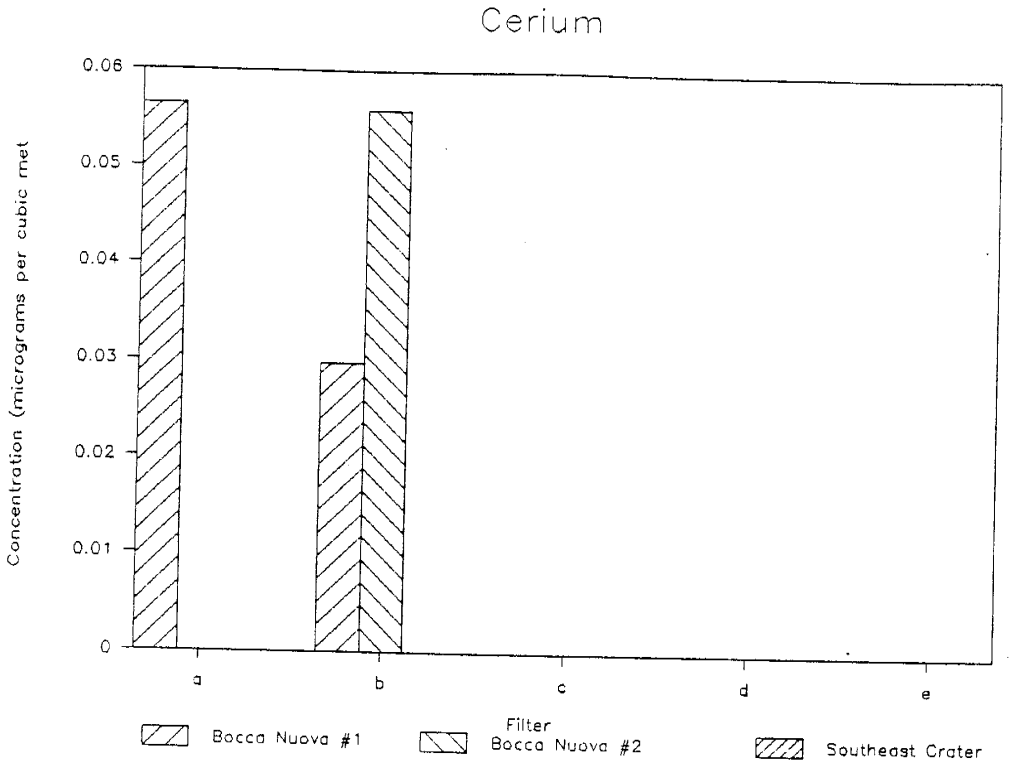
Cerium
Concentration (micrograms per cubic met
0.06
0.05
0.04
0.03
0.02
0.01
0
a
b
c
d
e
Filter
Bocca Nuova #1
Bocca Nuova #2
Southeast Crater

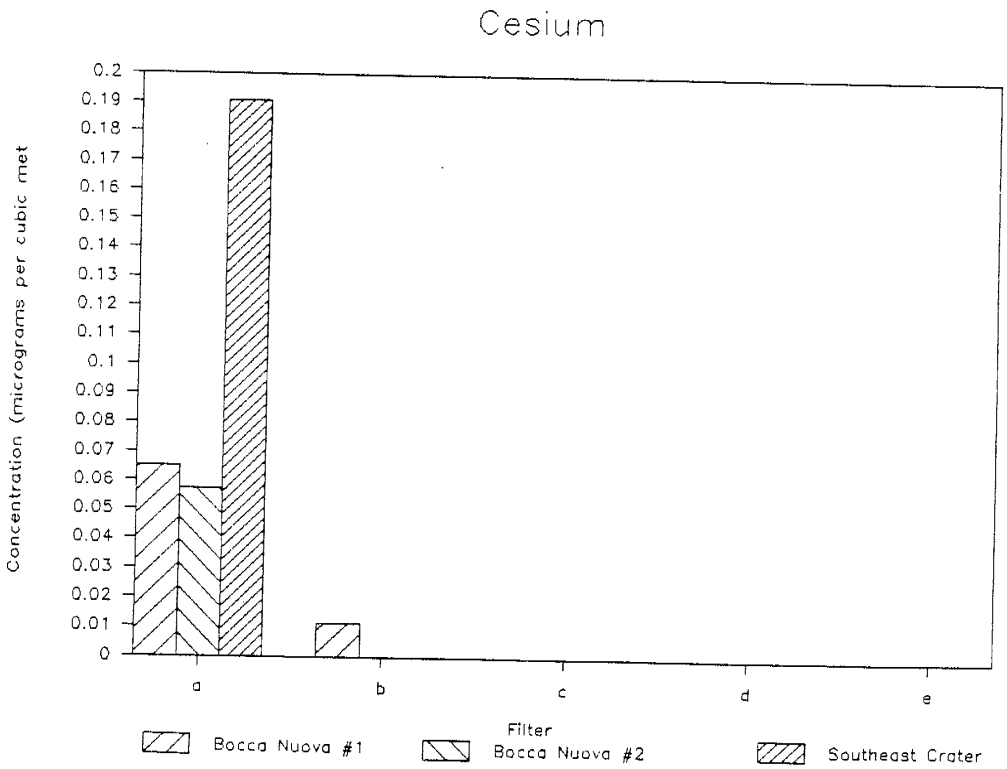
Cesium
Concentration (micrograms per cubic met
0.2
0.19
0.18
0.17
0.16
0.15
0.14
0.13
0.12
0.11
0.1
0.09
0.08
0.07
0.06
0.05
0.04
0.03
0.02
0.01
0
a
b
c
d
e
Filter
Bocca Nuova #1
Bocca Nuova #2
Southeast Crater

Chlorine

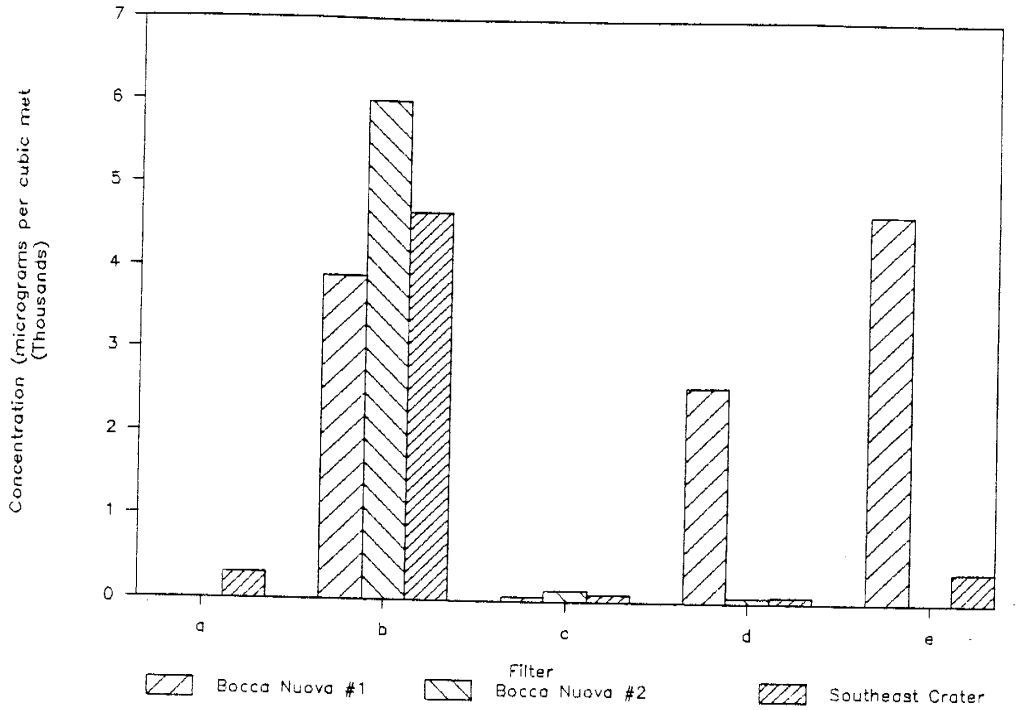

Cobalt

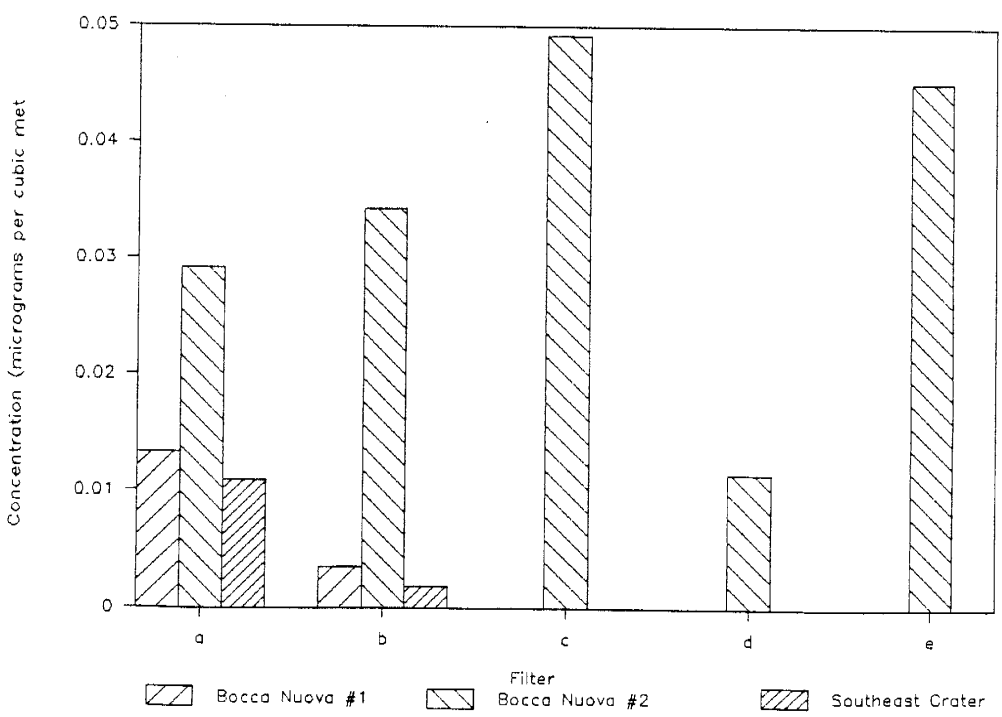

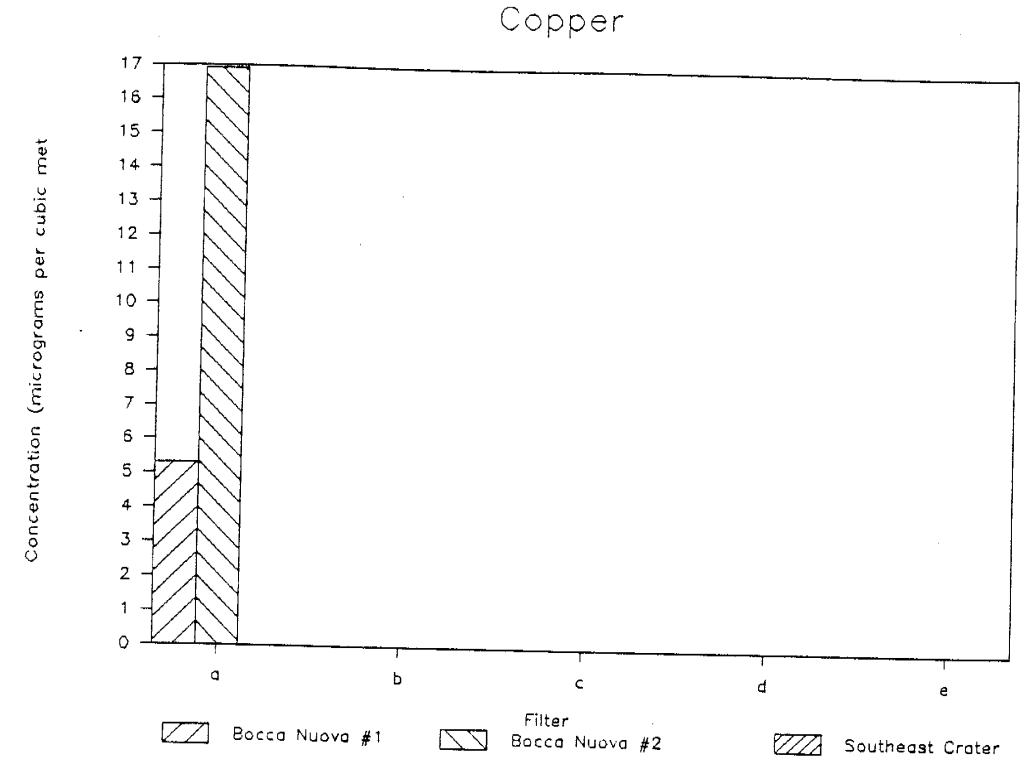
Copper
Concentration (micrograms per cubic met
17
16
15
14
13
12
11
10
9
8
7
6
5
4
3
2
1
0
a
b
c
d
e
Filter
Bocca Nuova #1
Bocca Nuova #2
Southeast Crater

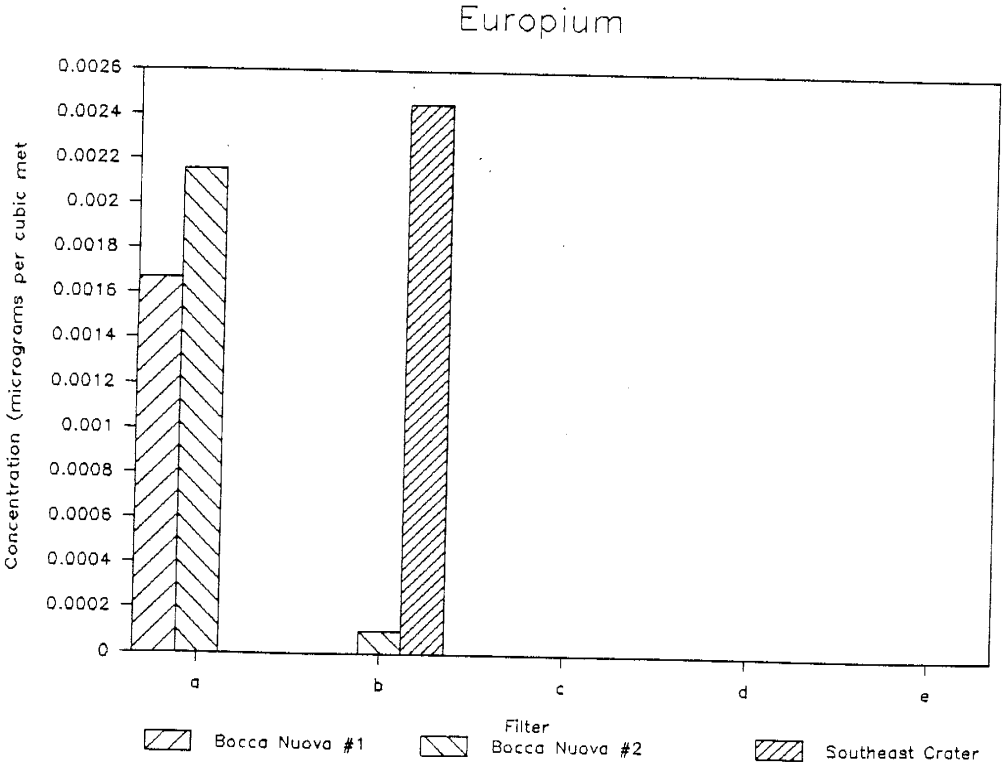
Europium
Concentration (micrograms per cubic met
0.0026
0.0024
0.0022
0.002
0.0018
0.0016
0.0014
0.0012
0.001
0.0008
0.0006
0.0004
0.0002
0
a
b
c
d
e
Filter
Bocca Nuova #1
Bocca Nuova #2
Southeast Crater

Fluorine

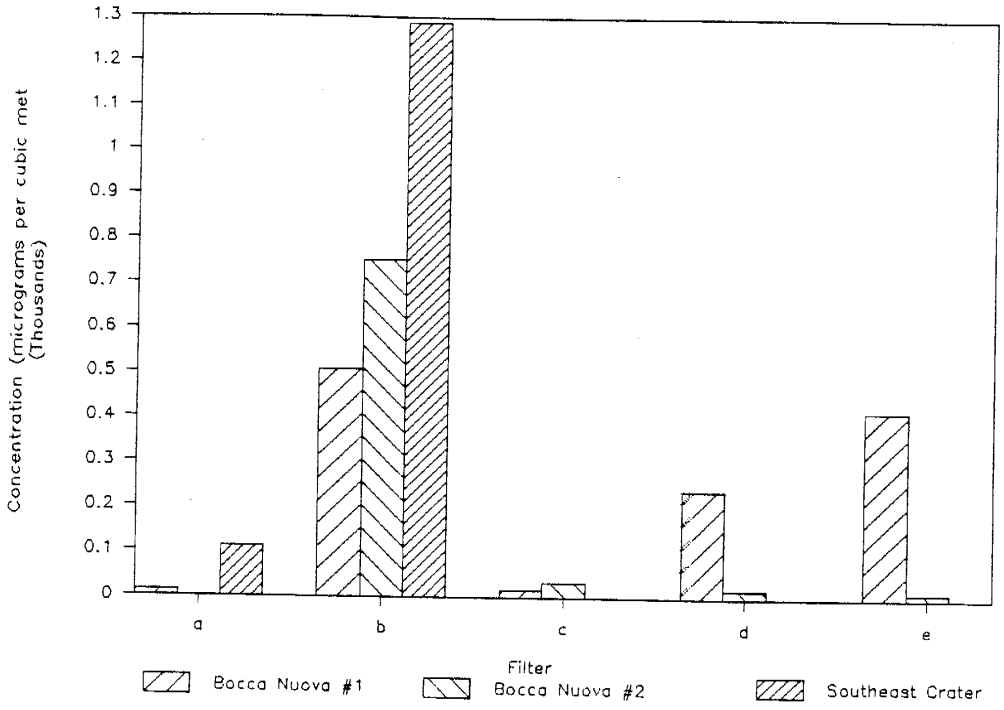

Gold

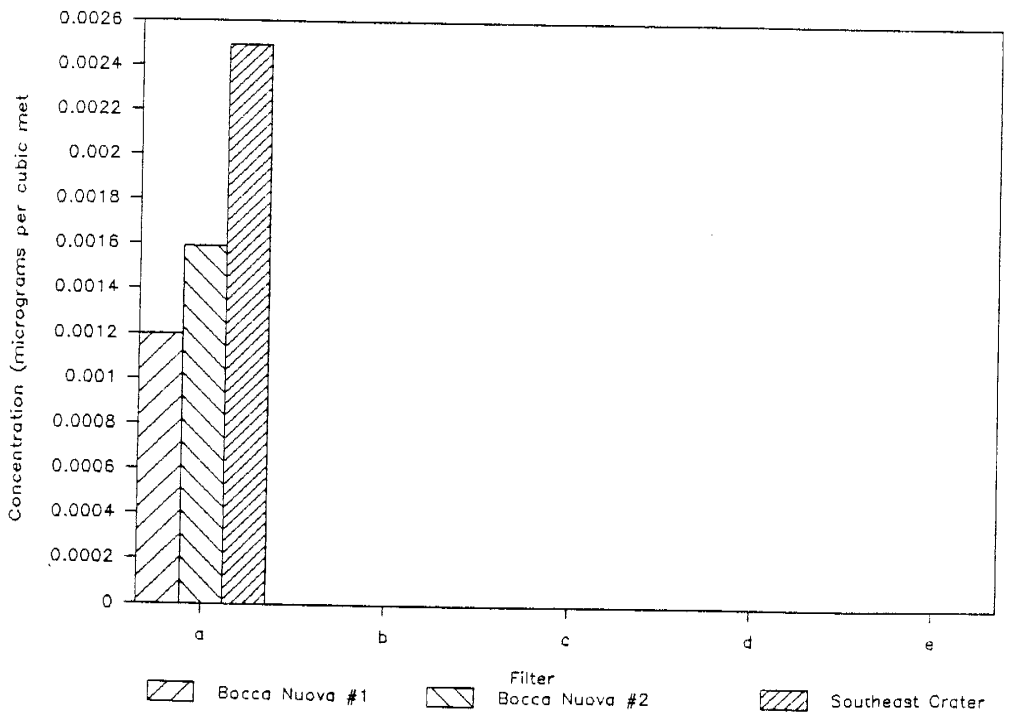

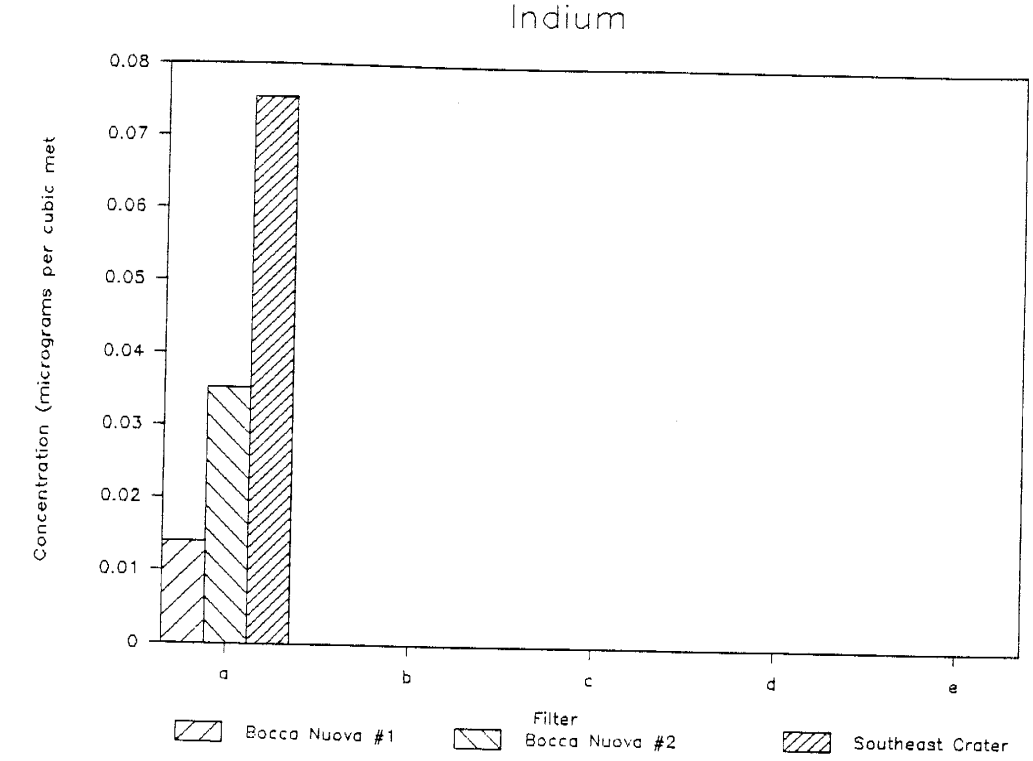
Indium
Concentration (micrograms per cubic met
0.08
0.07
0.06
0.05
0.04
0.03
0.02
0.01
0
a
b
c
d
e
Filter
Bocca Nuova #1
Bocca Nuova #2
Southeast Crater

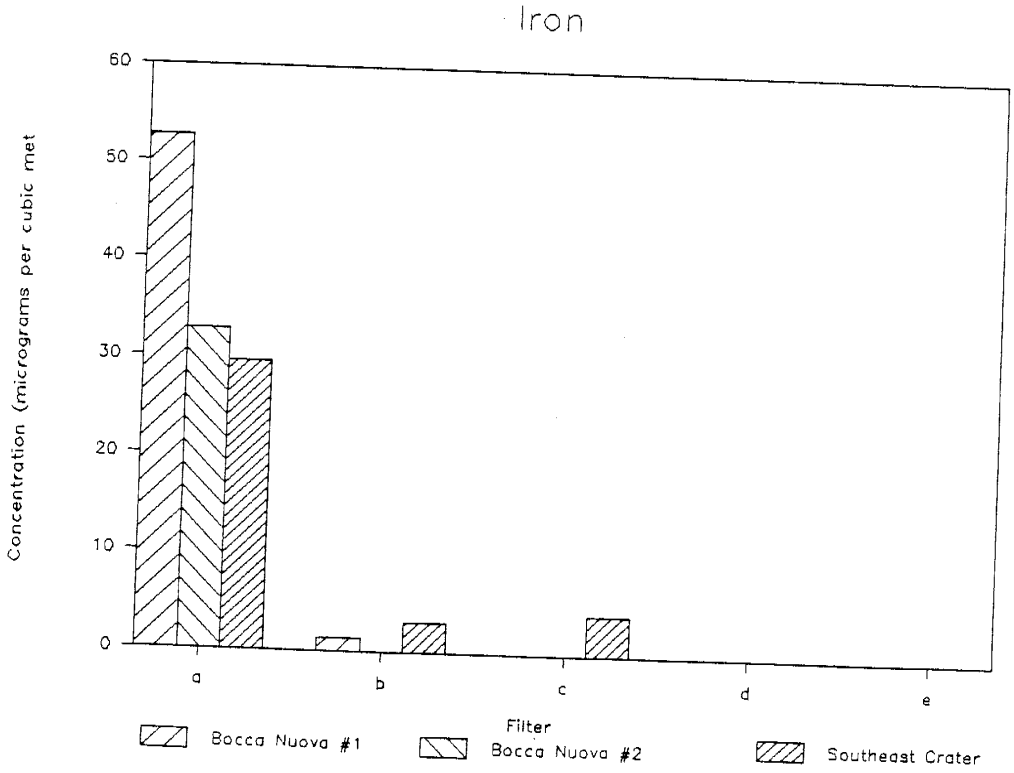
Iron
Concentration (micrograms per cubic met
60
50
40
30
20
10
0
a
b
c
d
e
Filter
Bocca Nuova #1
Bocca Nuova #2
Southeast Crater

Lanthanum

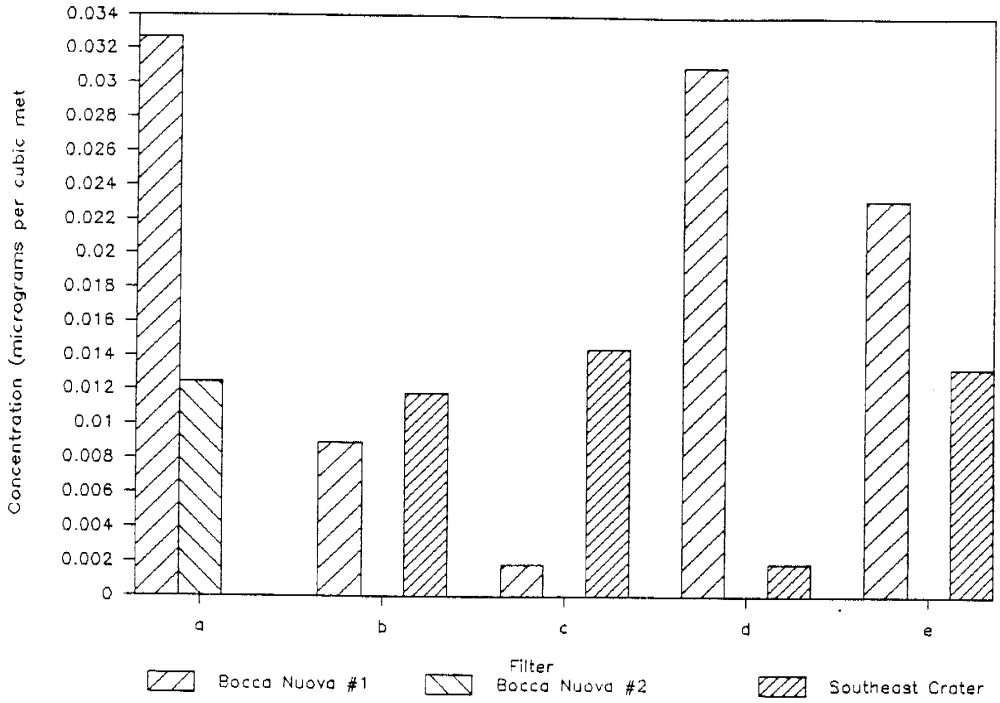

Manganese

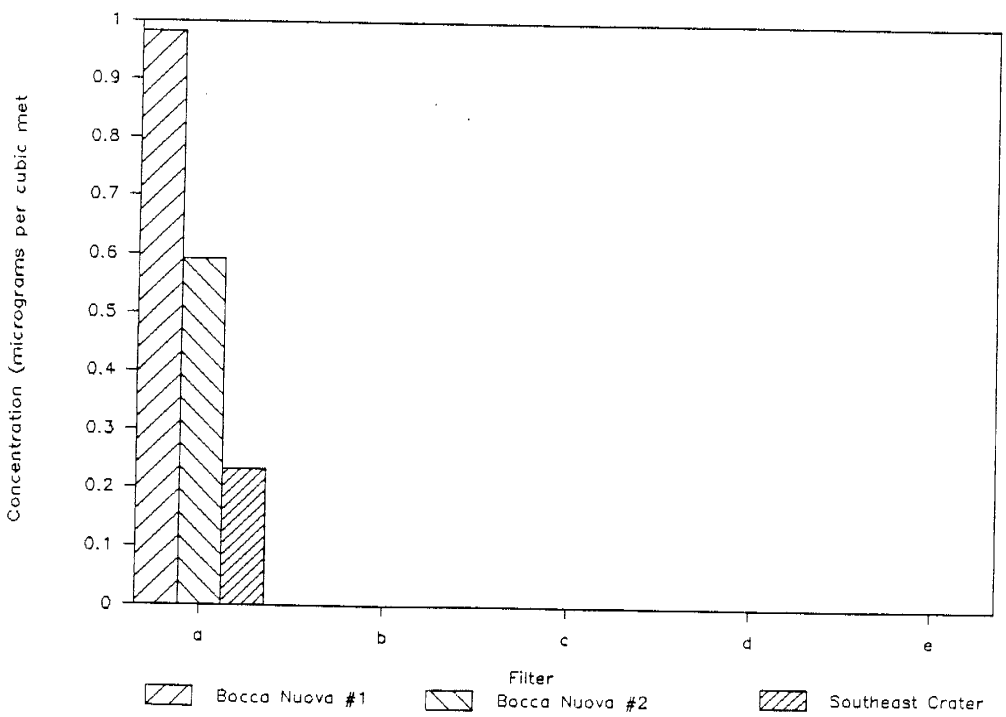

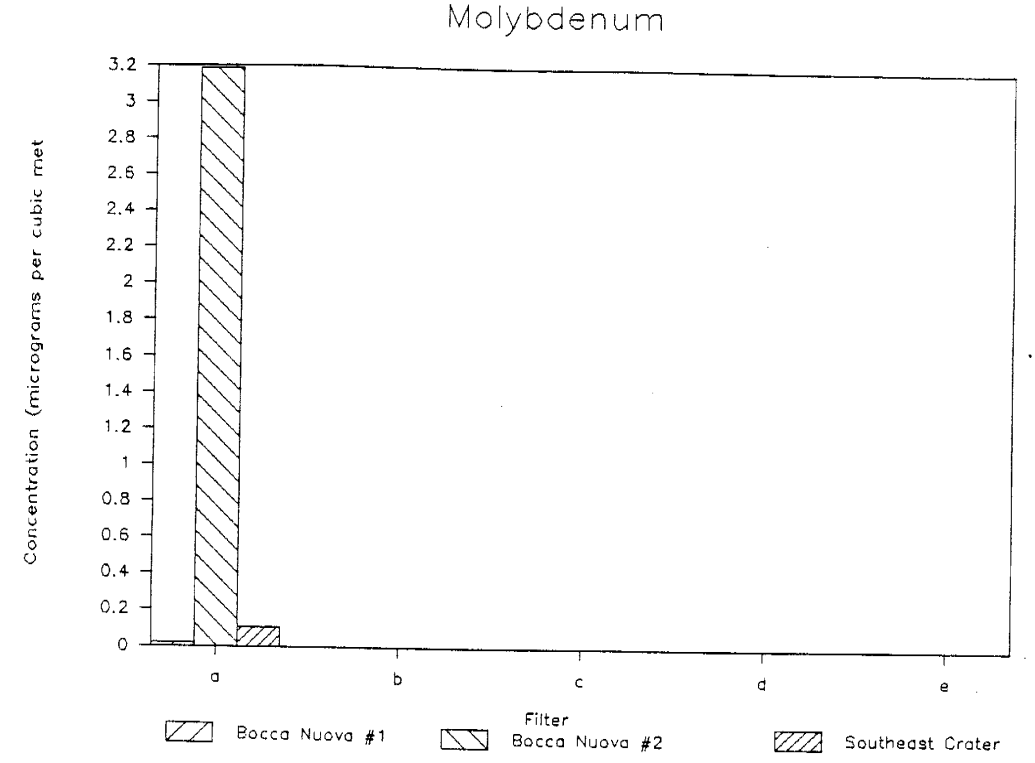
Molybdenum
Concentration (micrograms per cubic met
3.2
3
2.8
2.6
2.4
2.2
2
1.8
1.6
1.4
1.2
1
0.8
0.6
0.4
0.2
0
a
b
c
d
e
Filter
Bocca Nuova #1
Bocca Nuova #2
Southeast Crater

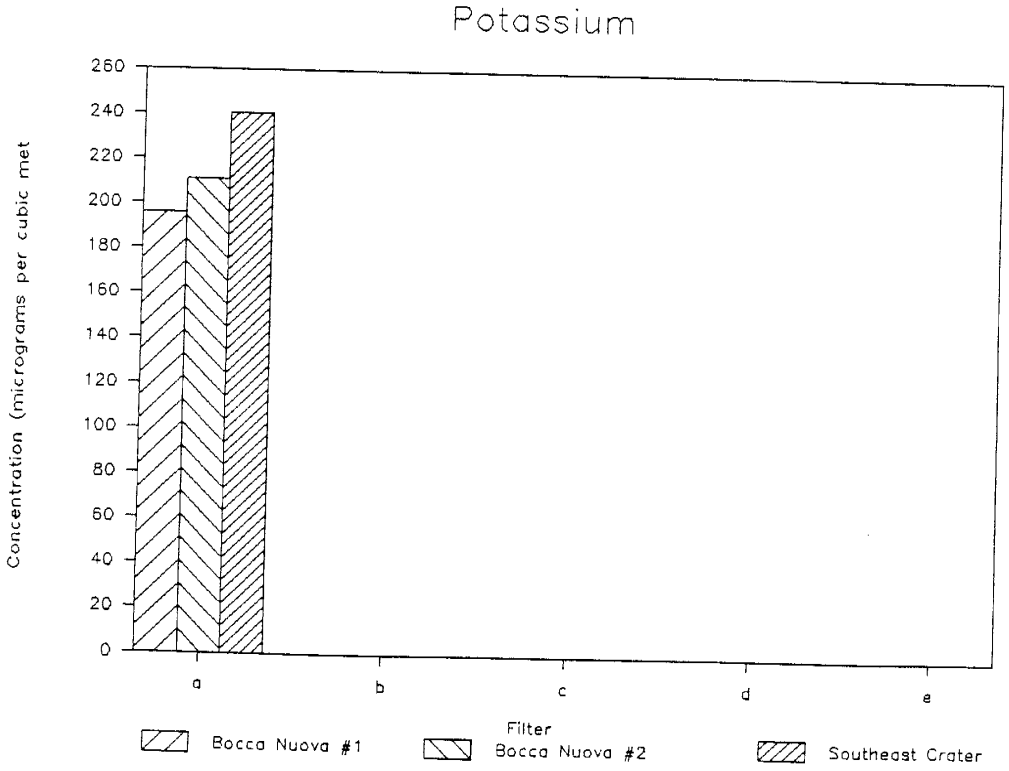
Potassium
Concentration (micrograms per cubic met
260
240
220
200
180
160
140
120
100
80
60
40
20
0
a
b
c
d
e
Filter
Bocca Nuova #1
Bocca Nuova #2
Southeast Crater

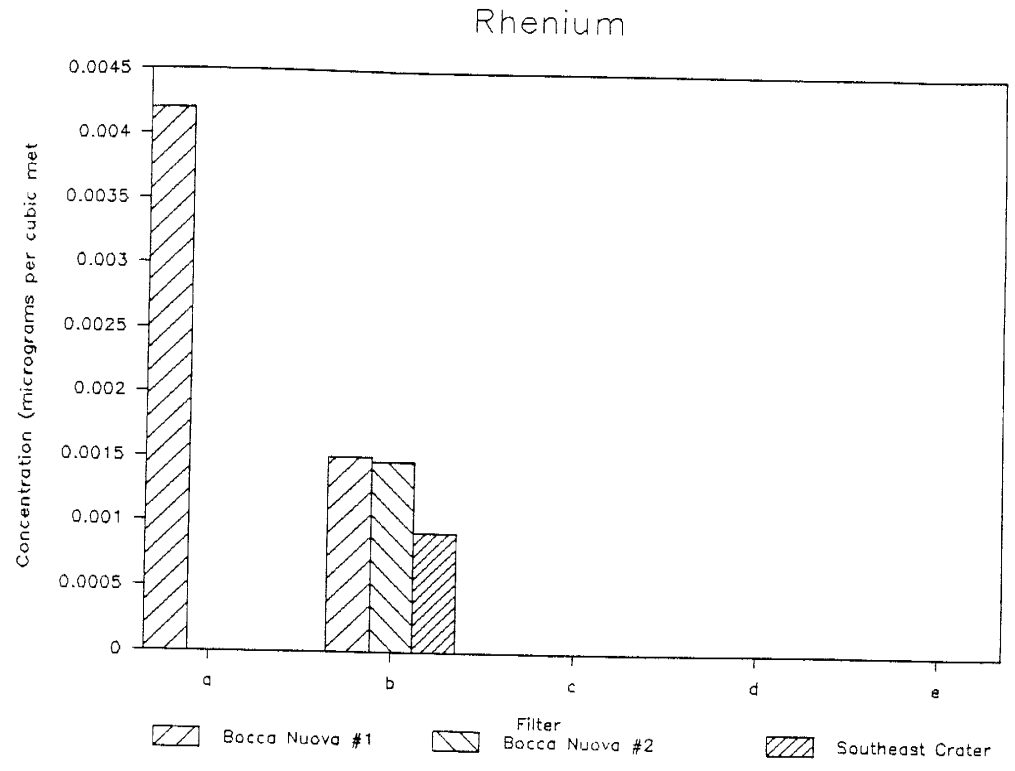
Rhenium
Concentration (micrograms per cubic met
0.0045
0.004
0.0035
0.003
0.0025
0.002
0.0015
0.001
0.0005
0
a
b
c
d
e
Filter
Bocca Nuova #1
Bocca Nuova #2
Southeast Crater

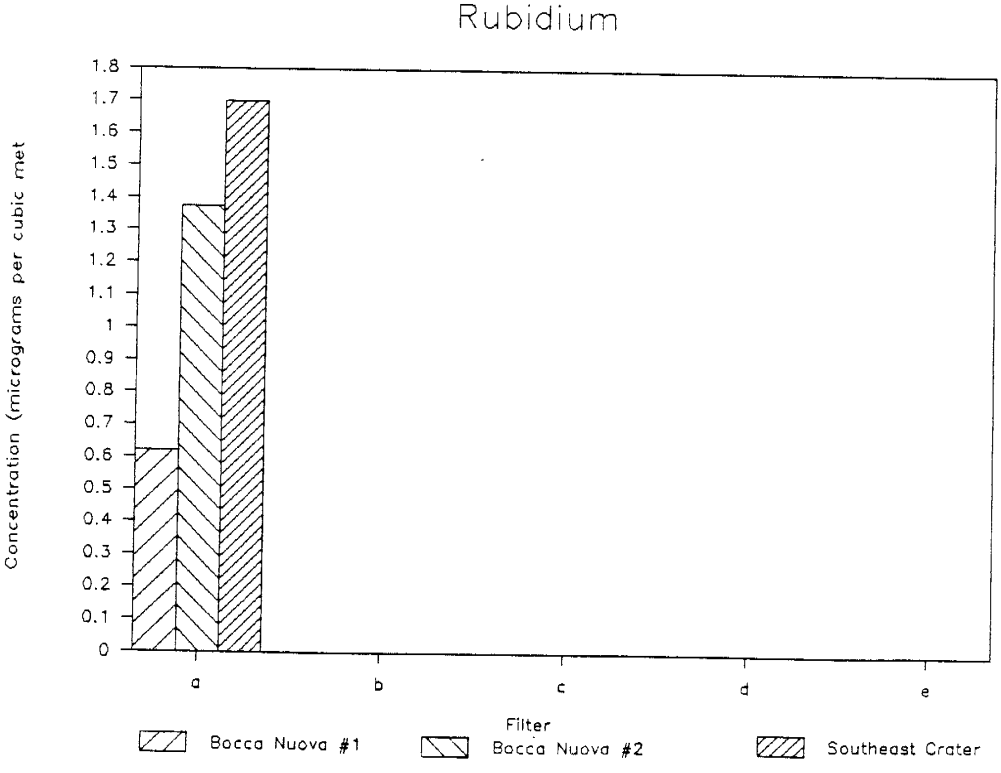
Rubidium
Concentration (micrograms per cubic met
1.8
1.7
1.6
1.5
1.4
1.3
1.2
1.1
1
0.9
0.8
0.7
0.6
0.5
0.4
0.3
0.2
0.1
0
a
b
c
d
e
Filter
Bocca Nuova #1
Bocca Nuova #2
Southeast Crater

Samarium

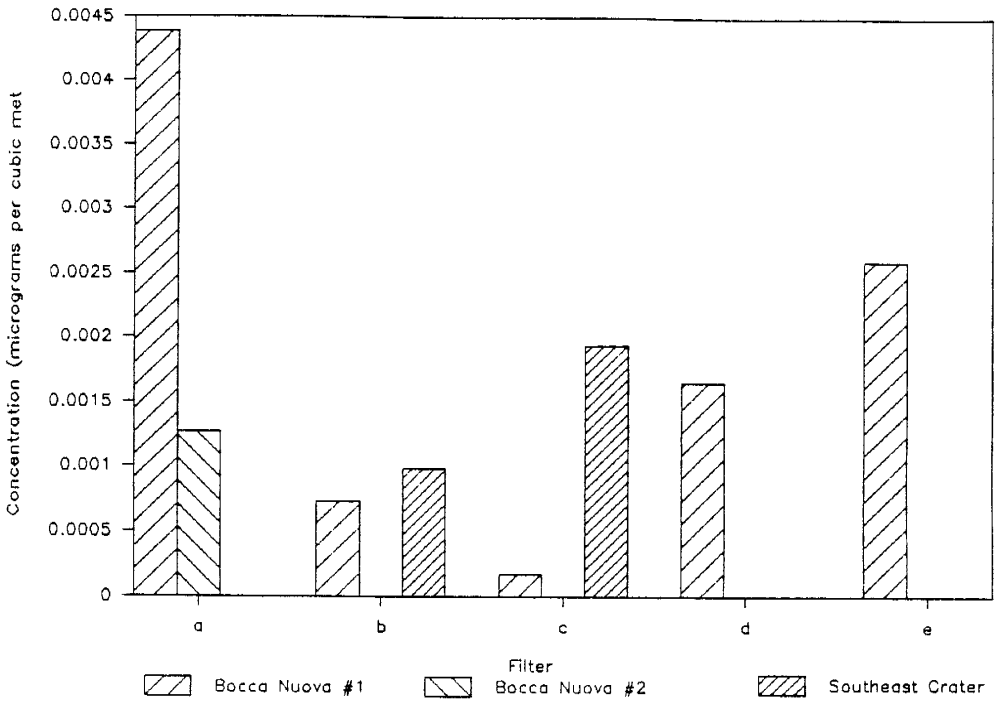

Scandium

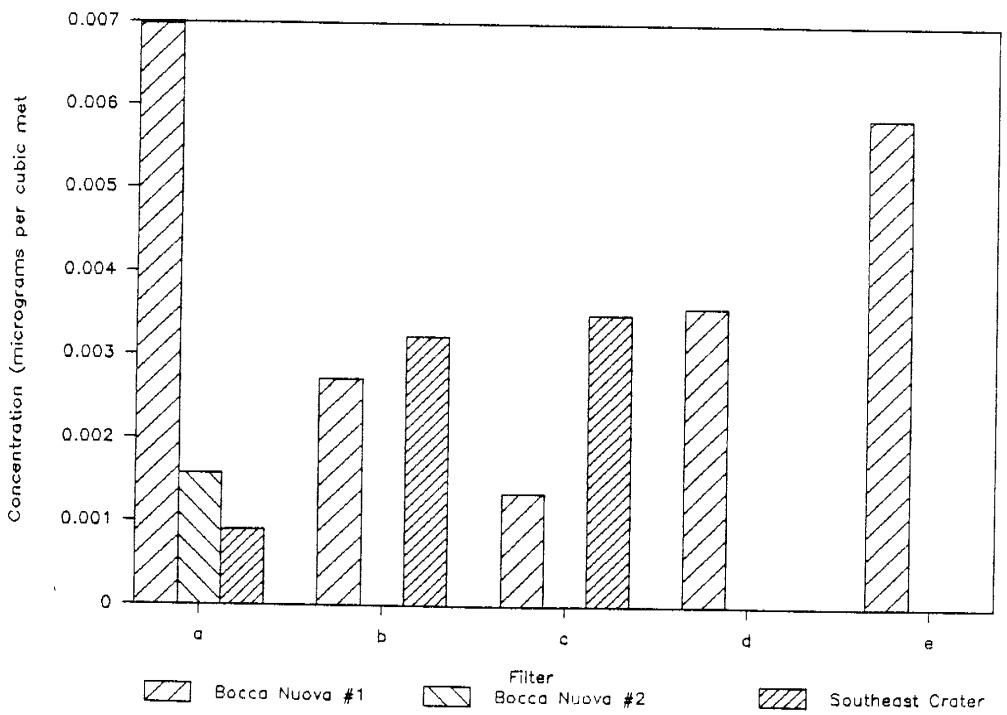

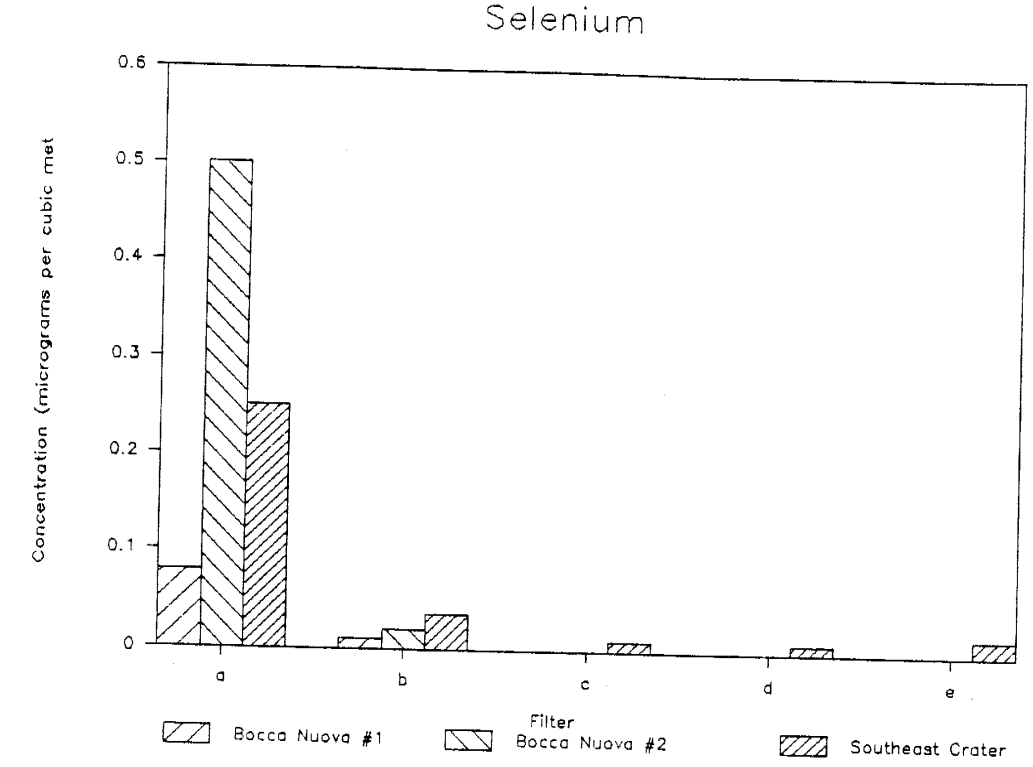
Selenium
Concentration (micrograms per cubic met
0.6
0.5
0.4
0.3
0.2
0.1
0
a
b
c
d
e
Filter
Bocca Nuova #1
Bocca Nuova #2
Southeast Crater

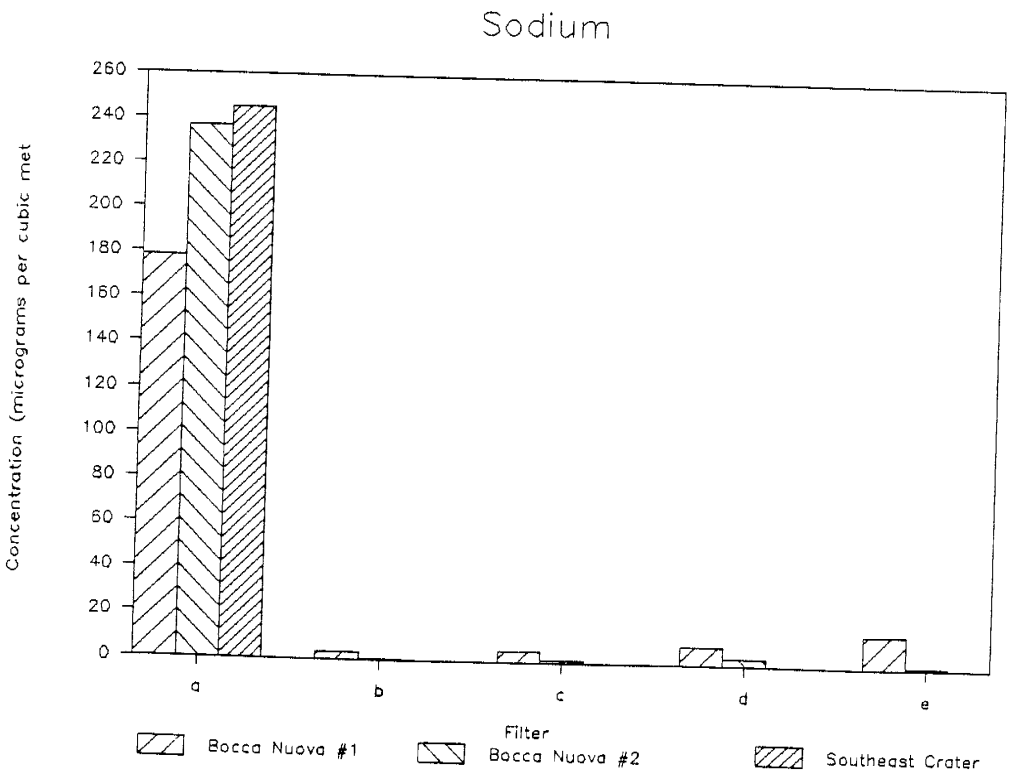
Sodium
Concentration (micrograms per cubic met
260
240
220
200
180
160
140
120
100
80
60
40
20
0
a
b
c
d
e
Filter
Bocca Nuova #1
Bocca Nuova #2
Southeast Crater

Sulfur

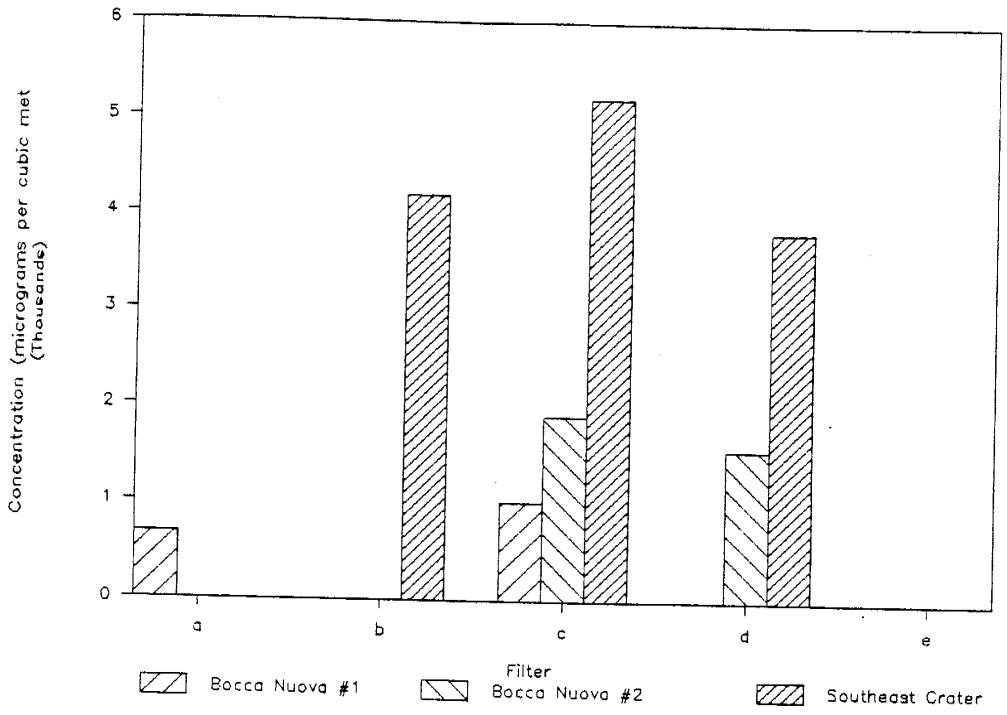

Tungsten

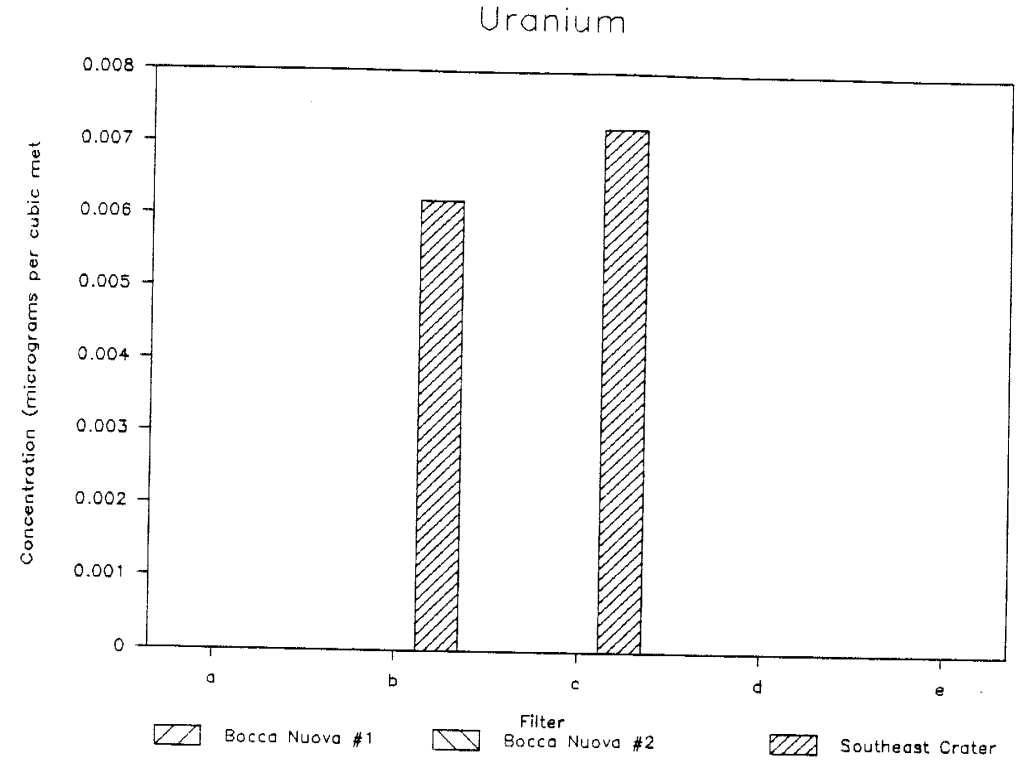
Uranium
Concentration (micrograms per cubic met
0.008
0.007
0.006
0.005
0.004
0.003
0.002
0.001
0
a
b
c
d
e
Filter
Bocca Nuova #1
Bocca Nuova #2
Southeast Crater

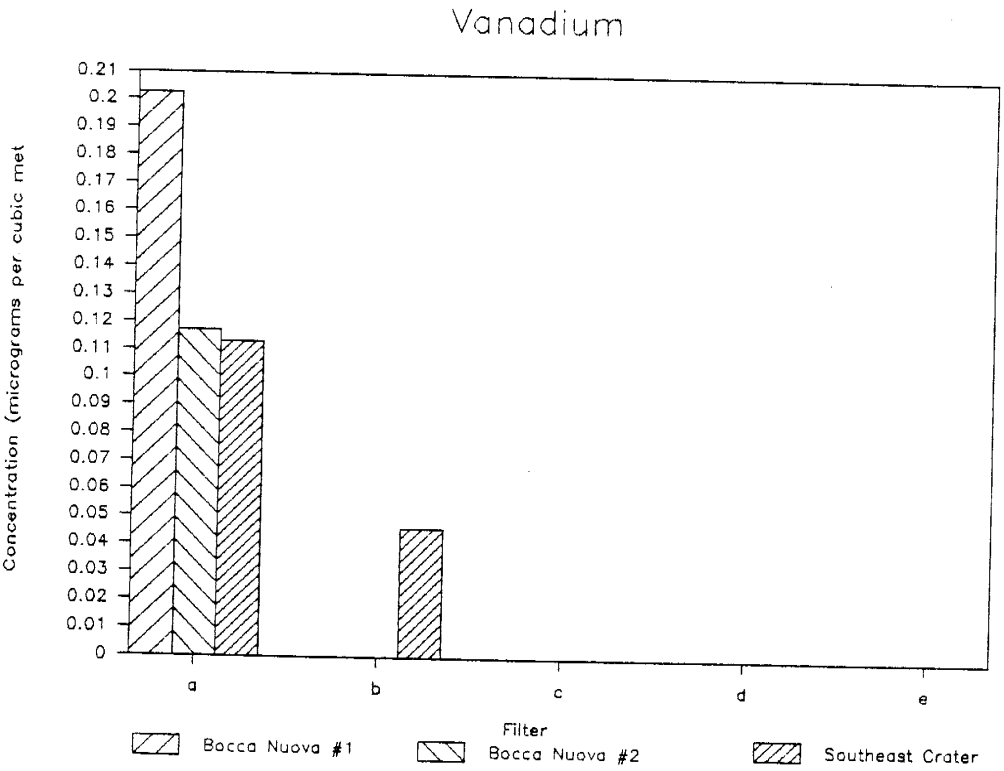
Vanadium
Concentration (micrograms per cubic met
0.21
0.2
0.19
0.18
0.17
0.16
0.15
0.14
0.13
0.12
0.11
0.1
0.09
0.08
0.07
0.06
0.05
0.04
0.03
0.02
0.01
0
a
b
c
d
e
Filter
Bocca Nuova #1
Bocca Nuova #2
Southeast Crater

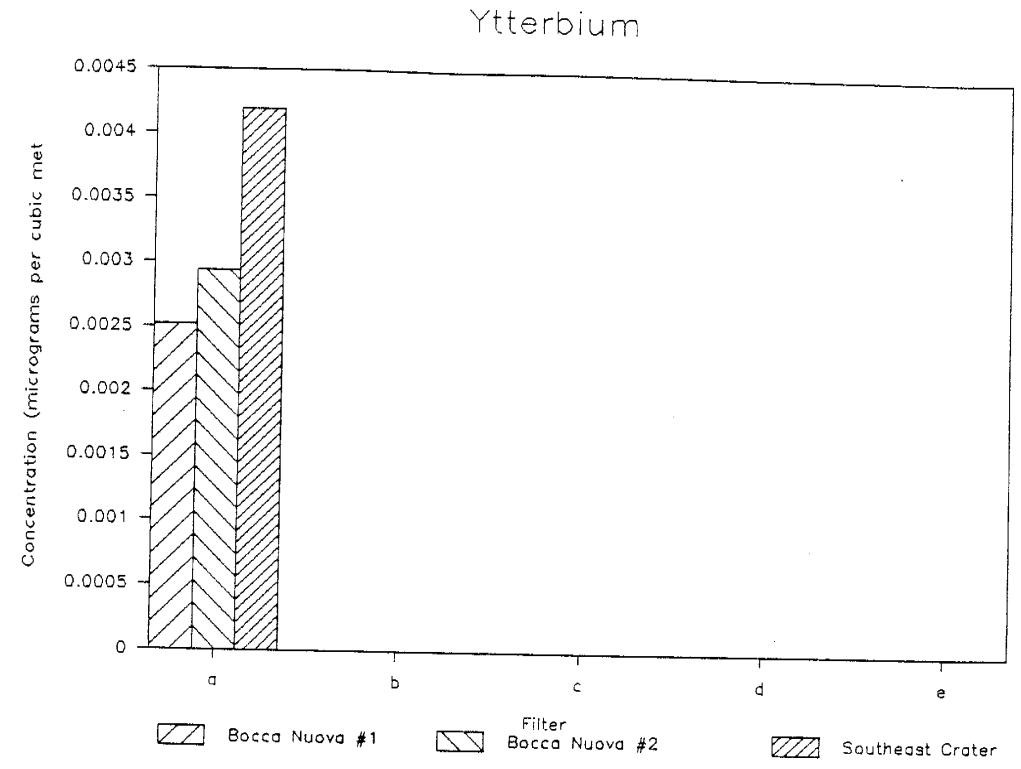
Ytterbium
Concentration (micrograms per cubic met
0.0045
0.004
0.0035
0.003
0.0025
0.002
0.0015
0.001
0.0005
0
a
b
c
d
e
Filter
Bocca Nuova #1
Bocca Nuova #2
Southeast Crater

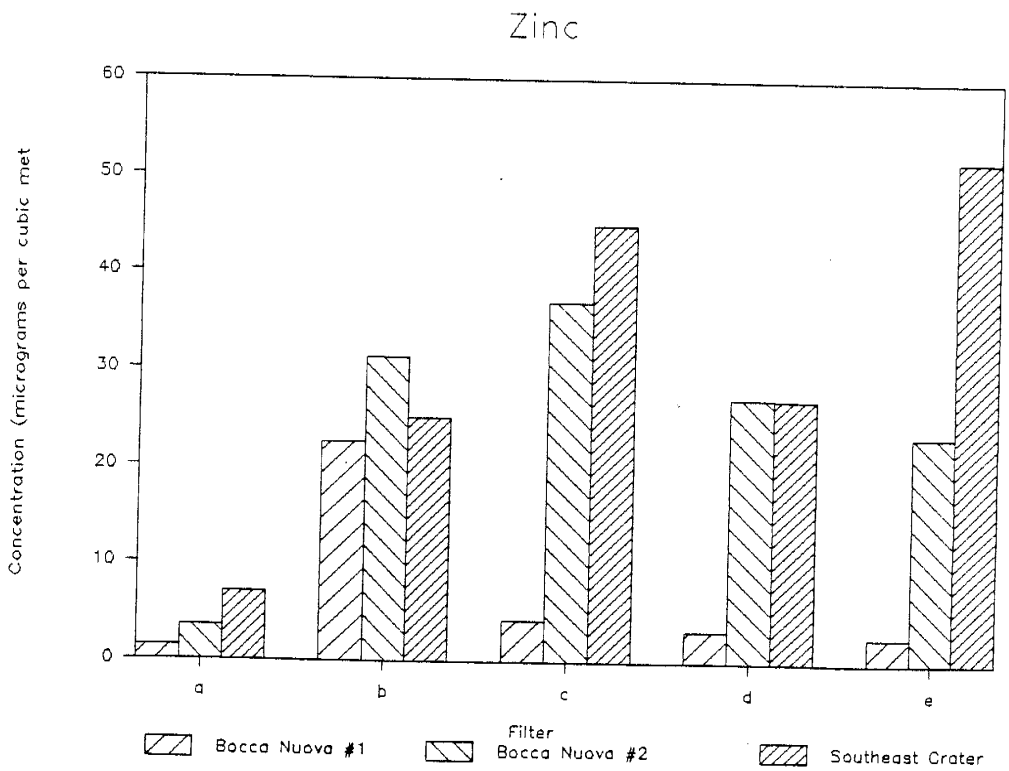
Zinc
Concentration (micrograms per cubic met
60
50
40
30
20
10
0
a
b
c
d
e
Filter
Bocca Nuova #1
Bocca Nuova #2
Southeast Crater

REFERENCES

Aki, K. and Koyanagi, R. 1981. Deep volcanic tremor and magma ascent mechanism under Kilauea, Hawaii. Journal of Geophysical Research. 86. 7095-7109.

Allard, P. 1983. The origin of hydrogen, carbon, sulphur, nitrogen and rare gases in volcanic exhalations: Evidence from isotope geochemistry. in Forecasting Volcanic Events, edited by H. Tazieff and J-C. Sabroux. New York: Elsevier. 337-386.

Andres, R. J., Kyle, P. R., Rose, W. I. and Stokes, J. B. in prep. SO_2 emissions during eruptive episode 48A, Kilauea Volcano, Hawaii.

Barberi, F., Civetta, L., Gasparini, P., Innocenti, F. and Scandone, R. 1974. Evolution of a section of the Africa-Europe plate boundary: paleomagnetic and volcanological evidence from Sicily. Earth and Planetary Science Letters. 22. 123-132.

Berresheim, H. and Jaeschke, W. 1983. The contribution of volcanoes to the global atmospheric sulfur budget. Journal of Geophysical Research. 88. 3732-3740.

Bloomfield, P. 1976. Fourier Analyses of Time Series: An Introduction. New York: John Wiley and Sons. 258 pp.

Buat-Ménard, P. and Arnold, M. 1978. The heavy metal chemistry of atmospheric particulate matter emitted by Mount Etna volcano. Geophysical Research Letters. 5. 245-248.

Burtscher, H., Cohn, P., Scherrer, L., Siegmann, H. C., Faraci, G., Pennisi, A. R., Privitera, V., Cristofolini, R. and Scribano, V. 1987. Investigation of submicron volcanic aerosol-particles by photoelectron emission. Journal of Volcanology and Geothermal Research. 33. 349-353.

Cadle, R.D. 1980. A comparison of volcanic with other fluxes of atmospheric trace gas constituents. Reviews of Geophysics and Space Physics. 18. 746-752.

_____, Lazrus, A. L., Huebert, B. J., Heidt, L. E., Rose, Jr., W. I., Woods, D. C., Chuan, R. L., Stoiber, R. E., Smith, D. B. and Zielinski, R. A. 1979. Atmospheric implications of studies of Central American volcanic eruption clouds. Journal of Geophysical Research. 84. 6961-6968.

Carter, S. R. and Civetta, L. 1977. Genetic implications of the isotope and trace element variations in the eastern Sicilian volcanics. Earth and Planetary Science Letters. 36. 168-180.

Casadevall, T.J., Johnston, D. A., Harris, D. M., Rose, Jr., W. I., Malinconico, L. L., Stoiber, R. E., Bornhorst, T. J., Williams, S. N., Woodruff, L. and Thompson, J. M. 1981. SO_2 emission rates at Mount St. Helens from March 29 through December, 1980. United States Geological Survey Professional Paper 1250. 193-200.

_____, Rose, Jr., W. I., Fuller, W. H., Hunt, W. H., Hart, M. A., Moyers, J. L., Woods, D. C., Chuan, R. L. and Friend, J. P. 1984. Sulfur dioxide and particles in quiescent volcanic plumes from Poás, Arenal, and Colima volcanoes, Costa Rica and Mexico. Journal of Geophysical Research. 89. 9633-9641.

Chartier, T. A. 1986. Detailed record of SO_2 emissions from Pu'u O'o between episodes 33 and 34 of the 1983-86 East Rift Zone eruption of Kilauea, Hawaii. Thesis. Michigan Technological University.

Chester, D. K., Duncan, A. M., Guest, J. E. and Kilburn, C. R. J. 1985. Mount Etna: The anatomy of a volcano. Stanford: Stanford University Press. 404 pp.

Chouet, B. 1985. Excitation of a buried magmatic pipe: A seismic source model for volcanic tremor. Journal of Geophysical Research. 90. 1881-1893.

_____, Koyanagi, R. Y. and Aki, K. 1987. Origin of volcanic tremor in Hawaii, Part II, Theory and discussion. United States Geological Survey Professional Paper 1350. 1259-1280.

Chuan, R. L., Woods, D. C. and McCormick, M. P. 1981. Characterization of aerosols from eruptions of Mount St. Helens. Science. 211. 830-832.

Condomines, M., Tanguy, J. C., Kieffer, G. and Allègre, C. J. 1982. Magmatic evolution of a volcano studied by ^{230}Th-^{238}U disequilibrium and trace elements systematics: the Etna case. Geochimica et Cosmochimica Acta. 46. 1397-1416.

CRC Handbook of Chemistry and Physics. 1986. edited by Weast, R. C., Astle, M. J. and Beyer, W. H. Boca Raton, Florida: CRC Press, Inc.

Cristofolini, R., Ghiara, M. R., Stanzione, D. and Tranchina, A. 1984. Petrologic and geochemical features of rocks from recent eruptions at Mount Etna, Sicily. Neues Jahrbuch fur Mineralogie Abhandlungen. 149. 267-282.

_____, Ghisetti, F., Scarpa, R. and Vezzani, L. 1985. Character of the stress field in the Calabrian Arc and southern Apennines (Italy) as deduced by geological, seismological and volcanological information. Tectonophysics. 117. 39-58.

_____, Menzies, M. A., Beccaluva, L. and Tindle, A. 1987. Petrological notes on the 1983 lavas at Mount Etna, Sicily, with reference to their REE and Sr-Nd isotope composition. Bulletin of Volcanology. 49. 599-607.

_____ and Romano, R. 1982. Petrologic features of the Etnean volcanic rocks. Memorie della Societa Geologica Italiana. 23. 99-115.

_____ and Tranchina, A. 1980. Aspetti petrologici delle vulcaniti Etnee: Caratteri dei fenocristalli isolati ed in aggregati. Rendiconti Societa Italiana di Mineralogia e Petrologia. 36. 751-773.

Crowe, B. M., Finnegan, D. L., Zoller, W. H. and Boynton, W. V. 1987. Trace element geochemistry of volcanic gases and particles from 1983-1984 eruptive episodes of Kilauea Volcano. Journal of Geophysical Research. 92. 13,708-13,714.

Day, A. L. and Shepherd, E. S. 1913. Water and volcanic activity. Bulletin of the Geological Society of America. 24. 573-606.

De la Roche, H., Leterrier, J., Grandclaude, P. and Marchal, M. 1980. A classification of volcanic and plutonic rocks using R_1R_2-diagram and major element analyses - its relationships with current nomenclature. Chemical Geology. 29. 183-210.

Del Pezzo, E., Guerra, I., Lo Bascio, A., Luongo, G., Nappi, G. and Scarpa, R. 1974. Microtremors and volcanic explosions at Stromboli - Part 2. Bulletin Volcanologique. 38. 1023-1036.

Devine, J. D., Sigurdsson, H., Davis, A. N. and Self, S. 1984. Estimates of sulfur and chlorine yield to the atmosphere from volcanic eruptions and potential climatic effects. Journal of Geophysical Research. 89. 6309-6325.

Ferrazzini, V. and Aki, K. 1987. Slow waves trapped in a fluid-filled crack: Implication for volcanic tremor. Journal of Geophysical Research. 92. 9215-9223.

Ferrick, M. G., Qamar, A. and St. Lawrence, W. F. 1982. Source mechanism of volcanic tremor. Journal of Geophysical Research. 87. 8675-8683.

Finlayson-Pitts, B. J. and Pitts, Jr. J. N. 1986. Atmospheric Chemistry: Fundamentals and Experimental Techniques. New York: John Wiley and Sons. 46, 645-667.

Finnegan, D. L., Kotra, J. P., Hermann, D. M. and Zoller, W. H. 1988. The use of ^{7}LiOH impregnated filters for the collection of acidic gases and analysis by instrumental neutron activation analysis. in press.

Gerlach, T. M. 1979. Evaluation and restoration of the 1970 volcanic gas analyses from Mount Etna, Sicily. Journal of Volcanology and Geothermal Research. 6. 165-178.

_____. 1980. Evaluation of volcanic gas analyses from Kilauea Volcano. Journal of Volcanology and Geothermal Research. 7. 295-317.

_____. 1981. Restoration of new volcanic gas analyses from basalts of the Afar region: Further evidence of CO_2-degassing trends. Journal of Volcanology and Geothermal Research. 10. 83-91.

_____. 1986. Exsolution of H_2O, CO_2, and S during eruptive episodes at Kilauea Volcano, Hawaii. Journal of Geophysical Research. 91. 12,177-12,185.

_____ and Graeber, E. J. 1985. Volatile budget of Kilauea Volcano. Nature. 313. 273-277.

Goldberg, E. D. 1976. The Health of the Oceans. Paris: UNESCO Press. 172 pp.

Greenland, L. P., Rose, W. I. and Stokes, J. B. 1985. An estimate of gas emissions and magmatic gas content from Kilauea Volcano. Geochimica at Cosmochimica Acta. 49. 125-129.

Grindley, G. W. 1973. Structural control of volcanism at Mount Etna. Philosophical Transactions of the Royal Society of London, Series A. 274. 165-175.

Guest, J. E. 1982. Styles of eruption and flow morphology on Mt. Etna. Memorie della Societa Geologica Italiana. 23. 49-73.

Huntingdon, A. T. 1973. The collection and analysis of volcanic gases from Mount Etna. Philosophical Transactions of the Royal Society of London, Series A. 274. 119-128.

Jaeschke, W., Berresheim, H. and Georgii, H-W. 1982. Sulfur emissions from Mt. Etna. Journal of Geophysical Research. 87. 7253-7261.

Jaggar, T. A. 1940. Magmatic gases. American Journal of Science. 238. 313-353.

Krauskopf, K. B. 1979. An Introduction to Geochemistry; Second edition. New York: McGraw-Hill Book Company. 367-393.

Lambert, G., Le Cloarec, M-F. and Pennisi, M. 1988. Volcanic output of SO_2 and trace metals: A new approach. Geochimica et Cosmochimica Acta. 52. 39-42.

Lantzy, R. J. and Mackenzie, F. T. 1979. Atmospheric trace metals: global cycles and assessment of man's impact. Geochimica et Cosmochimica Acta. 43. 511-525.

Le Guern, F. 1973. The collection and analysis of volcanic gases. Philosophical Transactions of the Royal Society of London, Series A. 274. 129-135.

Lentini, F. 1982. The geology of the Mt. Etna basement. Memorie della Societa Geologica Italiana. 23. 7-25.

Lepel, E. A., Stefansson, K. M. and Zoller, W. H. 1978. The enrichment of volatile elements in the atmosphere by volcanic activity: Augustine Volcano 1976. Journal of Geophysical Research. 83. 6213-6220.

Lo Bascio, A., Luongo, G. and Nappi, G. 1973. Microtremors and volcanic explosions at Stromboli (Aeolian Islands). Bulletin Volcanologique. 37. 596-606.

Lo Giudice, E., Patané, G., Rasá, R. and Romano, R. 1982. The structural framework of Mount Etna. Memorie della Societa Geologica Italiana. 23. 125-158.

Lombardo, G. and Patané, G. 1982. Etnean seismicity from macroseismic data and its relations with main tectonic features. Memorie della Societa Geologica Italiana. 23. 166-173.

Malinconico, Jr., L. L. 1979. Fluctuations in SO_2 emission during recent eruptions of Etna. Nature. 278. 43-45.

_____. 1987. On the variation of SO_2 emission from volcanoes. Journal of Volcanology and Geothermal Research. 33. 231-237.

Marple, V. A. and Willeke, K. 1976. Inertial impactors: Theory, design and use. in Fine Particles: Aerosol Generation, Measurement, Sampling, and Analysis, edited by B. Y. H. Liu. New York: Academic Press. 412-446.

Martin, D., Ardouin, B., Bergametti, G., Carbonnelle, J., Faivre-Pierret, R., Lambert, G., Le Cloarec, M. F. and Sennequier, G. 1986. Geochemistry of sulfur in Mount Etna plume. Journal of Geophysical Research. 91. 12,249-12,254.

_____, Granier, J. P., Imbard, M. and Strauss, B. 1984. Application of a long range transport model to a Mount Etna plume. Bulletin Volcanologique. 47. 1097-1106.

Mason, B. and Moore, C. B. 1982. Principles of Geochemistry, 4th edition. New York: John Wiley and Sons. 46-7.

Meeker, K. 1988. Master's thesis. in prep.

Millan, M. M., Gallant, A. J. and Turner, H. E. 1976. The application of correlation spectroscopy to the study of dispersion from tall stacks. Atmospheric Environment. 10. 499-511.

_____ and Hoff, R. M. 1978. Remote sensing of air pollutants by correlation spectroscopy - instrumental response characteristics. Atmospheric Environment. 12. 853-864.

Moffat, A. J. and Millán, M. M. 1971. The applications of optical correlation techniques to the remote sensing of SO_2 plumes using sky light. Atmospheric Environment. 5. 677-690.

Mroz, E. and Zoller, W. H. 1975. Composition of atmospheric particulate matter from the eruption of Heimaey, Iceland. Science. 190. 461-464.

Murray, J. B. 1987. Report of mission to Mount Etna; September 11th to October 16th 1987. London: University College London. 21 pp.

Murray, J. B., Kilburn, C. R. J., Sanderson, T. J., Benazon, S., Crookes, C. and Pullen, A. 1981. Sommità del Mt. Etna, Settembre 1981. Map. Southampton: Ordnance Survey.

Newcomb, G. S. and Millan, M. M. 1970. Theory, applications, and results of the long-line correlation spectrometer. IEEE Transactions on Geoscience Electronics. GE-8. 149-157.

Pollack, J. B., Toon, O. B., Sagan, C., Summers, A., Baldwin, B. and Van Camp, W. 1976. Volcanic explosions and climatic change: A theoretical assessment. Journal of Geophysical Research. 81. 1071-1083.

Rampino, M.R. and Self, S. 1984. Sulfur-rich volcanic eruptions and stratospheric aerosols. Nature. 310. 677-679.

Rittmann, A. 1973. Structure and evolution of Mount Etna. Philosophical Transactions of the Royal Society of London, Series A. 274. 5-16.

Romano, R. 1982. Succession of the volcanic activity in the Etnean area. Memorie della Societa Geologica Italiana. 23. 27-48.

_____, and Sturiale, C. 1982. The historical eruptions of Mt. Etna (Volcanological data). Memorie della Societa Geologica Italiana. 23. 75-97.

_____, Sturiale, C., Lentini, F. et al. 1979. Geological Map of Mount Etna, scale 1:50,000. National Research Council. Italian Geodynamic Project. International Institute of Volcanology. Catania, Italy.

Rose, Jr., W. I., Chuan, R. L., Cadle, R. D. and Woods, D. C. 1980. Small particles in volcanic eruption clouds. American Journal of Science. 280. 671-696.

_____, Symonds, R. B., Chartier, T., Stokes, J. B. and Brantley, S. 1985. Simultaneous experiments with two correlation spectrometers at Kilauea and Mount St Helens. EOS. 66. 1142.

Schick, R., Cosentino, M., Lombardo, G. and Patané, G. 1982. Volcanic tremor at Mount Etna - a brief description. Memorie della Societa Geologica Italiana. 23. 191-196.

_____, Lombardo, G. and Patané, G. 1982. Volcanic tremors and shocks associated with eruptions at Etna (Sicily), September 1980. Journal of Volcanology and Geothermal Research. 14. 261-279.

Self, S. and Rampino, M. R. 1988. The relationship between volcanic eruptions and climatic change: Still a conundrum? EOS. 69. 74-86.

Sharp, A. D. L. 1982. Deep seismic sounding of Mount Etna - a review. Memorie della Societa Geologica Italiana. 23. 197-205.

Sigurdsson, H. 1982. Volcanic pollution and climate: The 1783 Laki eruption. EOS. 63. 601-602.

Stoiber R. E., Malinconico, Jr., L. L. and Williams, S. N. 1983. Use of the correlation spectrometer at volcanoes. in Forecasting Volcanic Events, edited by H. Tazieff and J-C. Sabroux. New York: Elsevier. 425-444.

_____, Williams, S. N. and Huebert, B. 1987. Annual contribution of sulfur dioxide to the atmosphere by volcanoes. Journal of Volcanology and Geothermal Research. 33. 1-8.

Tanguy, J. C. 1979. The storage and release of magma on Mount Etna: A discussion. Journal of Volcanology and Geothermal Research. 6. 179-188.

Tazieff, H. 1971. New investigations on eruptive gases. Bulletin Volcanologique. 34. 421-438.

Varekamp, J. C., Thomas, E., Germani, M. and Buseck, P. R. 1986. Particle geochemistry of volcanic plumes of Etna and Mount St. Helens. Journal of Geophysical Research. 91. 12,233-12,248.

Vié le Sage, R. 1983. Chemistry of the volcanic aerosol. in Forecasting Volcanic Events, edited by H. Tazieff and J-C. Sabroux. New York: Elsevier. 445-474.

Wadge, G. 1977. The storage and release of magma on Mount Etna. Journal of Volcanology and Geothermal Research. 2. 361-384.

_____. 1979. The storage and release of magma on Mount Etna: A reply to a discussion by J.C. Tanguy. Journal of Volcanology and Geothermal Research. 6. 189-195.

_____ and Guest, J. E. 1981. Steady-state magma discharge at Etna 1971-81. Nature. 294. 548-550.

Williams, D. J., Carras, J. N., Milne, J. W. and Heggie, A. C. 1981. The oxidation and long-range transport of sulphur dioxide in a remote region. Atmospheric Environment. 15. 2255-2262.

Zettwoog, P. and Haulet, R. 1978. Experimental results on the SO_2 transfer in the Mediterranean obtained with remote sensing devices. Atmospheric Environment. 12. 795-796.

This thesis is accepted on behalf of the faculty of the Institute by the following committee:

Philip R. Kyle

Advisor

Andrew Campbell

Carl Popp

18 June 1988

Date